From Molecular Cores to Planet Forming Disks (c2d)

A *Spitzer* Space Telescope Legacy Program

c2d Spectroscopy Explanatory Supplement

Edited by: Fred Lahuis and Jacqueline E. Kessler-Silacci

30 November 2006

Colophon

The c2d Spectroscopy Explanatory Supplement was compiled and edited by Fred Lahuis and Jacqueline E. Kessler-Silacci with contributions from all c2d spectroscopy team members:

Neal J. Evans II (University of Texas, c2d Principal Investigator),
Geoffrey A. Blake (California Institute of Technology, c2d Co-Investigator),
Ewine F. van Dishoeck (Leiden Observatory, c2d Co-Investigator),
Jean-Charles Augereau (Observatoire de Grenoble),
Zita Banhidi (Stockholm Observatory),
A. C. Adwin Boogert (AURA/NOAO-South),
Joanna M. Brown (California Institute of Technology),
Vincent C. Geers (Leiden Observatory),
Jes K. Jørgensen (Harvard-Smithsonian Center for Astrophysics),
Jacqueline E. Kessler-Silacci (University of Texas),
Claudia Knez (University of Texas, University of Maryland),
Fred Lahuis (Leiden Observatory, SRON),
Bruno Merín (Leiden Observatory, ESA),
Johan Olofsson (Observatoire de Grenoble),
Klaus M. Pontoppidan (California Institute of Technology)

In publications, refer to this document as:

Lahuis, F., Kessler-Silacci, J. E., Evans, N. J., II, Blake, G. A., van Dishoeck, E. F., Augereau, J.-C., Banhidi, Z., Boogert, A. C. A., Brown, J. M., Geers, V. C., Jørgensen, J. K., Knez, C., Merín, B., Olofsson, J., & Pontoppidan, K. M. 2006, "c2d Spectroscopy Explanatory Supplement," (Pasadena: *Spitzer* Science Center)

Questions regarding this document should be directed to the *Spitzer* Science Center helpdesk *help@spitzer.caltech.edu*.

This document and the c2d legacy data described herein are accessible via the legacy archive at the *Spitzer* Science Center
http://ssc.spitzer.caltech.edu/legacy/c2dhistory.html.

More information on the "Cores to Disks" legacy program itself can be found on the "Cores to Disks" homepage
http://peggysue.as.utexas.edu/SIRTF/.

Contents

1. Introduction

This document describes the final delivery of the spectroscopy section of the "Cores to Disks" or c2d Legacy team. The organization of this document is as follows:

- A brief summary of the program and the delivery (this introduction)
- A description of the processing of IRS pointed observations (Section 2)
- A description of the delivered products for IRS pointed observations (Section 3)
- A description of the processing of IRS maps (Section 4.1)
- A description of the delivered products for the IRS maps (Section 4.2)
- A description of the processing of MIPS SED data (Section 5.1)
- A description of the delivered products for MIPS SED (Section 5.2)
- A summary (Section 6)
- Appendices

The observational strategy is described in detail in Evans et al. (2003). The 75 hour c2d IRS program consisted primarily of IRS observations of point sources, with only a small portion dedicated to IRS spectral maps of the south-eastern Serpens molecular core and the Barnard 1 (B1) outflow and followup mini-maps of extended gas-phase and polycyclic aromatic hydrocarbon (PAH) emission around point source targets. High-S/N spectra were obtained within the 5–38 μm range (high resolution [R≈600] over the 10–37 μm range) for 226 sources at all phases of star and planet formation up to ages of $\sim$5 Myr. Additionally, the MIPS SED mode at 50–100 μm was used in the second year of the program to characterize the longer wavelength silicate and ice features of a small subsample of disks. Previous spectroscopic studies, e.g., with ISO, had the sensitivity to probe only high- or intermediate-mass young stellar objects. *Spitzer* permits the first comprehensive mid-infrared spectroscopic survey of solar-type young stars.

The c2d IRS program was divided into two sets with roughly equal time, the first-look (PID #172) consisting of observations of known embedded, pre-main-sequence stars, and background stars and the second-look (PID #179) consisting of IRS follow-up spectroscopy of sources discovered in the IRAC and MIPS mapping surveys. The source list for the first-look program was restricted primarily to low-mass young stars, defined as having masses $M < 2\ M_{\odot}$, with ages younger than $\sim$5 Myr, for minimal overlap with existing infrared spectroscopy. Within these criteria, the selection contains a broad representative sample of young stars with ages down to 0.01 Myr and masses down to the hydrogen-burning limit or even less, if possible. The second-look IRS campaign was more focused on observations of new or interesting types of sources found in the c2d IRAC and MIPS maps, including IRS staring observations of samples of very low-mass stars and brown dwarfs, weak-line T Tauri Stars, edge-on disks, very low luminosity objects (VeLLOs), and cold disks, as well as IRS mapping observations of extended outflows and followup mini-maps of extended gas-phase and PAH emission and 4 MIPS SED observations of interesting targets from the first-look campaign.

Almost all first-look targets were observed using the IRS staring mode in each of its four modules: short-low with two sub-slits (SL2: $R = \lambda/\delta\lambda \approx 60 - 120$, $\lambda_{\rm SL2} = 5.2 - 8.7\,\mu$m and SL1: $R \approx 60 - 120$, $\lambda_{\rm SL1} = 7.4 - 14.5\,\mu$m), long-low with two sub-slits (LL2: $R \approx 60 - 120$, $\lambda_{\rm LL2} = 14.0 - 21.3\,\mu$m and LL1: $R \approx 60 - 120$, $\lambda_{\rm LL1} = 19.5 - 38.0\,\mu$m), short-high (SH: $R \approx 600$, $\lambda_{\rm SH} = 9.9$–19.6 μm), and long-high (LH: $R \approx 600$, $\lambda_{\rm LH} = 18.7$–37.2 μm). The longest wavelength ends of SL1 and LL1 suffer from light leaks from higher orders and are therefore removed from the delivered spectra. For those sources that are part of various GTO programs involving the low-resolution modules, only the high-resolution 10–37 μm (SH,LH) spectra were acquired as part of the c2d IRS effort. In contrast to the scheduled GTO observations of large numbers of young stars, typically with the low-resolution IRS modules, the c2d IRS program focuses on long integration times in the high resolution modules, ensuring high dynamic range even on weak sources. For all first-look observations, the integration times for the short-high and long-high modules were fixed such that theoretical S/Ns of at least 100 and 50 were obtained for sources brighter and fainter than 500 mJy, respectively. The spectra taken using the short-low modules always reach theoretical S/Ns of greater than 100. Second-look IRS staring targets were observed in various modules depending on the source type and flux. The S/N limits of first-look were achieved where possible, but since second-look consisted of primarily very weak sources, this was not always the case. See Table 2 for a list of the details of each of the observed IRS AORs. A number of sources have been observed twice. These have the addition _AOR1 and _AOR2 added to the name in the delivered products and in the feature identification tables.

As part of the second-look program, followup mini-maps of extended gas-phase and PAH emission around point source targets were taken using the IRS mapping mode. In addition, IRS spectral maps of the south-eastern Serpens molecular core and the B1 outflow were obtained. All mapping observations are listed at the end of Table 2 and labeled with AOT_mode “irsmap”. The Serpens molecular core was imaged over more than 7 arcmin^2 to a 1σ sensitivity of 2 mJy using the low-resolution IRS spectral mapping mode. This core contains several deeply embedded sources and possesses a complex physical structure with outflows on a scale of 30″–60″ (∼0.05–0.1 pc) from the driving sources. Section 4 gives details on the observing strategy, the IRS mapping reduction and the IRS mapping products provided in this delivery.

As a means of quickly assessing the nature of the observed sources an automated feature identification of the most prominent spectral features is performed on all IRS staring observations and all extracted spectra of individual map pointings. The results are listed in the product logfiles and, for all IRS staring observations and source map pointings, listed in Tables 7 and 8.

The MIPS SED observations taken as part of the second-look program were all "FixedSingle" observations, meaning that they were non-mapping, non-clustered AORs. The exposure time for all observations was 10 s, repeated as necessary to get S/N of 30–50 based on IRAS 60 μm and MIPS 70 μm fluxes and the 2004 sensitivity estimates for MIPS SED mode. Table 5 lists the details of each of the observed MIPS SED AORs.

Table 1 gives an overview of the campaigns in which c2d IRS program observations have been executed. Table 2 and 5 give all relevant observational details of the IRS and MIPS SED observation included in this delivery. All delivery product for observations from campaigns up to IRS–29 were derived using data from SSC pipeline S13.2.0, for later campaigns S14.0.0 pipeline data was used.

Table 1: Summary of c2d observations

Campaign	Obs. dates	#aors
IRS-01	14 Dec 2003 – 17 Dec 2004	1
IRS-02	04 Jan 2004 – 09 Jan 2004	1
IRS-03	04 Feb 2004 – 08 Feb 2004	2
IRS-05	22 Mar 2004 – 28 Mar 2004	11
IRS-10	13 Jul 2004 – 18 Jul 2004	3
IRS-11	07 Aug 2004 – 11 Aug 2004	3
IRS-12	27 Aug 2004 – 02 Sep 2004	36
IRS-13	26 Sep 2004 – 04 Oct 2004	6
IRS-14	20 Oct 2004 – 26 Oct 2004	3
IRS-15	11 Nov 2004 – 17 Nov 2004	1
IRS-18	04 Feb 2005 – 18 Feb 2005	12
MIPS-19	25 Feb 2005 – 10 Mar 2005	4
IRS-19	11 Mar 2005 – 23 Mar 2005	12
IRS-20	14 Apr 2005 – 24 Apr 2005	10
IRS-23.2	08 Aug 2005 – 17 Aug 2005	6
IRS-24	06 Sep 2005 – 14 Sep 2005	56
IRS-29	04 Mar 2006 – 22 Mar 2006	10
IRS-30	16 Apr 2006 – 26 Apr 2006	7
TOTAL		184

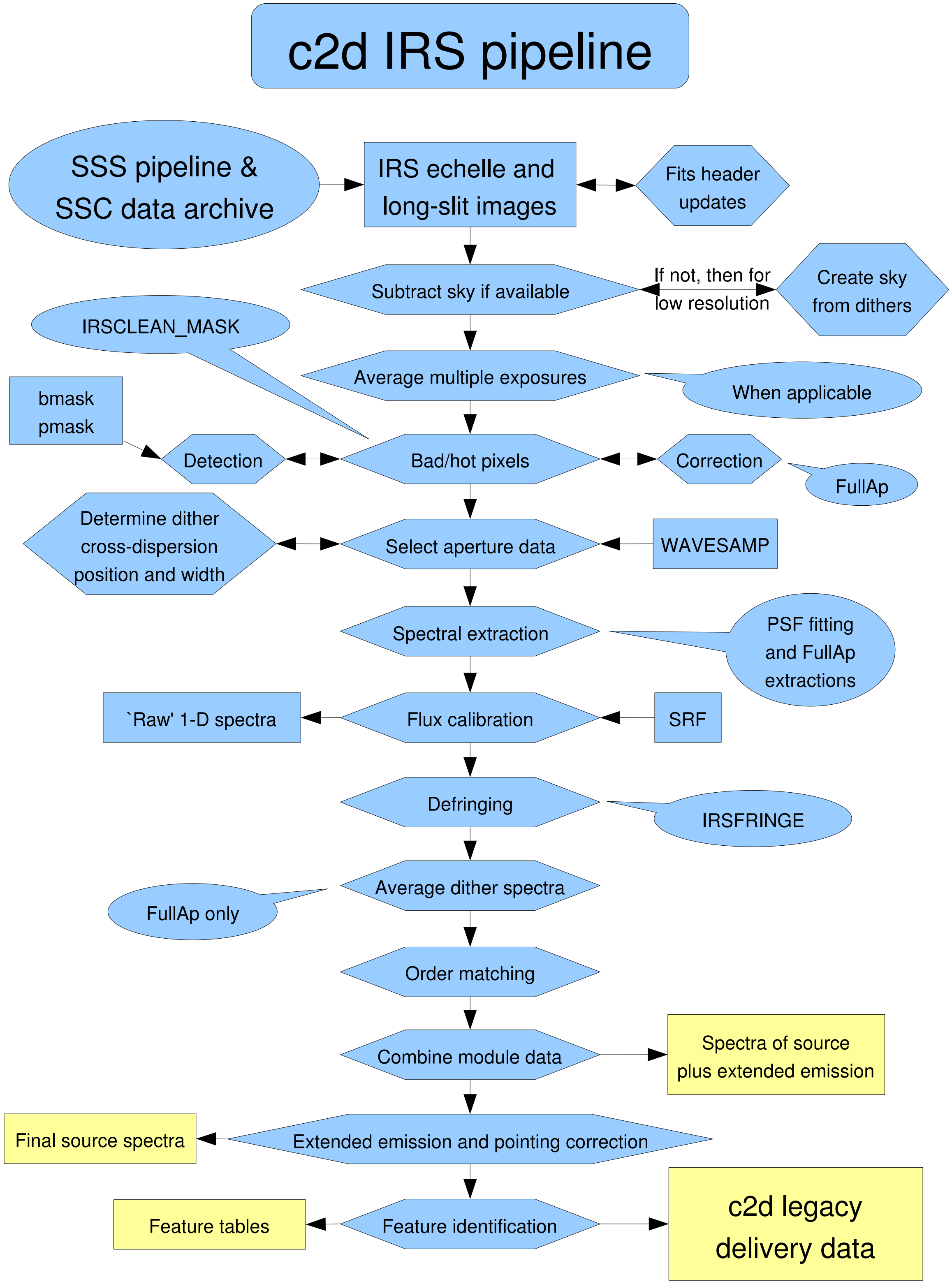

Fig. 1.— Schematic overview of the data reduction and legacy product generation for IRS staring mode observations in the c2d pipeline. Rectangles include data and products, polygons include tasks, and dialog baloons include descriptions. The products in the yellow boxes are part of the delivery. The reduction and products are described in detail in Sections 2 and 3.

2. Reduction of IRS pointed observations

The *Spitzer* archive products include Basic Calibrated Data (BCD; *_bcd.fits) files, which are two dimensional spectra that have been processed through the SSC pipeline, including saturation flagging, dark-current subtraction, linearity correction, cosmic ray correction, ramp integration, droop correction, stray light removal or crosstalk correction, and flat-field correction. The IRS reduction starts from the intermediate RSC products (*_rsc.fits), which have had the stray light removed (for SL) or cross-talk corrected (for SH,LH) but no flat-field applied. LL has no known stray light issues and therefore no corrections are made. In our reduction, 1-D spectra are extracted from the long-slit (SL,LL) and echelle (SH,LH) images using two extraction methods (see Section 2.2). The first is a full aperture extraction (Section 2.2.1) from images in which known bad/hot pixels have been corrected (see Section 2.1). The second is an optimal PSF extraction (Section 2.2.2) based on fitting an analytical cross dispersion point spread function plus extended emission (assumed to be uniform over the adopted extraction aperture) to all non bad/hot image pixels (see Section 2.1). The optimal PSF extraction uses an analytical fit to the good pixels only, and therefore bad/hot pixel correction is not required. The 1-D spectra for both extraction methods are flux calibrated using a spectral response function (SRF) derived from a suite of calibrator stars using Cohen templates and MARCS models provided by the *Spitzer* Science Center (Decin et al. 2004). After extraction, the 1-D spectra are corrected for instrumental fringe residuals (see Section 2.5) and, finally, an empirical order matching is applied (see Section 2.6). For all extracted spectra, a log file, overview plot and an IPAC spectral table are generated. In the log file a list of the strongest spectral features is given (see Section 3.6).

The c2d pipeline incorporates routines from OSIA,[1] IRSFRINGE,[2] SMART[3] (Higdon et al. 2004), and IRSCLEAN_MASK.[4] The pipeline also uses advanced reduction tools and calibration routines developed by the c2d and FEPS[5] legacy teams for full aperture extraction, optimal PSF extraction, automated product generation, and pointing correction (in development).

---

[1] OSIA is a joint development of the ISO–SWS consortium. Contributing institutes are SRON, MPE, KUL and the ESA Astrophysics Division. http://sws.ster.kuleuven.ac.be/osia/

[2] IRSFRINGE is developed for the *Spitzer* science community by the "Cores to Disks" c2d legacy team. IRSFRINGE has been integrated into SMART but is also available as a stand-alone package from http://ssc.spitzer.caltech.edu/postbcd/irsfringe.html

[3] http://ssc.spitzer.caltech.edu/postbcd/smart.html

[4] The IRSCLEAN_MASK software was developed by the IRS Instrument Support Team at SSC in conjunction with the Cornell IRS Science Center. It can be retrieved from http://ssc.spitzer.caltech.edu/archanaly/contributed/irsclean/

[5] See http://ssc.spitzer.caltech.edu/legacy/fepshistory.html for the FEPS Data Explanatory Supplement.

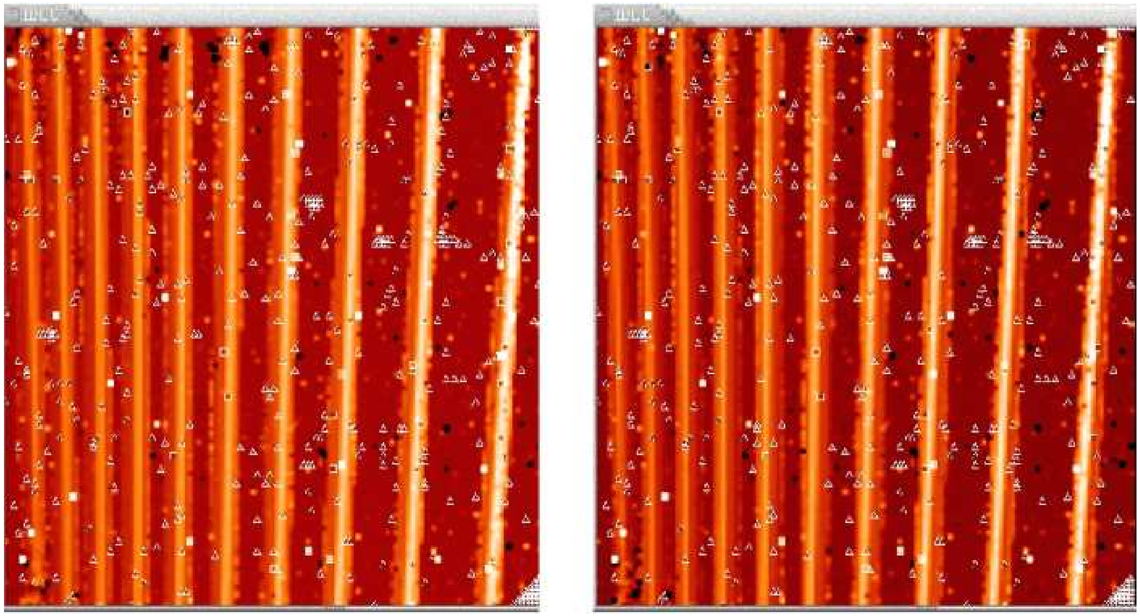

Fig. 2.— Two-dimensional BCDs of two dither positions in the LH module. Triangles and squares denote bad pixels, most of which are defined in the SSC bad pixel (‘`pmask and bmask`’) files.

2.1. Bad/Hot Pixels

The ‘`pmask.fits`’ and ‘`bmask.fits`’ files provided by the SSC contain masks for permanently bad IRS array pixels (‘hot’ pixels), pixels affected by cosmic rays or full saturation, and a number of pixels with long-term transients as a result of solar flares or cosmic ray hits. The SSC pipeline interpolates over ‘NaNs’ in the images and ignores pixels flagged as fatal in the raw SSC pipeline. See the IRS Data Handbook[6] for full details on the SSC IRS pipeline and extraction. In our reduction, an attempt is made to identify additional bad pixels in the optimal PSF extraction, and to correct all known bad pixels for the full aperture extraction.

The LH array is particularly affected by bad or hot pixels (see Figure 2). Although only $\lesssim 7\%$ of the pixels in LH are affected, collapsing the spectra along the spatial dimension of the slit during the extraction process results in $\sim$20% of the final spectral data points being affected. In reality, this number may be much larger, as the SSC mask files do not identify all transient, or ‘hot’ pixels, particularly at wavelengths $> 30\ \mu$m. Correction of the identified bad-pixels significantly improves the extracted spectra (Figure 3), but artifacts remain. In the SL, SH and LL modules the problem is much less severe but still requires attention as artifacts resulting from bad pixels can still be present.

[6]http://ssc.spitzer.caltech.edu/irs/dh/

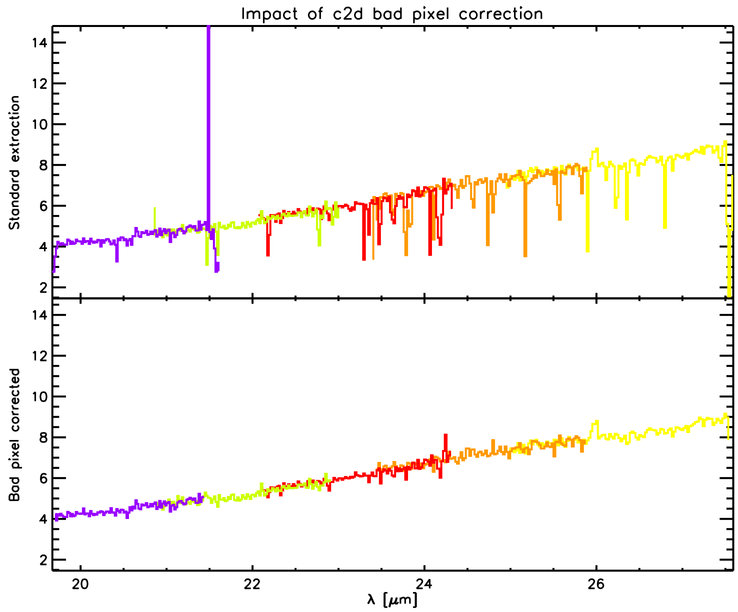

Fig. 3.— A demonstration of c2d bad pixel correction on part of the S11 IRS long high spectrum (color coded by order) of IRAS-08242-5050 (HH46). The upper panel shows the result of the standard extraction without full bad-pixel correction. The lower panel shows the result of the c2d full aperture extraction which includes a correction for hot and bad pixels. Not correcting for bad pixels clearly increases the risk of false feature identification, but also leads to the effective loss of a significant part of the spectral samples.

It is particularly important to identify as many bad pixels as possible which fall within the extraction window before the 2-D data are processed into 1-D spectra. These include the hot pixels identified by the `pmask.fits` files and bad pixels identified by the BCD pipeline that are included in the `bmask.fits` files. The latter includes pixels affected in the data acquisition and pixels for which the calibration or reduction in the BCD pipeline failed. Aside from the known bad/hot pixels, additional affected pixels are identified using the IRSCLEAN_MASK program provided by the *Spitzer* Science Center.[7] For a more detailed description of the SSC pipeline processing, see the IRS Data Handbook.

After identifying as many bad pixels as possible, the c2d pipeline interpolates over the bad pixels for the full aperture extraction and ignores the bad pixels for the optimal PSF extraction. Specifically, the bad pixel correction is done by interpolating over the bad pixels in the cross-dispersion direction for all apertures as defined by the `wavesamp` calibration file in the former case. The optimal PSF extraction profile is used as the interpolation function (see Section 2.2.2). Significant improvement in data quality for both the SH and LH modules is thus achieved. (See Figure 3 for the result of the c2d bad pixel correction on part of a LH spectrum).

[7] http://ssc.spitzer.caltech.edu/archanaly/contributed/irsclean/

2.2. Spectral Extraction

Once the bad/hot pixels have been corrected, the spectra are extracted using a full aperture or optimal PSF extraction. Prior to extraction, the c2d pipeline averages the RSC images of each dither position. For the full aperture extraction, 1-D spectra are extracted for each dither position, which are combined after correction for the spectral response function. For the optimal PSF extraction, both dither positions are combined and one single 1-D spectrum is extracted. This gives the best overall noise reduction and spectral stability, as is required for automated pipeline processing. Averaging before extraction also has the added benefit that missing pixels in one single image will be corrected for by good data in the other exposures.

2.2.1. full aperture extraction

The first method of extraction employed in the c2d pipeline for both the low resolution and high resolution modules is similar to that employed in the SSC pipeline. The main difference is that the c2d pipeline performs a fixed-width aperture extraction from RSC products and then corrects for a spectral response function (SRF), while the SSC pipeline performs a varying aperture extraction from flat-field corrected BCD products. For the low resolution modules, the c2d pipeline implements an extraction aperture with a fixed width in pixels over the whole order. The source position in the slit is determined and the extraction aperture is centered on the source. The width is sufficiently wide that 99% of the flux of a point-source falls within the window. For the high resolution modules, the full slit width is used in the extraction.

The spectra are extracted separately for each dither position and later averaged into one single spectrum, with weights inversely dependent on the error.

For low resolution staring observations, the dither positions are used for the sky correction. For the high resolution modules, a sky estimate for the full aperture extraction is derived using the optimal PSF extraction method.

2.2.2. optimal PSF extraction

Optimal extraction is performed on the combined RSC data after correcting for the cross dispersion offsets of the separate dither position images. The observed signal is assumed to be that of a point-source or slightly resolved source plus a uniform zero level (over the IRS extraction aperture). The zero level will in most cases represent the local extended emission close to the source, but it may also contain residuals of e.g., the raw pipeline dark current subtraction (see also Section 3.3).

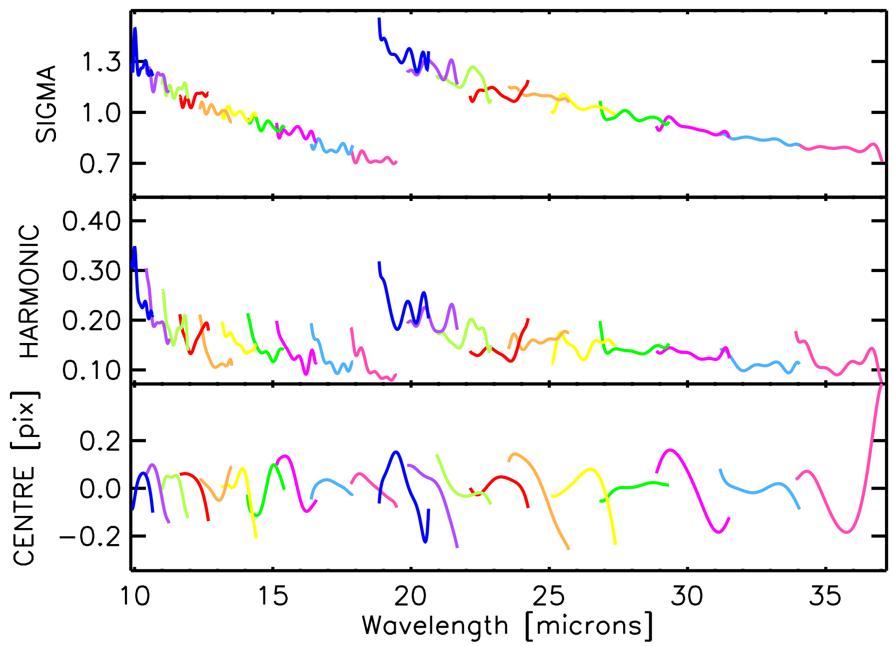

Fig. 4.— Parameters defining the IRS SH and LH cross dispersion profiles for unresolved sources. The variation with wavelength within each order is, for high signal to noise calibrators, consistently reproduced from observation to observation and assumed to be real. These most likely result from mechanical and optical defects in the instrument.

Sky corrected high signal-to-noise calibrator data are used to define the IRS point spread function (PSF) in the cross dispersion direction. From these the detailed profile characteristics, the width of the profile, the offsets with respect to the pre-orbit definition of the order-traces, and the amplitude of the harmonic distortions are retrieved.

The IRS cross dispersion profile is described by the analytical function S;

$$S(x,\lambda) = \mathrm{sinc}^2(\sigma(\lambda) \times (x - c(\lambda))) + a_H(\lambda) \times H1(\lambda) + a_H(\lambda)^2 \times H2(\lambda).$$

The sinc width σ relates to the $FWHM$ by $\sigma = e/(2 * FWHM)$, c is the location of the profile center, more specifically the offset of the observed profile with respect to the pre-orbit defined order-trace, $H1$ and $H2$ are the first and second even harmonics, and a_H the harmonic amplitude. The σ, c, and a_H wavelength dependence is shown in Figure 4. For the extended emission, the flat field cross-dispersion profile is used which has been derived by the *Spitzer* Science Center.

When applied to an individual observation, the cross dispersion offset of the trace and a scale factor for the width (for slightly extended sources) are determined from the collapsed order data (see Figure 5). Subsequently the 1-D spectra are extracted for all apertures defined in the IRS WAVESAMP files. The PSF profile is fit to the aperture data keeping all parameters, except the profile amplitude and the zero level, fixed. After the extraction, the 1-D spectrum is flux calibrated using the SRF described in Section 2.3.

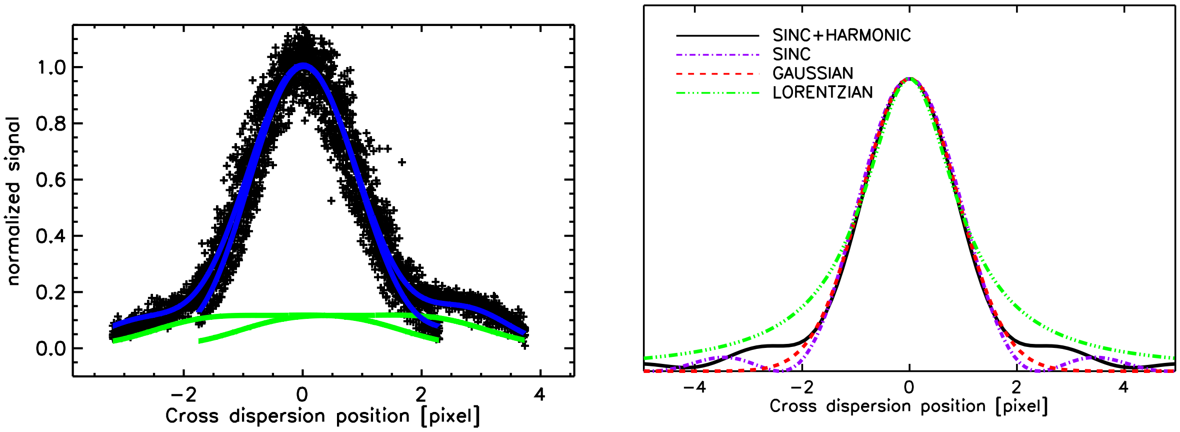

Fig. 5.— Example of the cross dispersion profile. The left plot shows a fit to the collapsed and cross-dispersion position corrected data (black pluses) from both dither positions of SH order 11 for GW Lup (see also Figure 8). The blue lines denote the source profile plus extended emission (green) for each dither position. The variations between the two dither positions reflect the flat-field profile of the zero level at the uncorrected slit position. The right plot shows a comparison of the IRS profile for a given width (σ) and harmonic amplitude compared to an undistorted sinc, a Gaussian, and a Lorentzian profile with the same FWHM. Note the significant variation in the strength and shape of the profile wings. The correct characterization of both the width and the wings of the profile is essential for extracting the proper source and sky spectra.

The advantages of PSF fitting are that it is less sensitive to bad data samples and unidentified bad pixels, that it gives an estimate of the data zero level and/or local sky contribution, and that it provides information on the extended nature of spectral features (see e.g. Geers et al. 2006).

The PSF fitting is sensitive to undersampling which can result in poorly defined continua. The short wavelength ends of the SH and LH modules suffer from this for some sources, but orders 2 and 3 of the SL and LL modules are most affected by undersampling. Therefore, we have chosen to include optimal extraction data only for the high resolution modules and for order 1 of the SL and LL modules. For the SL and LL order 2 and 3 data also no usable sky estimate can be obtained and these columns in the delivered IPAC tables contain zeros for these orders.

2.3. Spectral Response Function (SRF)

Both the full aperture extraction and the optimal PSF extraction are calibrated from standard stars observed within the regular *Spitzer* Calibration program (see Table 3). A set of Cohen templates and MARCS code model atmospheres (Decin et al. 2004) provided by the *Spitzer* Science Center[8] are used to derive the spectral response functions. The low resolution full aperture calibration

[8] http://ssc.spitzer.caltech.edu/irs/calib/templ/

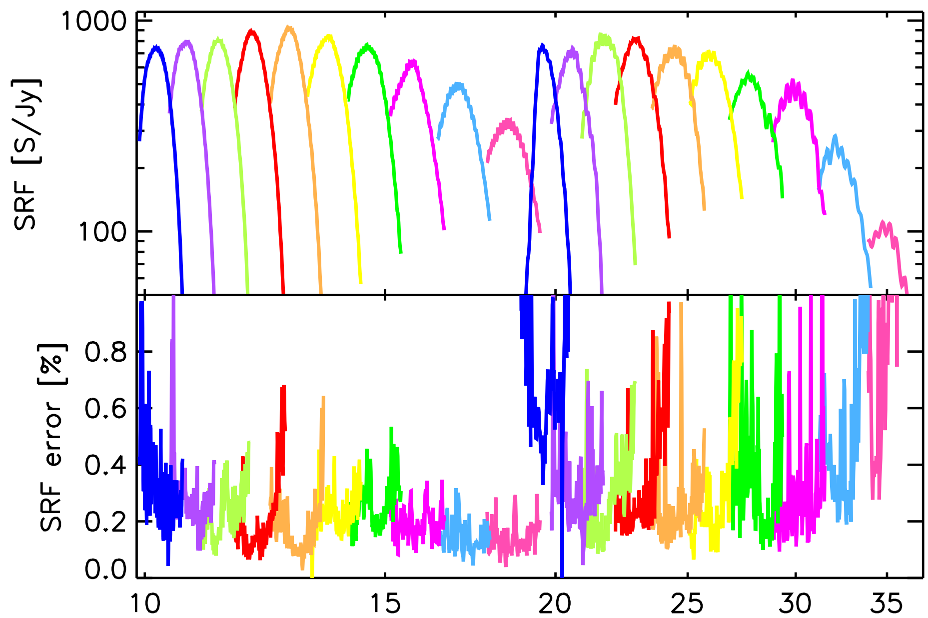

Fig. 6.— Spectral Response Function (SRF) for SH and LH for the optimal PSF extraction in units of S/Jy where S is the signal unit of the RSC echelle images. The orders are color coded, same for SH and LH. The SRF functions for the full aperture extraction show a similar profile and only change in detail and absolute level.

uses additional calibration refinements derived from a sample of stars observed within the FEPS legacy program. The low resolution full aperture calibration is discussed in detail in the FEPS Data Explanatory Supplement[9] and will therefore not be discussed in detail in this document.

Only standard stars observed with high accuracy pointing accompanied by dedicated sky observations are used to derive the spectral response function. Table 3 gives a list of all AORs included in the derivation. The same procedures used for the science extraction are used for the calibration, but the last stage of flux calibration is omitted. Despite the high accuracy pointing, small pointing errors will be present. To limit the impact of these on the final calibration, the observations are sorted by signal strength and the observations from the weakest quarter (assumed to be the sources with the most extreme pointing error) are excluded.

For the optimal PSF extraction, the derivation of the SRF and the PSF parameters are intimately coupled. The derivation is done in steps. In the first iteration, the PSF function is characterized and then, in the second iteration, this PSF function is used in the extraction of the 1-D spectra used to derive the SRFs.

Figure 6 shows the derived SRFs and errors for SH and LH modules. The SRF errors depict

[9] Available from the SSC FEPS legacy page http://ssc.spitzer.caltech.edu/legacy/fepshistory.html

the point-to-point uncertainty. Table 4 lists the average absolute flux calibration uncertainty per order and module for high precision pointing observations. The PSF definition is discussed in more detail in Section 2.2.2.

2.4. Error propagation

An error is assigned to each spectral data point during extraction. This error is propagated in each step of the pipeline and includes the relative spectral response uncertainty (Figure 6), the absolute flux calibration uncertainty for high precision pointing (Table 4), and, for the full aperture extraction, the deviation between the dither positions. The SSC S13 and S14 products do not contain fully propagated and usable errors and are not included. Full error propagation for the SSC pipeline is foreseen for S15. However, that is beyond the lifetime of the c2d legacy program.

The c2d extraction error is estimated from the residuals of the profile fit to the observed (source+sky) signal. The profile fitting is performed using the CURFIT routine provided by the OSIA package, which uses a non-linear least squares fit. The error is estimated from the fit residuals,

$$e_{\rm signal}(\lambda) = \sqrt{\frac{\sum_{i=1}^{\rm n}(signal(i) - fit(i))^2}{{\rm n}\times({\rm n}-1)}},$$

where $e_{\rm signal}(\lambda)$ is the estimated extraction error for a given wavelength λ. $signal(i)$ is the observed source+sky signal for a RSC image pixel, $fit(i)$ is the fitted PSF profile plus extended emission, and $\rm n$ the number of good pixels in the aperture for the given wavelength λ as defined in the SSC `wavesamp` calibration file.

After the extraction, the absolute flux calibration and the SRF are applied to the signal and sky estimate. Then the SRF error and the absolute flux calibration uncertainty are added to the extraction error;

$$e_{\rm flux}(\lambda) = \sqrt{e_{\rm signal}(\lambda)^2 + \frac{signal^2(\lambda) * (e^2_{SRF}(\lambda) + e^2_F(\lambda))}{SRF^2(\lambda)}}.$$

The absolute flux uncertainty is valid for observations obtained with high precision pointing. For observations obtained with lower accuracy peakup or no peakup, the absolute flux uncertainty will be larger, see Figure 12 and Section 3.4.

For the full aperture extraction both dither position are averaged using a weighted mean with $1/e^2_{\rm flux}(\lambda)$ as weights. At each wavelength the absolute difference of the flux in both dither positions is included in the final error.

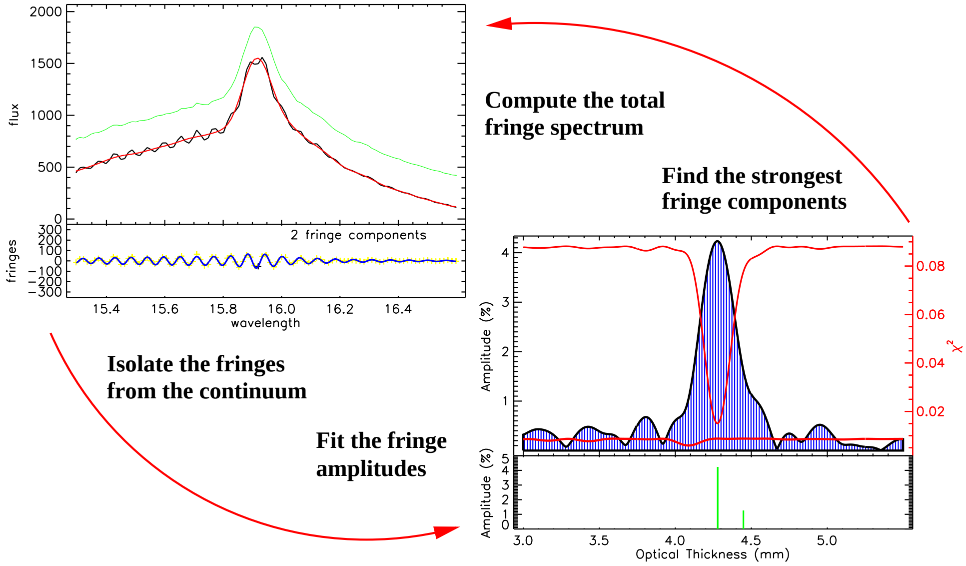

Fig. 7.— Defringing IRS spectra in practice. The left figure shows the original spectrum (black), with continuum (red). The final defringed spectrum is shown offset in green. In the lower panel, the continuum subtracted data (yellow) and the computed fringe spectrum (blue) are plotted. In the right figure, the derived fringe amplitude (blue) and the effective decrease in chi-squared (red) are plotted for the selected range of optical thickness. In the lower panel, the selected fringe components are shown (green).

2.5. Defringing

After extraction and flux calibration, the high resolution (SH and LH) and the LL order 1 spectra are defringed using the IRSFRINGE package developed by the c2d team. The IRSFRINGE documentation and software can be downloaded from the *Spitzer* Post-BCD website.[10] Also see Lahuis & Boogert (2003) for an introduction to IRS defringing.

Fringes originate on plane-parallel surfaces in the light path of the instrument. These surfaces act as Fabry-Pérot etalons, each of which can add unique fringe components to the source signal. The major components in SH and LH originate from the detector substrates. The LL1 fringes are believed to be the result of a filter de-lamination discovered prior to launch. The SL data and LL2 data do not contain any identified fringe residuals.

The fringes observed in the final spectra are residuals of the observed fringes after flux calibration. The observed fringe spectrum is modified during calibration due to wavelength shifts resulting from pointing offsets or a complex source morphology within the slit. No application of a response function (be it the SRFs used in the c2d extractions or the flat field in the SSC BCD

[10] http://ssc.spitzer.caltech.edu/postbcd/irsfringe.html

extraction) will therefore fully correct for these effects and small residual fringes will be present in most spectra. The amplitudes of the fringe residuals can be up to ∼5% and depend on source morphology, pointing, order, and wavelength.

IRSFRINGE uses a fringe model based on robust sine-wave fitting to remove fringe-residuals from the spectra. Figure 7 gives an illustration on how the defringing works (see also Lahuis & Boogert 2003). To avoid overfitting, a conservative signal-to-noise cutoff is used in the defringing. This means that residual fringing can still be present in the delivered data and for specific science applications manual defringing may be required on all or part of the spectra.

The c2d IPAC data tables can be read into IRSFRINGE using the IPAC2IRS routine in the current versions of IRSFRINGE or SMART

```
AAR = IPAC2IRS('MY_PET_SOURCE.TBL').
```

This command creates an IDL data structure with tags with names and contents that are identical to the columns of the IPAC table, plus an additional (empty) tag called FLUX. IRSFRINGE operates on the data in the FLUX tag. Before defringing, one has to copy the appropriate data into this tag, e.g.,

```
AAR.DATA.FLUX = AAR.DATA.FULLAP.
```

Then the data in the FLUX tag can be defringed, and the new FLUX data copied back into the proper column in the IPAC table as follows,

```
AAR = IRSFRINGE(AAR,NFRINGES=2)
AAR.DATA.FULLAP = AAR.DATA.FLUX
IRS2IPAC,AAR,'MY_PET_SOURCE_DEFR.TBL'.
```

See the documentation accompanying IRSFRINGE for more details on the defringing process and the options available in IRSFRINGE.

2.6. Order Matching

In order to produce cleaner spectra for the SH and LH modules, orders within each module are scaled in flux such that consecutive overlapping orders are matched. For SL and LL this is not done as order mismatches for these modules can be useful for assessing pointing errors.

First, a reference wavelength and flux are determined from the data of both overlapping orders in each overlap area. The weighted order wavelength and flux is then determined separately for both sides of each order and each order is corrected using a first order polynomial. For the first and the last order, only a single weighted wavelength and flux is calculated and a zero order correction is applied. The correction is made by scaling the flux of the order, unless the correction slope becomes negative within the order wavelength range, in which case the correction is made by adding/subtracting a flux offset.

To enable an evaluation of the consistency of the spectral slope in the inter-order regions, order clipping is not applied. For example, a slope discontinuity may be a signature that features have been introduced after order matching due to order tilts. This and other spectral artifacts will be discussed in detail in Section 3.5.

3. Data Products of IRS pointed observations

For all pointed IRS observations three products are generated:

1. A spectrum for each IRS target as an IPAC table.
2. Two PostScript files for each delivered spectrum.

    a PostScript file with the integrated spectrum and extended emission estimates.

    a PostScript file with the optimized source spectrum, see Section 3.4.

3. A log file describing each observation (see Appendix A for an example).

Table 2 gives a complete overview of all observations. For some sources multiple observations exist, and these are delivered as separate products. The following subsections describe the data products and how they can be used.

3.1. IRS c2d Products

The IRS pipeline, calibration, and extraction procedures remain in a state of constant development. As a result, the most optimum end-to-end reduction for any observation depends on various parameters that are currently not yet fully understood. In any extracted spectrum, artifacts will be present at some level. Therefore, we employ a number of extraction methods in our reduction pipeline and deliver two spectra for each source.

The c2d observations consist primarily of single staring-mode observations. Since the majority of the sources lie in complex star forming regions, no individual sky observations were taken. For this reason, none of the spectra have been corrected using direct measurements of the local sky. An estimate of the local sky contribution (as estimated in the c2d optimal PSF extraction, see Section 2.2) is therefore calculated and included in the delivered products. Also a best estimate source spectrum with extended emission and pointing corrections applied is included (see Section 3.4). An example is given in Figure 8.

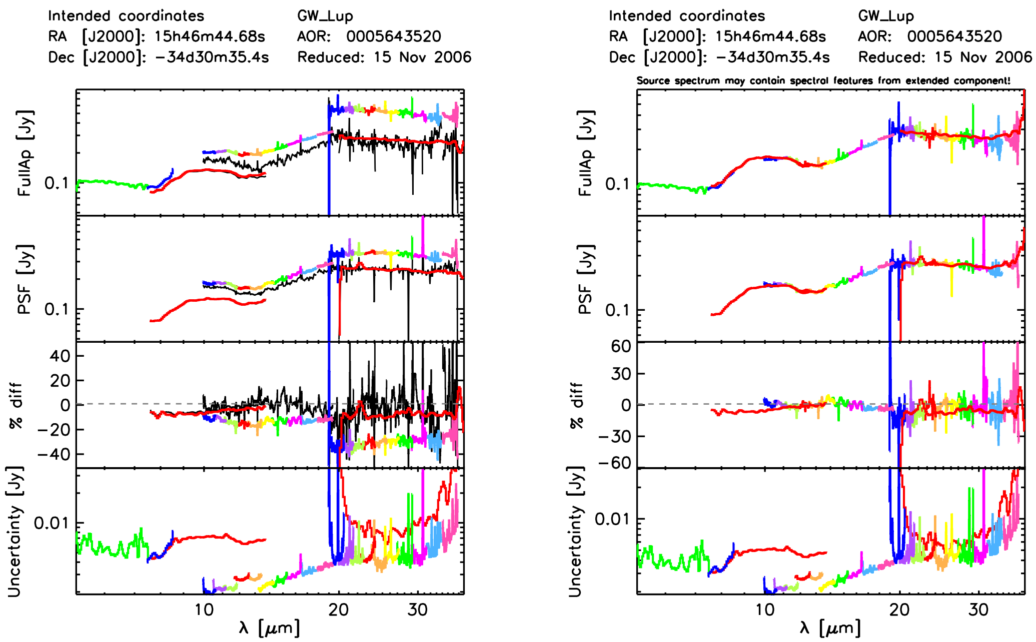

Fig. 8.— PostScript plots provided with the delivered spectra. Left: the extracted IRS spectra (SL: green, blue, red; LL: red; SH and LH: various colors for each order) and estimates of the extended emission subtracted from the spectra (in black) for all modules. Right: the final optimized source spectrum with an SED correction for the extended emission and a pointing correction the correct for module discontinuities. Shown from top to bottom are, (i) the full aperture extraction, (ii) the PSF extraction, (iii) the relative difference between Fullap and PSF, and (iv) the propagated errors. This source illustrates two issues with IRS spectral data: extended emission and pointing errors. The observed spectra show a strong offset of LH with respect to SH and LL, and of SH with respect to SL. After correcting for extended emission in SH and LH, both match. The discontinuity between SL1 and SL2 and SL1 and SH indicate a pointing error for SL; this is corrected for in the right plot (see Section 3.4). Note that the final optimized spectra may still contain artifacts, see Section 3.5 for more details and examples.

The products delivered to the SSC include an IPAC format ASCII table that contains the combined 1-D spectra extracted from all observed modules and log files that briefly describe each observation. Included in the log file is a list of the most prominent spectral features (see Section 3.6). For a first impression, a PostScript plot of the combined spectrum has been generated for each target.

The IPAC tables can easily be read into an IDL data structure within IRSFRINGE or SMART using the command

STRUCT = IPAC2IRS('YOUR_FAVOURITE_SOURCE.TBL').

The log files include a summary of the source nomenclature and coordinates along with the observation date, mode, and integration times, basic source parameters and identified spectral features. Appendix A gives an example of one of the log files.

The PostScript plots give a quicklook overview of the spectra contained in the data files. Figure 8 shows an example of the two plots delivered for each observation.

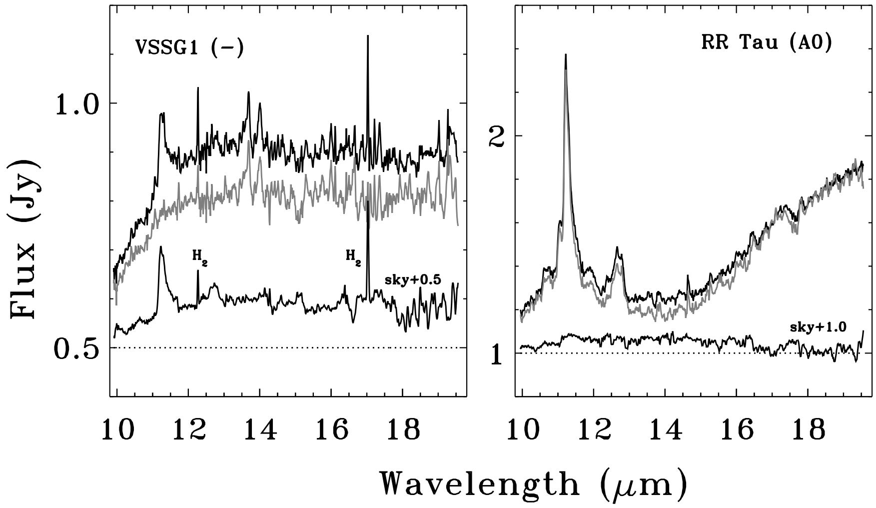

Fig. 9.— Using the estimate of the local extended emission in the study of PAH spectral features. Shown is the observed spectra and estimated sky emission (offset for clarity) in black and the sky corrected spectrum in gray. Toward VSSG1, all PAH emission is extended and no PAH intrinsic to the source is observed. Toward RR Tau, all PAH emission is local to the source without confusion by extended emission in the IRS aperture. (Geers et al. 2006).

3.2. Source parameters

Basic source characteristics, including the source size (after correction for the PSF size) and location within the slit, are determined within the PSF extraction. These are listed in the log file.

The source size is determined from the width of the PSF function fitted to the source compared to the width of the PSF function fit to standard calibrator stars. A source size of zero implies the source is not extended to the Spitzer-IRS instrument. For staring observations, cross-dispersion positions for both dither positions are determined for all modules. The offset listed in the log file is the offset with respect to the average cross-dispersion positions for the sample of standard stars which have been observed with high accuracy peak-up. The cross dispersion offsets can be used as a first order estimate of the dispersion offset, and thereby the flux loss, of the orthogonal slits. This means the LH cross dispersion offset gives an estimate for the SH dispersion offset and vice versa. The same applies to the SL and LL modules.

3.3. Extended emission

The optimal PSF extraction and the full aperture extraction for the SL1, LL1, SH, and LH modules provide a direct measure of the amplitude of the zero level of the spectrum. This zero level is a combination of extended emission in the direct vicinity of the source, be it sky or envelope emission, and residuals of, e.g., the dark current subtraction in the SSC pipeline. For the full

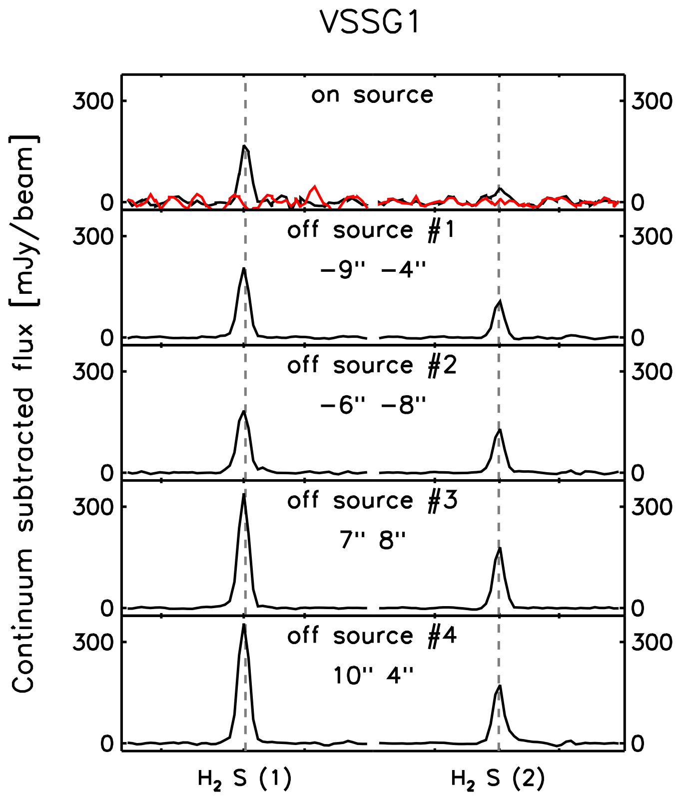

Fig. 10.— Example of line emission of molecular hydrogen toward VSSG 1. Plotted in red in the top panel is the emission toward the source corrected for the estimated extended component. Plotted in black in all panels is the extended emission toward the source and four off positions. This illustrates the problem of detecting unresolved emission toward young stars; the extended emission is often significantly stronger than the unresolved source component and can vary with position. In this example, no compact on-source emission has been detected.

aperture extraction, the extended emission is estimated from the PSF extraction scaled to the full aperture size. Though for SL1 and LL1 a sky correction derived from the other dither position is applied, extended emission can still be present, e.g. as a result of incorrect straylight correction for SL1 or because the extended sky emission varies strongly over the grid.

The flux values delivered in the c2d products contain the signal of the source plus the extended emission. For the full aperture extraction the flux is in units of Jy/Aperture and for the PSF extraction it is in Jy/beam. Thus, for a point source without extended emission, this flux is in Jy.

It is possible to spot extended spectral features in the spectra in two ways. The first one is to directly subtract the estimated extended emission of the observed spectrum, see Figures 9 and 10 for examples. The second way is to compare the peak strength of the feature. For extended features, the peak strength in the full aperture extraction will be stronger than in the PSF extraction reflecting the difference in aperture ($\sim 10-12\,\mathrm{pixel}^2$) versus beam ($\sim 3-5\,\mathrm{pixel}^2$), see e.g. the H_2 S(1) emission line presented in Figure 13.

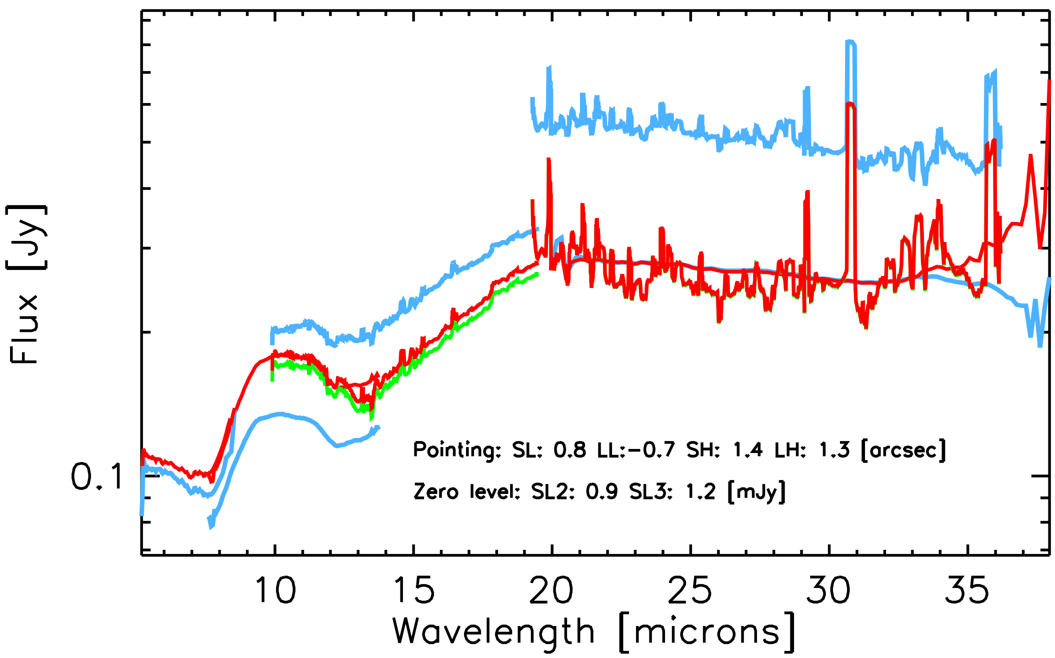

Fig. 11.— Producing a final spectrum for a source that has both extended emission and a pointing offset (GW Lup). In blue the observed signal (Fullap), in green the signal of SH and LH corrected for extended emission, and in red the final spectrum (see Section 3.4 for details). Note that green and red for LH are on top of each other. The optimum pointing offsets and zero level corrections are printed below the spectrum. Note that the final spectra often still contain artifacts, in particular the LH module, see Section 3.5 for more details and examples. The pointing correction was done using a β-version of the pointing fluxloss calibration and software, a collaborative effort of the c2d and FEPS legacy teams.

The estimate of the extended emission is, by nature of the fitting process, inherently more noisy and uncertain than the total signal. Therefore, care should be taken when correcting for the extended emission. When used for SED analysis or the study of resolved features, a smoothed version of the extended emission spectrum can be used (e.g., see studies of extended PAH emission by Geers et al. (2006) and the example in Figure 9). When analyzing unresolved features (e.g., studies of H_2 emission lines by Lahuis (in preparation) and the example in Figure 10), a direct subtraction of the extended emission or a correction of a Gaussian line fit to the extended emission is required to obtain the unresolved source component.

3.4. Final source spectrum

In order to provide the most useful products, that reflect more closely the on-source emission, additional corrections are applied to the results of the Fullap and PSF extractions (see Figures 11 and 8 for an example). First for SL1, LL1, SH, and LH the estimated extended emission com-

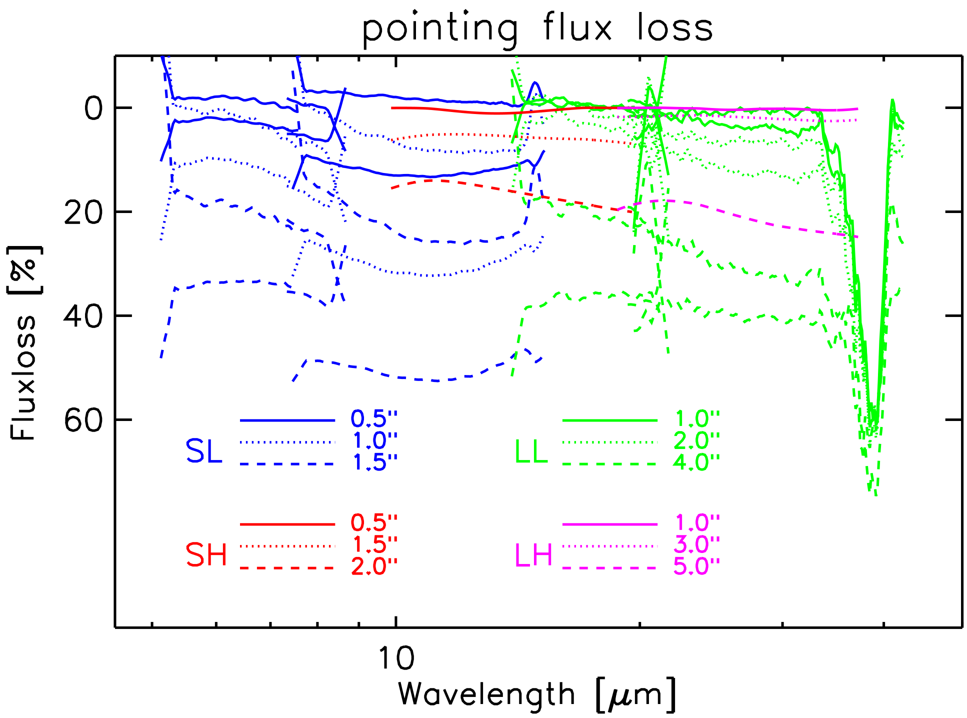

Fig. 12.— Fluxloss as a result of pointing errors. The SL and LL fluxloss functions have been derived from multiple mapping observations of standard stars, the SH and LH fluxloss functions are derived from the optimal extraction cross dispersion PSF assuming a spherical PSF. Empirical fluxloss functions for SH and LH will have to be derived at a later date. For SL and LL it should be noted that the PSF is not centered on the slit. Therefore, for SL and LL, two curves for each offset value are given, for a positive and a negative pointing error. The characterization of the pointing fluxloss is a collaborative effort of the c2d and FEPS legacy teams.

ponent (see Section 3.3) is subtracted. After this, pointing errors are corrected based on optimal module matching. The optimization is done by minimizing the difference between the modules over the complete overlap range to maximally exploit the strong wavelength dependence of the fluxloss functions (see Figure 12). The module overlap regions of SL2/SL1, SL1/SH, SH/LH, LL2/LL1, and LL/SH+LH are used.

Since the extended emission estimates inherently contain more noise and artifacts than the complete (source+extended emission) spectrum, a smoothed version over the complete module wavelength range is subtracted from the observed spectrum. The extended emission estimates are smoothed with a broad median filter and then fit with a low order polynomial (4th order for low resolution and 6th order for high resolution). To suppress edge effects the spectra are padded on both wavelength ends. For the low resolution modules, an extended emission correction is applied during extraction. Residual extended emission can still be present as a result of, e.g., a varying local sky, SL straylight residuals, or dark current residuals. For SL1 and LL1, the ex-

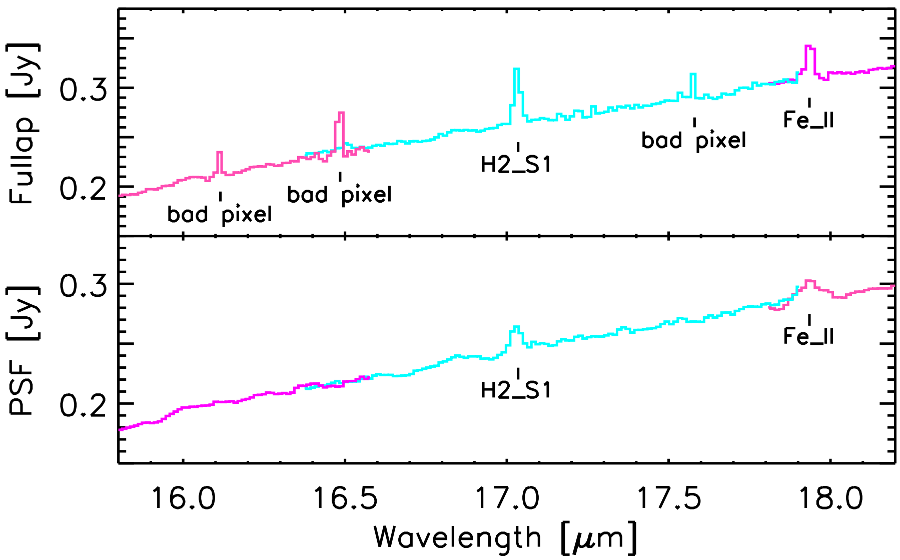

Fig. 13.— Example of a source spectrum (Sz 102) with bad pixels and gas-phase features. In this region of the spectrum, there are clearly identified bad pixels (near 16.1 and 17.6 μm), one multi-pixel spike near 16.5 μm, and strong multi-pixel gas phase lines (H2_S1 at 17.04 μm and Fe_II at 17.9 μm). Comparing the two spectra helps to identify the bad pixels. Note the difference in the strength of the H_2 S(1) between the extractions as a result of the line emission being extended while the continuum emission comes from the unresolved source.

tended emission estimate is used for the correction, but this is not usable for SL and LL order 2 and 3. Instead, for these orders, an additional zero level correction is included in the module optimization.

If for a particular module *no* unresolved (or slightly extended) source component could be identified during extraction, then the final source spectrum is set to zero for that module. For example, an extremely blue or extremely red object may have no detectable source signal in only the long or short wavelength modules, respectively. If the source is fully extended in all modules, then the source spectrum contains the original spectrum without correction.

The pointing offsets (in arcseconds) and zero level offsets (in Jy) required to optimally match the modules in the spectra are listed in the IPAC table header. The pointing offset estimates are listed using the keywords SLPE_PSF (pointing offset for PSF spectrum), SLPE_SRF (pointing offset for FullAp spectrum) and similar for the other modules. The SL and LL zero level offsets are included in the header using SL2Z_PSF (SL order 2 zero level for PSF spectrum), and similar for order 3, the FullAp extraction (_SRF), and the LL modules.

It should be noted that since only a smoothed low resolution correction for the extended emission is applied, spectral features, such as H_2 emission lines and PAH emission bands, arising from extended emission components are not removed from the final spectra. If extended spectral features are present, then a careful examination of the original spectrum and estimated extended emission

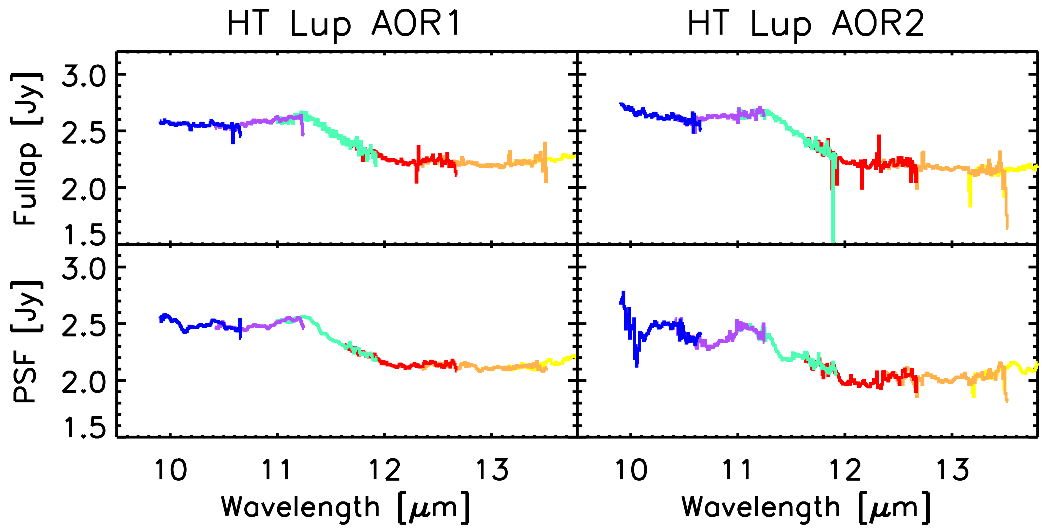

Fig. 14.— Extracted spectra for HT Lup AOR1 (IRS staring mode, left) and AOR2 (IRS mapping mode, right) are shown. The differences in the shapes of the lowest wavelength SH orders (where the spatial sampling to which the PSF extraction is sensitive becomes critical) between the extractions exemplifies order curvature type artifacts. The AOR2 spectrum shows that the PSF extraction becomes less reliable when used for the spectral extraction from single map pointings as a result of the narrower cross dispersion baseline compared to wider baseline in the combined two dither positions for the staring observation. Note that due to the order curvature artifacts, the user must be careful when interpreting the shape of the amorphous silicate 10 μm feature and/or the identification of crystalline forsterite or PAH features (both near 11.3 μm). In the case of HT Lup, we are fortunate to have 2 different observations to compare, in most cases, one must use the error estimates and comparisons of PSF vs. Fullap extractions to determine whether order curvature is a factor.

(see Section 3.3) is required in order to use the spectra for science analysis.

3.5. IRS Artifacts

As noted above, the c2d correction of bad/hot pixels, as well as pixels flagged in the BCD pipeline, greatly improves the final S/N ratio of the spectra. This does not mean, however, that the spectra are free of artifacts. The inclusion of spectra extracted using two different extraction techniques can be used to recognize the presence of some artifacts, but this is not guaranteed to be foolproof. Artifacts, both resolved and unresolved, can be present in the delivered spectra and great care should be taken when interpreting any "features."

Therefore, we will now discuss various types of artifacts that we have found to be present in the c2d spectra. This list is not meant to be all-inclusive, but should be viewed as examples of the types of artifacts that are most common. These artifacts may arise from a variety of factors.

Narrow (1–2 pixel wide) spikes in the spectrum can often be associated with 'hot' or bad pixels that were not identified and corrected using the interpolation routines (see Section 2.1 and Figures 2 and 3). As discussed above, these artifacts are most prominent in the LH spectra, but they also appear in the LL, SH, and, occasionally, SL modules. The PSF and Fullap extractions use different methods to correct for bad pixels; for the Fullap method, the pipeline finds and interpolates bad pixels prior to extraction and the PSF method only includes pixels identified as "good" in the extraction. Therefore, comparing the resulting spectra from the two extractions can often help to identify bad pixels (see Figure 13), as they may appear in only one spectrum. Additionally, true gas-phase lines will usually be a bit broader (2-3 pixels wide) than spikes due to bad pixels, but it is often difficult to distinguish real emission and (1–2 pixel wide) spikes should always be treated with caution.

Artifacts located at the edges of orders may be present due to "order curvature," "order tilt," or "bad order matching" (that is, there can sometimes be large differences in flux or spectral shape between successive orders). Such problems often arise when the source is not centered in the slit. The PSF correction applied to both full slit and source profile fitting extractions has reduced the frequency and severity of these types of artifacts, but they are still often present, and are particularly common in cases with large pointing offsets. Order curvature often results in "V" shaped dips or increases in the flux of the spectrum at the intersection of two orders. These can easily be misinterpreted as solid-state emission or absorption features (See Figure 14). Order tilt in successive orders, if corrected by scaling the orders to match in the overlap regions, can result in an increase in the continuum slope in the affected spectral region. If left uncorrected, order tilts or bad order matches result in sharp jumps in the spectrum in the order overlap region. In most cases, one must use the error estimates and comparisons of PSF vs. Fullap extractions to determine whether order curvature is an artifact. If the log file indicates that there is a pointing offset, order artifacts will likely be corrected in the final pointing corrected source spectrum.

Additionally, there may be significant differences in the flux of consecutive modules (see Figure 11). This is particularly true in the overlap between high resolution and low resolution modules, particularly for the full slit extraction, due to differing contributions from background flux. Pointing offsets will also result in flux differences between modules, as the module slits are oriented perpendicular to one another. Again, if these issues are due to pointing offsets, then they should be corrected in the final source spectrum.

3.6. Spectral features

To provide a quick assessment of the nature of the observed sources, an automated feature identification, restricted to the most prominent features, is included in the c2d pipeline. The identified features for each source are listed in the log files (Appendix A) and complete lists of features found in all sources are presented in Tables 7–8. Also included in Table 8 are the integrated

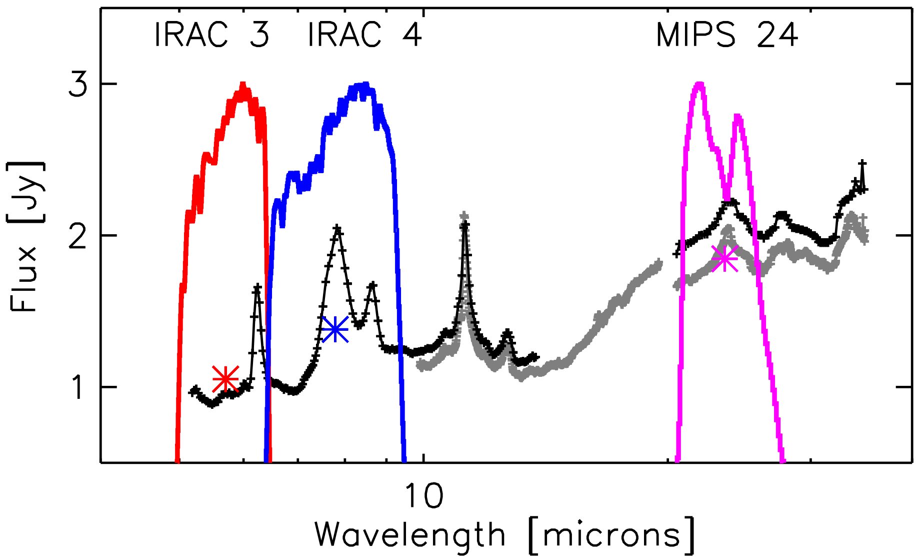

Fig. 15.— The observed Spitzer-IRS spectrum of RR_Tau and the IRAC 3, IRAC 4, and MIPS 24 filter profiles used to derive the continuum values listed in Table 8 and plotted here with asterisk symbols. In grey are the SH and LH spectra and in black the SL and LL spectra.

fluxes of the IRS spectra over the IRAC 3, IRAC 4, and MIPS 24 photometric bands using the instrumental filter profiles (see Figure 15 for an example). The feature tables have been checked by eye by c2d team members and comments (about suspect features, etc.) are noted in the logs. Given the complexity of the data and the observed features (e.g., the presence of extended emission and pointing uncertainties), no feature strengths or optical depths are derived. To do so requires more sophisticated fitting procedures.

In order to reduce the mis-identification of features the extended emission and pointing corrected spectra (see Section 3.4) are used as input for the feature identification. Remaining offsets between consecutive modules are corrected such that the overlapping regions match in flux. The modules are matched pairwise, SL1 to SH, SL2 to SL1, LH to SH, and LL to combined data from SH and LH. This additional module matching is only done to facilitate the feature ID process. As mentioned in Section 3.5, the difference in flux between modules is likely due to differences in background emission and/or pointing offsets. Simply scaling the modules may not be the correct approach for determining the strength or composition of features, but is acceptable for determining the *presence* of the strongest, most easily identified features, as done here.

Table 6 lists the feature information and constraints used by the feature identification script. The wavelength (λ) and FWHM are used to initialize the fit parameters of the feature profile and are allowed to vary within a limited range ($\sim$0.3$\times$FWHM). The continuum points define two regions on either side of the feature, one on the short wavelength side (between wavelengths cont 1a and cont 1b) and one on the long wavelength side (between cont 2a and cont 2b). These continuum regions are used to make an initial estimate of the continuum parameters. After parameter initialization, a Gaussian profile and a 2nd order polynomial is fitted to the data between cont 1a and cont 2b. When two values are listed for λ and FWHM in Table 6, a two component Gaussian fit is made. This is the case for overlapping features, e.g., ICE_6 and PAH_7_8, and for features with shapes that are non-Gaussian and require a multiple component fit, e.g, for CO_2, SiO_s, and SiO_b. Though a simple two-component fit is insufficient to accurately reproduce the shape of the latter bands, it is sufficient to establish their presence or absence.

A number of gas-phase emission lines are searched for by the feature identification program. This includes all molecular hydrogen lines in the IRS range, from H_2 S(0) to H_2 S(7), and a number of atomic forbidden lines. As these lines are expected to be unresolved, the FWHM is set to the instrument resolution and wavelengths to determine the continuum are set to the following, cont 1a=-4×FWHM, cont 1b=-1.5×FWHM, cont 2a=1.5×FWHM, and cont 2b=4×FWHM. For all lines, a Gaussian profile with a center position and a width are fit to within 25% of the instrument resolution. A larger offset in the center position is not acceptable considering the accuracy of the IRS wavelength calibration.

The most prominent features from polycyclic aromatic hydrocarbons (PAHs), near 6.2, 7.7, 8.6, 11.3 and 12.7 μm, are included in the c2d feature identification. The 6.2 and 12.7 μm features are fairly isolated, but the 7.5 and 8.6 μm features overlap with each other and the 11.3 μm feature overlaps with the broad 9.8 μm silicate feature. For this reason, the feature ID program groups the 7.5 and 8.6 features together as "PAH_7_8," fitting a profile that is the combination of two Gaussian profiles. The feature fit for the 11.3 μm feature uses the underlying silicate feature as the "continuum" looking for a narrow feature with a width of $<$0.2 μm. PAH features, when identified, are subtracted from the spectrum before silicate features are fit.

The c2d feature identification program searches for the most prominent silicate features, which are broad amorphous olivine/pyroxene Si-O stretching and O-Si-O bending modes, in emission or absorption, at 9.8 and 18 μm (labeled "SiO_s" and "SiO_b"), and a crystalline silicate (forsterite/enstatite) lattice mode emission feature at 33–35 μm ("SiO_l"). There are several crystalline silicate emission features overlapping with the broad amorphous features, but the exact wavelengths of these features are dependent on the grain size and composition (Kessler-Silacci et al. 2006). They are difficult to be reliably identified in this automated method and are therefore not included. The one exception is a crystalline forsterite feature near 11.3 μm, which often can be distinguished from the 9.8 μm amorphous feature. However, this feature overlaps with the narrow 11.3 μm PAH feature, but appears to be broader in sources with verified crystalline silicates. For this reason, in cases where a feature can be identified near 11.3 μm, but the feature is broader (width $\sim$0.6 μm) than typically seen for PAH, we label it as "Em_11.3." In some cases, identification of Em_11.3 could be due to an SiO_s feature with a flattened shape, possibly indicative of grain growth. Detailed compositional modeling of the spectra are required to determine if this feature is due to PAH or forsterite emission. The identification of the broad amorphous SiO_s and

SiO_b features can sometimes be confused by the presence of strong, narrow crystalline silicate emission features. In addition, for a number of observations, SL order 1 data is not available, thus cutting off a significant part of the SiO_s feature. In some cases, such issues can lead to a non-detection, false detection, or the mis-classification of the nature of the features.

There are several ice absorption features, but the c2d feature identification includes only the most prominent: the CO_2 feature near 15.1 μm and two overlapping ice features near 6.0 and 6.85 μm (combined as "ICE_6").

Several features in the spectra are blended with other features, e.g. H_2 emission lines on top of the ICE_6 band, PAH 11.3 μm emission on top of a Si-O stretching mode band, and CO_2 absorption on the very broad Si-O bending mode profile. For this reason, a feature is removed from the spectrum (only for the purposes of feature identification) after it has been positively identified.

Complete lists of features identified in the observed spectra are presented in Tables 7–8. Table 7 lists the detection status for all gas phase molecular hydrogen and atomic lines and Table 8 lists the detection status for all solid-state features, including features from PAHs, ices, and silicates. Also listed, in the last 3 columns of Table 8, are the spectral fluxes integrated over the IRAC 3, IRAC 4, and MIPS 24 photometric bands. In both Tables 7 and 8, a check mark (✓) denotes that the feature has been detected at $> 5\sigma$, averaged for both the full slit and source profile fitting extractions, and at least 3σ in both extractions. For the 9.8 and 18 μm silicate bands, "✓(A)" and "✓(E)" denote that the feature was detected in absorption or emission, respectively. A question mark (?) denotes that the feature has been detected at 3–5σ, averaged for both the full slit and source profile fitting extractions. Dashes ("-") indicate non-detections. These tables can be used to get an overview of the most prominent features in each spectrum, but should not be considered as a complete or definitive inventory. In the case of extended emission, for example, the PSF extraction will show a much weaker feature than the full aperture extraction, and thus the feature may not meet the above criteria. In cases where the feature identifications made by the automated routine are determined by visual inspection to be incorrect or questionable, a note will be made in the log file and in the tables, but the feature will still be listed in the log file and in Tables 7–8.

It should also be noted that many of the observed emission lines and several PAH features have shown to result from extended emission close to the source (Section 3.3). Therefore, the features identified in the spectrum and attributed to a particular target in Tables 7–8 may not be due to on-source emission. For a number of these extended emission lines (Lahuis, in prep.) and PAH features (Geers et al. 2006) no source emission or only a (weak) source component is found by carefully using the sky estimate derived from the optimal PSF extraction.

4. c2d IRS maps

Within the first-look program, a few sources (HT Lup and HD 163296) were observed with the IRS mapping mode and with the IRS staring mode for comparison. As part of the second-look program, IRS mini-maps of extended gas-phase and PAH emission were taken around point source targets that showed evidence of emission in the first-look observations. In addition, IRS spectral maps of the south-eastern Serpens molecular core and the Barnard 1 outflow were obtained. All IRS mapping mode observations are labeled with AOT_mode "irsmap" in Table 2. Note that the map of the Serpens core was split up into two AORs, named SerpensCoreNW_1 and SerpensCoreNW_2.

The IRS mini-maps taken to look for extended gas-phase and PAH emission were observed with the short-high 9.9–19.6 μm module, which includes the PAH 11.3 μm emission feature and the H_2 S(1), H_2 S(2), Ne II, Ne III, Fe II, and S III gas-phase lines.

IRS spectral mapping of the B1 outflow was also performed with the SH module, primarily to map the H_2 emission. The central position of the map is RA = 3 33 17.4, DEC = +31 09 36.0 [J2000]. A grid of 36 by 2 pointings was used, with step sizes of $4.0''$ and $10''$ parallel and perpendicular to the slit, respectively. The observed area is 151.3×14.7 square arcseconds. Each position was observed once with a ramp time of $\sim$31.46 seconds.

The IRS mapping observations of the south-eastern part of the Serpens core have been carried out in the long-low (LL) and the short-low (SL) modules, covering a spectral region of 5.2–40 μm. The central position of the map is RA = 18 29 56.6, DEC = +1 13 30.0 [J2000]. For the LL modules, the map consists of 16 slit positions stepped in $9.5''$ intervals resulting in an observed area of 152×168 square arcseconds. Each pointing was observed twice with a ramp time of 31.46 seconds resulting in a total integration time of 62.92 seconds. For the SL modules, a grid of 43 by 5 pointings was used, with step sizes of $3.5''$ and $50''$ parallel and perpendicular to the slit, respectively. The observed area is 257×151 square arcseconds. Each position was observed twice resulting in a ramp time of 2×14.68 seconds. The maps in the different modules (SL, LL) are shifted relative to each other by roughly $60''$ due to the different locations of the modules in the IRS field of view. A screenshot showing the SL1 observed map of the Serpens core is displayed via ds9 in Figure 16.

4.1. Reduction of IRS mapping observations

All IRS mapping observations were reduced first with the same routines and calibration as the IRS staring observations (as described in Sections 2 and 3), with the spectrum of one module extracted for each position in the map. The IRS mapping observations differ from the IRS staring

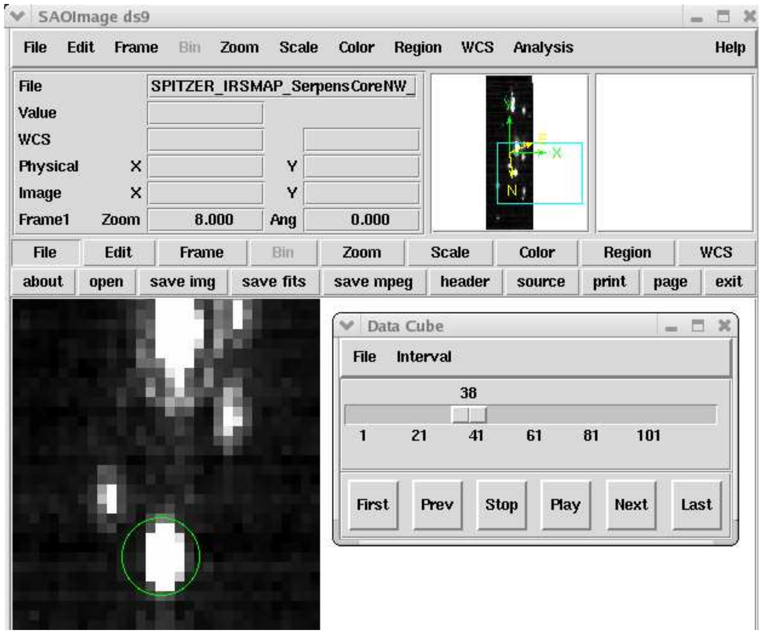

Fig. 16.— Screenshot showing one of the IRS mapping data cubes (module SL1) viewed with ds9.

observations in that they have one dither position per commanded map position instead of two. For the PSF extraction this results in an effectively smaller cross dispersion baseline and more limited sampling, which reduces the effectiveness of the profile fitting for unresolved sources (see Figure 14 for a comparison between an IRS mapping and an IRS staring mode observation).

In addition, three dimensional data cubes, consisting of one wavelength and two spatial dimensions, were produced for the Serpens core. The production of these data cubes began with the S13.2.0 version of the BCD two-dimensional spectra (*_bcd.fits).

First, frames taken at the same positions were co-added in order to increase the S/N; the mean of the value at every position of the two frames was taken as the co-added value. Next, the data for each position are combined to make a complete map of the region by stacking the spectra together. The pixel sizes of the final map are defined by the pixel sizes of the initial 2D spectra and the step sizes between the individual spectra. The partial slit overlap causes an overestimation of the flux of the order of ∼4% in each pixel. Finally, the trace from bright sources in the 2D-spectra was used to correct for distortion in the spectral map. The IRS `wavesamp` calibration files provided by the SSC were also distortion corrected, as the wavelength is also affected by the distortion. But since the distortion is only a factor along the spatial axes in the 2D spectra, and the distortion in that direction is small, the error should also be small when compared to the spectral resolution of the instrument.

By comparing the mapping observations of, e.g., EC82 to pointed observations in the SL spectra (see Figure17), a flux accuracy of about 15% can be estimated for the spectral maps.

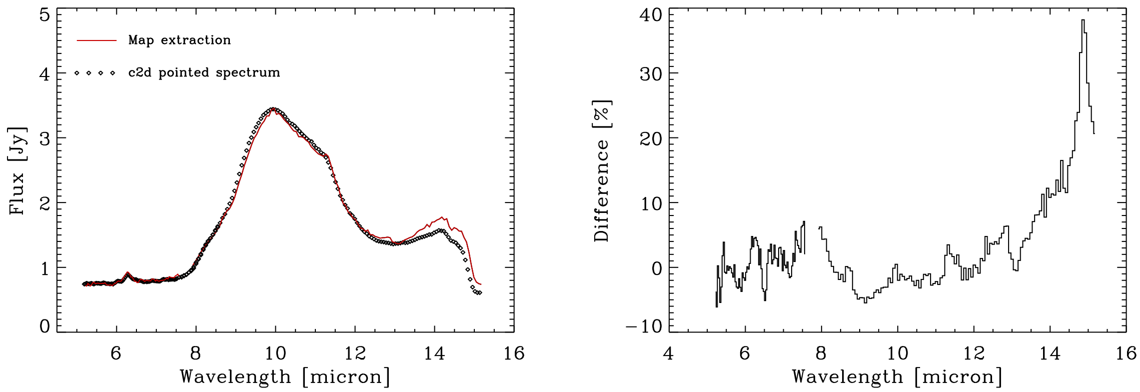

Fig. 17.— Left panel: A comparison of a spectrum extracted from the Serpens cube at the location of EC 82 (scaled down by 15%) and the spectrum of the IRS staring observation of EC 82. Right panel: The % difference between the two spectra as a function of wavelength.

4.2. Data products of IRS mapping observations

4.2.1. *Individual map pointings*

For all IRS mapping observations three products are produced for each position in the map in a manner identical to IRS pointed observations. The difference between IRS mapping observations and IRS staring observations is that only one dither position instead of two is available per commanded position. As mentioned in Section 4.1, the smaller cross dispersion baseline and more limited sampling may reduce the quality of the products in particular for the highest orders of the high resolution modules.

The delivered products for each map position are:

1. A spectrum as an IPAC table.
2. A PostScript file of the delivered spectrum.
3. A log file describing the observation (see Appendix A for an example).

4.2.2. *Serpens core data cubes*

For the Serpens core, the following additional products are delivered:

1. A data cube for each order observed (SL1, SL2, LL1, and LL2).
2. Wavelength definition files for each data cube.

Each data cube has two spatial dimensions and one wavelength dimension. The cubes are named SPITZER_IRSMAP_SerpensCoreNW_SL1.fits, etc. The signal is in units of Jy/pixel. The wavelength definition files, SPITZER_IRSMAP_SerpensCoreNW_SL1_wave.fits, etc., specify the (approximate) wavelength in μm for every pixel in the cube. The data cubes can be read and plotted with ds9 (see Figure16).

At the time the c2d spectral maps for Serpens were reduced the *CUbe Builder for IRS Spectral Maps* (CUBISM) was not available. Hence the spectral maps provided in this delivery are not optimal and intended for quick-look purposes only. Users should consider using their own data reduction (e.g., using CUBISM) to obtain publishable results.

5. c2d MIPS SED observations

During the c2d second-look program, the MIPS SED mode was used to obtain low resolution ($R = 15$–25) spectroscopy in the 55–95 μm wavelength range. This data was intended to characterize the longer wavelength SED, as well as silicate and ice emission features, for 4 sources (SX Cha, Haro 1-1, Sz 102, and CoKu Tau 4) when combined with IRS spectra taken during the c2d first-look campaign. The reduction techniques and delivered products for these 4 MIPS SED observations are described below.

5.1. MIPS SED Data Reduction

The c2d data reduction of MIPS SED data started from the two dimensional BCD images, version S13.2.0, provided by the SSC. An SED AOR consists of a set of BCDs observing several positions in the sky called cluster positions. For each cluster position there are on-the-source and off-the-source BCDs. The BCDs for each source were coadded using the MOPEX software package, version 030106.[11] The MOPEX mosaicing script *mosaic_sed.pl* reads in a list of input images, splits them into cluster positions and on-the-source and off-the-source subsets, coadds the appropriate frames and extracts the spectrum from the resulting image. All of the c2d MIPS SED observations are done in the non-mapping mode, "Fixed Single," i.e. a cluster of only 1 cluster position. In this case, the lists of input images are separated into the on- and off-source subsets only.

The resulting coadded images were extracted separately with MOPEX and with IRAF. In both cases either a 3 column or 5 column extraction was used, such that the aperture is sufficiently wide that the full source flux falls within the window. MOPEX uses a fixed width aperture extraction centered on the 3 or 5 brightest columns in the coadded image. In this version of MOPEX the aperture was defined automatically, with MOPEX choosing the brightest columns in the coadded image. For weak sources, this often resulted in an extraction aperture centered on the first 3 (or 5) columns of the coadded image, which are noisy, and not the source emission (which is typically columns 12-16). It was not possible to move the center of the aperture. In these cases, the MOPEX extraction should be discarded and the IRAF "hands-on" extraction should be used. An example of this case is shown in Figure 18.

The MOPEX "namelist" configuration file (see Appendix C) contains blocks of various parameter settings, input image names, and running options. Appendix B shows an example of the namelist files used in the c2d data reduction of SX Cha. A complete description and default settings for

[11] MOPEX post-BCD software is available via the SSC http://ssc.spitzer.caltech.edu/postbcd/download-mopex.html.

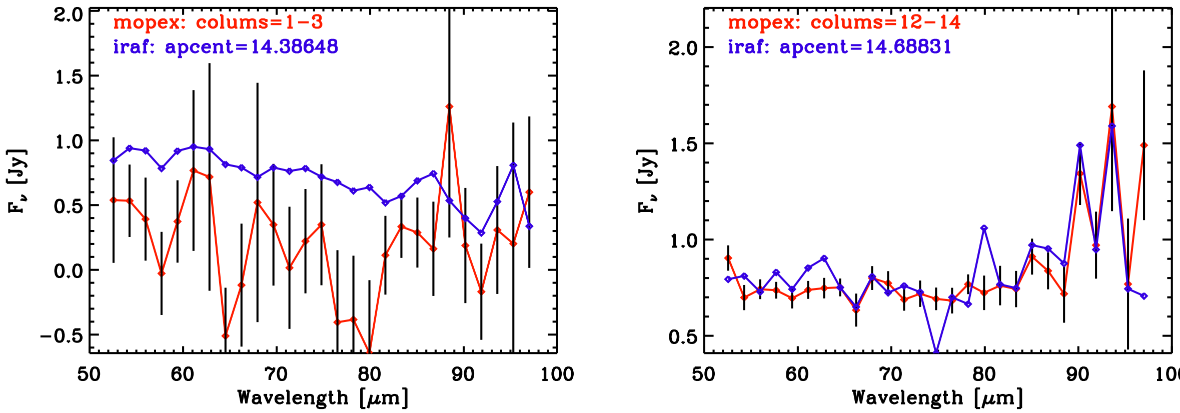

Fig. 18.— Examples of IRAF (blue) and MOPEX (red) extracted spectra for SX Cha (left) and Haro1-1 (right). Error bars are overplotted for the MOPEX extraction. The columns used for the extraction are shown in the upper left. The extraction aperture in this version of MOPEX is automatically centered on the brightest columns. This can result in erroneous extractions. For SX Cha the MOPEX extraction was centered on columns 1–3, off source, while the IRAF extraction was centered on column 14, on source. Thus, the IRAF spectrum should be used and the MOPEX spectrum should be discarded. For Haro1-1 the MOPEX extraction was centered on roughly the same columns as the IRAF extraction and can therefore be assumed to be on source.

the parameters specified in the namelist file can be found in the MOPEX mosaic_sed documentation file.[12] In general, default values are used with the following exceptions. The mosaics of the input uncertainty images are made (CREATE_UNC_MOSAIC=1, HAVE_UNCERTANTIES=1), and are used to compute the uncertainties of the extracted spectrum (USE_UNC_FOR_EXTRACT=1). The maximum number of bad pixels in a column for the column to be included in spectrum computation, MAX_BAD_PIXELS_IN_COLUMN was set to 20, instead of the default of 10, as this made for more robust extractions of weak sources. The spectra were extracted with either N_COLUMNS=3 or N_COLUMNS=5. The sample calibration file supplied with MOPEX, MIPS70_SED_sample_calibration.tbl, was used for wavelength and flux calibration.

The IRAF extraction was performed using NOAO/TWODSPEC/APEXTRACT/APALL. This routine allows the user to reset the center of the aperture, so the IRAF apertures were always centered on the brightest part of the on-source emission (typically columns 12-16). Again, either 3 column or 5 column fixed-width extractions were performed in order to include most the source flux. For bright sources, the trace was calculated from the BCD, for weaker sources, the trace from brighter sources was used. Wavelength and aperture dependent flux calibration and uncertainties were adopted from the MOPEX extractions.

---

[12] The mosaic_sed.pdf documentation file is available with the SSC post-BCD software (e.g., MOPEX) at http://ssc.spitzer.caltech.edu/postbcd/.

5.2. MIPS SED Data Products

For the MIPS SED observations, the following products are delivered:

1. A spectrum for each extraction (MOPEX, IRAF) as an IPAC table; see Appendix E for a header example.
2. A PostScript file for each MIPS SED target, with IRAF and MOPEX extractions overplotted (see Figure 18).
3. A logfile describing each observation (see Appendix C for an example).

The products delivered to the SSC include IPAC format ASCII tables that contain the 1-D extracted spectra and log files that briefly describe each observation. For each source, separate ASCII tables with MOPEX and IRAF extractions are provided. For a first impression, a single PostScript plot showing both the IRAF and MOPEX extractions has been generated for each target.

The ASCII tables can be read into an IDL structure within IRSFRINGE or SMART using the command

STRUCT = IPAC2IRS('YOUR_FAVOURITE_SOURCE.TBL').

The log files include basic information, including the source name, coordinates and the observation date and AOR_key and AOR_label. A typical log file for SX Cha is shown in Appendix D.

Figure 18 shows the PostScript files for SX Cha (left) and Haro 1-1 (right). These are plots of both the IRAF (blue) and MOPEX (red) extracted spectra in Jy, with errorbars included for the MOPEX extraction. Note that for SX Cha, the MOPEX extraction was centered on columns 1–3, off source, while the IRAF extraction was centered on column 14, on source. Thus, the IRAF spectrum should be used and the MOPEX spectrum should be discarded.

For Haro 1-1 (Figure 18, right panel), both the MOPEX extraction and the IRAF extraction were centered on roughly the same columns; therefore the MOPEX aperture can be assumed to be on source. The spectra are fairly similar, and through comparison of the two the user may decide which, if any, features are significant.

6. Summary

This document accompanies the final delivery of improved products from the c2d legacy project. It describes, in considerable detail, the delivered products and the algorithms and calibration products used to derive them. The delivery consists for the most part of IRS staring observations, but also includes some MIPS SED and IRS mapping observations. All observations are accompanied by illustrative plots and informative logfiles. This document is concise and as such is not able to address all issues of importance to the spectra, but it will serve as a solid base for using the spectra in further analysis.

The user should note that all IRS staring spectra and derived parameters are produced by an automated pipeline and artifacts are expected to be present in several spectra. By delivering spectra derived with two different extraction algorithms, estimates of the local extended emission, and a source spectrum corrected for extended emission and pointing effects, we provide the users with sufficient redundancy, in most cases, to assess the quality of the spectra.

All IRS mapping observations are extracted with the same routines and calibrations as the IRS staring observations, but the map pointings have only one dither position, rather than the two dither positions of the staring mode observations. Because of the reduced baseline and limited sampling, this results in a poorer PSF extraction for resolved sources with significant background emission. For the map of the Serpens NW core, three-dimensional (two spatial and one wavelength) data cubes are provided in addition to the standard extractions. These data cubes are preliminary and should be treated as illustrative and not of publishable quality.

The MIPS SED spectra have been coadded and extracted using the latest version of MOPEX but the MOPEX software and MIPS SED calibration are still under development and future versions may offer significant improvements. Because the aperture is set automatically within the current version of the MOPEX extraction, it is often centered off-source for weak sources. Therefore a "hands-on" extraction, performed using IRAF is also included in this delivery.

REFERENCES

Boogert, A.C. et al. 2004, ApJS, 154, 97, *Spitzer Space Telescope Spectroscopy of Ices toward Low-Mass Embedded Protostars*

Decin, L. et al. 2004, ApJS, 154, 408, *MARCS: Model Stellar Atmospheres and Their Application to the Photometric Calibration of the Spitzer Space Telescope Infrared Spectrograph (IRS)*

Evans, N. J., II et al. 2003, PASP, 115, 965, *From Molecular Cores to Planet-forming Disks: An SIRTF Legacy Program*

Higdon et al. 2004, PASP, 116, 975, *The SMART Data Analysis Package for the Infrared Spectrograph on the Spitzer Space Telescope*

Houck, J. R. et al. 2004, ApJS, 154, 18, *The Infrared Spectrograph on the Spitzer Space Telescope*

Geers, V.C. et al. 2006, A&A, in press, *c2d Spitzer-IRS Spectra of Disks Around T Tauri Stars*

Infrared Spectrograph Data Handbook Version 2.0, 2006, `http://ssc.spitzer.caltech.edu/irs/dh/`

Jorgensen, J.K. et al. 2005, ApJ, 631, L77, *Protostellar holes: Spitzer Space Telescope observations of the protostellar binary IRAS16293-2422*

Kessler-Silacci, J. et al. 2006, ApJ, 639, 275, *c2d Spitzer-IRS Spectra of Disks Around T Tauri Stars: I. Silicate Emission and Grain Growth*

Knez, C. et al. 2005, ApJ, 635, L145, *Spitzer Mid-Infrared Spectroscopy of Ices Toward Extincted Background Stars*

Lahuis, F., & Boogert, A. 2003, *How to get rid of Fringes in SIRTF/IRS data* in "Chemistry as a Diagnostic of Star Formation", August 2002, University of Waterloo, Canada

Lahuis, F. et al. 2006, ApJ, 636, L145, *Hot Organic Molecules Toward a Young Low-Mass Star: A Look at Inner Disk Chemistry*

Pontoppidan, K.M. et al. 2005, ApJ, 622, 463, *Ices in the Edge-on Disk CRBR 2422.8-3423: Spitzer Spectroscopy and Monte Carlo Radiative Transfer Modeling*

van Dishoeck, E.F. 2006, PNAS, 103, 33, 12249, *Chemistry in Low-Mass Protostellar and Protoplanetary Regions*

This preprint was prepared with the AAS LaTeX macros v5.2.

Table 2. List of Observed IRS AORs

Target	RA [J2000]	Dec [J2000]	Obs_date	AOR_key	AOT_type	Obs_mode	Modules	Version
LDN1448_IRS1	3h25m09.4s	30d46m21.7s	2004-09-01	0005656832	irsstare	TargetFixedSingle	SL1,SL2,SH,LH	S13.2.0
LDN1448_NA	3h25m36.5s	30d45m21.4s	2005-09-05	0005828096	irsstare	TargetFixedSingle	SL1,SL2,SH,LH	S13.2.0
IRAS_03235+3004	3h26m37.4s	30d15m27.9s	2005-09-05	0009835520	irsstare	TargetFixedSingle	SL1,SL2,LL1,LL2	S13.2.0
IRAS_03245+3002	3h27m39.0s	30d12m59.3s	2005-09-05	0006368000	irsstare	TargetFixedSingle	SL1,SL2,SH,LH	S13.2.0
L1455_SMM1	3h27m43.3s	30d12m28.8s	2005-09-08	0015917056	irsstare	TargetFixedSingle	SL1,SL2,LL1,SH	S13.2.0
RNO_15	3h27m47.7s	30d12m04.3s	2004-08-30	0005633280	irsstare	TargetFixedSingle	SL1,SL2,LL1,SH,LH	S13.2.0
L1455_IRS3	3h28m00.4s	30d08m01.2s	2005-09-08	0015917568	irsstare	TargetFixedSingle	SL1,SL2,LL1,SH	S13.2.0
IRAS_03254+3050	3h28m34.5s	31d00m51.2s	2005-02-08	0011827200	irsstare	TargetFixedSingle	SL1,SL2,LL1,SH,LH	S13.2.0
LkHA_325	3h28m52.2s	30d45m05.5s	2005-09-05	0015737600	irsstare	TargetMulti	SL1,SL2,LL1,LL2	S13.2.0
LkHA_270	3h29m17.7s	31d22m45.1s	2005-02-08	0005634048	irsstare	TargetFixedSingle	SL1,SL2,SH,LH	S13.2.0
LkHA_271	3h29m21.9s	31d15m36.3s	2005-02-10	0011827968	irsstare	TargetFixedSingle	SL1,SL2,SH,LH	S13.2.0
IRAS_03271+3013	3h30m15.2s	30d23m48.8s	2005-02-10	0005634304	irsstare	TargetMulti	SL1,SL2,LL1,SH,LH	S13.2.0
SSTc2d_J033036.0+303024	3h30m35.9s	30d30m24.4s	2005-09-05	0015737600	irsstare	TargetMulti	SL1,SL2,LL1,LL2	S13.2.0
SSTc2d_J033037.0+303128	3h30m37.0s	30d31m27.7s	2005-09-05	0015737600	irsstare	TargetMulti	SL1,SL2,LL1,LL2	S13.2.0
LkHA_326	3h30m44.0s	30d32m46.7s	2005-02-10	0005634304	irsstare	TargetMulti	SL1,SL2,LL1,SH,LH	S13.2.0
SSTc2d_J033052.5+305418	3h30m52.6s	30d54m18.1s	2005-09-05	0015737088	irsstare	TargetFixedSingle	SL1,SL2,LL1,LL2	S13.2.0
IRAS_03292+3039	3h32m18.0s	30d49m46.9s	2005-09-08	0015918848	irsstare	TargetFixedSingle	LL1	S13.2.0
SSTc2d_J033241.7+311046	3h32m41.8s	31d10m46.6s	2005-09-05	0015737344	irsstare	TargetFixedSingle	SL1,SL2,LL1,LL2	S13.2.0
IRAS_03301+3111	3h33m12.8s	31d21m24.2s	2004-02-03	0005634560	irsstare	TargetMulti	SL1,SL2,SH,LH	S13.2.0
SSTc2d_J033314.4+310711	3h33m14.4s	31d07m10.8s	2005-09-08	0015915776	irsstare	TargetFixedSingle	LL1,LL2	S13.2.0
B1-a	3h33m16.7s	31d07m55.1s	2005-09-08	0015918080	irsstare	TargetFixedSingle	SL1,SL2,LL1,SH	S13.2.0
B1-c	3h33m17.9s	31d09m31.0s	2005-09-05	0013460480	irsstare	TargetFixedSingle	SL1,SL2,LL1,SH	S13.2.0
B1-b	3h33m20.3s	31d07m21.4s	2005-09-08	0015916544	irsstare	TargetFixedSingle	SL1,SL2,LL1,LL2	S13.2.0
SSTc2d_J033327.3+310710	3h33m27.3s	31d07m10.2s	2005-09-08	0015918336	irsstare	TargetFixedSingle	SL1,SL2,LL1,SH	S13.2.0
LkHA_327	3h33m30.4s	31d10m50.4s	2004-02-03	0005634560	irsstare	TargetMulti	SL1,SL2,SH,LH	S13.2.0
SSTc2d_J033341.3+311341	3h33m41.3s	31d13m41.6s	2005-09-05	0015736832	irsstare	TargetFixedSingle	SL1,SL2,LL1,LL2	S13.2.0
IRAS_03380+3135	3h41m09.2s	31d44m38.0s	2005-09-05	0015736576	irsstare	TargetFixedSingle	SL1,SL2,LL1,LL2	S13.2.0
BD+31_634	3h41m39.2s	31d36m10.3s	2005-09-05	0015736320	irsstare	TargetFixedSingle	SL1,SL2,LL1,LL2	S13.2.0
SSTc2d_J034202.2+314802	3h42m02.2s	31d48m01.9s	2005-09-08	0015916032	irsstare	TargetFixedSingle	LL1,LL2	S13.2.0
SSTc2d_J034219.3+314327	3h42m19.3s	31d43m26.6s	2005-09-05	0015736064	irsstare	TargetFixedSingle	SL1,SL2,LL1,LL2	S13.2.0
RNO_19	3h42m56.0s	31d58m42.0s	2005-09-05	0015735552	irsstare	TargetFixedSingle	SL1,SL2,LL1,LL2	S13.2.0
IRAS_03406+3133	3h43m44.5s	31d43m09.1s	2005-09-05	0015735296	irsstare	TargetFixedSingle	SL1,SL2,LL1,LL2	S13.2.0
HH_211-mm	3h43m56.8s	32d00m50.5s	2005-02-08	0005826304	irsstare	TargetFixedSingle	SH,LH	S13.2.0
SSTc2d_J034438.5+320801	3h44m38.5s	32d08m00.6s	2006-03-08	0016755456	irsstare	TargetFixedSingle	SL1,SL2,LL1,LL2	S13.2.0

Table 2—Continued

Target	RA [J2000]	Dec [J2000]	Obs_date	AOR_key	AOT_type	Obs_mode	Modules	Version
LkHA_330	3h45m48.3s	32d24m11.8s	2004-09-02	0005634816	irsstare	TargetFixedSingle	SL1,SL2,LL1,SH,LH	S13.2.0
IRAS_03439+3233	3h47m05.5s	32d43m08.5s	2004-09-29	0005635072	irsstare	TargetMulti	SL1,SL2,LL1,SH,LH	S13.2.0
IRAS_03445+3242	3h47m41.6s	32d51m43.8s	2004-02-03	0005635328	irsstare	TargetFixedSingle	SL1,SL2,SH,LH	S13.2.0
IRAS_03446+3254	3h47m47.1s	33d04m03.4s	2004-09-29	0005635072	irsstare	TargetMulti	SL1,SL2,LL1,SH,LH	S13.2.0
IRAM_04191+1522	4h21m56.9s	15d29m45.8s	2006-03-15	0016754432	irsstare	TargetFixedSingle	LL1,LL2	S13.2.0
Elias3	4h23m24.5s	25d00m08.3s	2004-08-30	0005635584	irsstare	TargetFixedSingle	SL1,SL2	S13.2.0
Elias3	4h23m24.5s	25d00m08.3s	2005-02-08	0006372352	irsstare	TargetFixedSingle	SL1,SL2	S13.2.0
LkCa_8	4h24m57.1s	27d11m56.5s	2005-02-08	0009832960	irsstare	TargetFixedSingle	SH,LH	S13.2.0
SSTc2d_J042838.9+265135	4h28m39.0s	26d51m35.1s	2005-09-08	0015919360	irsstare	TargetFixedSingle	LL1,LL2	S13.2.0
IQ_Tau	4h29m51.6s	26d06m45.0s	2005-02-09	0009832704	irsstare	TargetFixedSingle	SH,LH	S13.2.0
FX_Tau	4h30m29.6s	24d26m45.1s	2005-02-10	0009832448	irsstare	TargetFixedSingle	SH,LH	S13.2.0
V710_Tau	4h31m57.8s	18d21m36.3s	2004-09-29	0005636608	irsstare	TargetFixedSingle	SH,LH	S13.2.0
RXJ0432.8+1735	4h32m53.2s	17d35m33.7s	2005-09-09	0015917824	irsstare	TargetFixedSingle	SL1,SL2,LL1,LL2	S13.2.0
Elias13	4h33m25.9s	26d15m34.0s	2004-08-31	0005636864	irsstare	TargetFixedSingle	SL1,SL2,SH	S13.2.0
DN_Tau	4h35m27.4s	24d14m58.8s	2005-02-10	0009831936	irsstare	TargetMulti	SH,LH	S13.2.0
CoKu_Tau_3	4h35m40.9s	24d11m08.6s	2005-02-10	0009831936	irsstare	TargetMulti	SH,LH	S13.2.0
Tamura2	4h37m28.2s	26d10m29.0s	2004-09-27	0005637632	irsstare	TargetMulti	SL1,SL2	S13.2.0
Tamura2	4h37m28.2s	26d10m29.0s	2005-09-09	0015913472	irsstare	TargetMulti	LL2	S13.2.0
Elias15	4h39m26.9s	25d52m59.3s	2004-09-27	0005637376	irsstare	TargetMulti	SL1,SL2	S13.2.0
Elias15	4h39m26.9s	25d52m59.3s	2005-09-09	0015913216	irsstare	TargetFixedSingle	LL2	S13.2.0
Elias16	4h39m38.9s	26d11m26.6s	2004-09-27	0005637632	irsstare	TargetMulti	SL1,SL2	S13.2.0
Tamura8	4h40m57.5s	25d54m13.4s	2004-09-27	0005637376	irsstare	TargetMulti	SL1,SL2	S13.2.0
Tamura8	4h40m57.5s	25d54m13.4s	2005-09-09	0015913472	irsstare	TargetMulti	LL2	S13.2.0
CoKu_Tau_4	4h41m16.8s	28d40m00.5s	2004-09-02	0005637888	irsstare	TargetFixedSingle	SH,LH	S13.2.0
BF_Ori	5h37m13.3s	-6d35m00.6s	2004-10-03	0005638144	irsstare	TargetFixedSingle	SL1,SL2,LL1,SH,LH	S13.2.0
RR_Tau	5h39m30.5s	26d22m27.0s	2004-09-28	0005638400	irsstare	TargetFixedSingle	SL1,SL2,LL1,SH,LH	S13.2.0
IRAS_08242-5050	8h25m43.8s	-51d00m35.6s	2003-12-15	0005638912	irsstare	TargetMulti	SL1,SL2,SH,LH	S13.2.0
IRAS_08261-5100	8h27m38.9s	-51d10m37.3s	2003-12-15	0005638912	irsstare	TargetMulti	SL1,SL2,SH,LH	S13.2.0
IRAS_08267-3336	8h28m40.7s	-33d46m22.3s	2004-11-11	0005639168	irsstare	TargetFixedSingle	SL1,SL2,LL1,SH,LH	S13.2.0
SX_Cha	10h55m59.7s	-77d24m39.9s	2004-08-31	0005639424	irsstare	TargetMulti	SH,LH	S13.2.0
SY_Cha	10h56m30.5s	-77d11m39.4s	2004-08-31	0005639424	irsstare	TargetMulti	SH,LH	S13.2.0
TW_Cha	10h59m01.1s	-77d22m40.8s	2004-09-01	0005639680	irsstare	TargetMulti	SH,LH	S13.2.0
Ced_110_IRS4	11h06m46.6s	-77d22m32.4s	2004-09-01	0005639680	irsstare	TargetMulti	SH,LH	S13.2.0
Ced_110_IRS6	11h07m09.2s	-77d23m04.3s	2004-09-01	0005639680	irsstare	TargetMulti	SH,LH	S13.2.0

Table 2—Continued

Target	RA [J2000]	Dec [J2000]	Obs_date	AOR_key	AOT_type	Obs_mode	Modules	Version
B35	11h07m21.5s	-77d22m11.8s	2004-09-01	0005639680	irsstare	TargetMulti	SH,LH	S13.2.0
VW_Cha	11h08m01.5s	-77d42m28.7s	2004-09-01	0005639680	irsstare	TargetMulti	SH,LH	S13.2.0
Hn_9	11h09m18.2s	-76d30m29.2s	2005-02-10	0009831168	irsstare	TargetFixedSingle	SL1,SL2,LL1,LL2	S13.2.0
VZ_Cha	11h09m23.8s	-76d23m20.7s	2004-09-02	0005640448	irsstare	TargetMulti	SH,LH	S13.2.0
WX_Cha	11h09m58.8s	-77d37m08.9s	2004-09-01	0005640192	irsstare	TargetMulti	SH,LH	S13.2.0
ISO-Cha237	11h10m11.4s	-76d35m29.2s	2004-09-02	0005640448	irsstare	TargetMulti	SH,LH	S13.2.0
C7-11	11h10m38.0s	-77d32m39.9s	2004-09-01	0005640192	irsstare	TargetMulti	SH,LH	S13.2.0
HM_27	11h10m49.6s	-77d17m51.7s	2004-09-01	0005640192	irsstare	TargetMulti	SH,LH	S13.2.0
XX_Cha	11h11m39.7s	-76d20m15.1s	2004-09-02	0005640448	irsstare	TargetMulti	SH,LH	S13.2.0
HD_98922	11h22m31.7s	-53d22m11.4s	2004-01-04	0005640704	irsstare	TargetFixedSingle	SH,LH	S13.2.0
HD_101412	11h39m44.5s	-60d10m27.7s	2005-02-10	0005640960	irsstare	TargetFixedSingle	SL1,SL2,SH,LH	S13.2.0
T_Cha	11h57m13.5s	-79d21m31.5s	2004-07-18	0005641216	irsstare	TargetFixedSingle	SH,LH	S13.2.0
IRAS_12535-7623	12h57m11.8s	-76d40m11.5s	2004-08-31	0011827456	irsstare	TargetMulti	SH,LH	S13.2.0
ISO-ChaII_13	12h58m06.7s	-77d09m09.5s	2005-09-13	0015918592	irsstare	TargetFixedSingle	SL1,SL2,LL1,LL2	S13.2.0
IRAS_12553-7651	12h59m06.6s	-77d07m40.0s	2005-03-12	0009830912	irsstare	TargetFixedSingle	SL1,SL2,LL1,SH,LH	S13.2.0
Off_position_3	13h00m00.0s	-77d20m00.0s	2004-03-25	0005654784	irsstare	TargetFixedSingle	SH,LH	S13.2.0
RXJ1301.0-7654	13h00m53.2s	-76d54m15.2s	2005-03-12	0009830656	irsstare	TargetFixedSingle	SL1,SL2,LL1,LL2	S13.2.0
Sz50	13h00m55.4s	-77d10m22.2s	2004-08-31	0011827456	irsstare	TargetMulti	SH,LH	S13.2.0
ISO-ChaII_54	13h00m59.2s	-77d14m02.7s	2005-08-13	0015735040	irsstare	TargetFixedSingle	SL1,SL2,LL1,LL2,SH	S13.2.0
SSTc2d_J130234.5-772252	13h02m34.5s	-77d22m52.3s	2005-09-13	0015919104	irsstare	TargetFixedSingle	SL1,SL2	S13.2.0
DL_Cha	13h06m08.4s	-77d06m27.3s	2004-07-14	0005642240	irsstare	TargetFixedSingle	SH,LH	S13.2.0
SSTc2d_J130718.0-774053	13h07m18.1s	-77d40m52.9s	2005-09-13	0015920384	irsstare	TargetMulti	SL1,SL2	S13.2.0
SSTc2d_J130827.2-774323	13h08m27.1s	-77d43m23.3s	2005-09-13	0015920384	irsstare	TargetMulti	SL1,SL2	S13.2.0
Sz62	13h09m50.7s	-77d57m24.0s	2005-03-12	0009830400	irsstare	TargetFixedSingle	SL1,SL2,LL1,LL2	S13.2.0
IRAS_13546-3941	13h57m38.9s	-39d56m00.2s	2004-07-17	0005642752	irsstare	TargetFixedSingle	SL1,SL2,SH,LH	S13.2.0
HD_132947	15h04m56.0s	-63d07m52.6s	2004-03-25	0005643008	irsstare	TargetFixedSingle	SL1,SL2,SH,LH	S13.2.0
HD_135344	15h15m48.4s	-37d09m16.0s	2004-08-08	0005657088	irsstare	TargetFixedSingle	SH,LH	S13.2.0
IRAS_15398-3359	15h43m02.3s	-34d09m06.7s	2005-09-09	0005828864	irsstare	TargetFixedSingle	SL1,SL2,LL1,SH,LH	S13.2.0
HT_Lup	15h45m12.9s	-34d17m30.6s	2004-08-30	0005643264	irsstare	TargetFixedSingle	SL1,SL2,SH,LH	S13.2.0
HT_Lup	15h45m12.9s	-34d17m30.6s	2004-08-28	0009829120	irsmap	TargetFixedSingle	SL1,SL2,SH,LH	S13.2.0
GW_Lup	15h46m44.7s	-34d30m35.4s	2004-08-30	0005643520	irsstare	TargetFixedSingle	SL1,SL2,LL1,SH,LH	S13.2.0
HM_Lup	15h47m50.6s	-35d28m35.4s	2004-08-30	0005643776	irsstare	TargetFixedSingle	SL1,SL2,LL1,LL2	S13.2.0
Sz73	15h47m57.0s	-35d14m35.1s	2004-08-30	0005644032	irsstare	TargetMulti	SL1,SL2,LL1,SH,LH	S13.2.0
GQ_Lup	15h49m12.1s	-35d39m05.0s	2004-08-30	0005644032	irsstare	TargetMulti	SL1,SL2,LL1,SH,LH	S13.2.0

Table 2—Continued

Target	RA [J2000]	Dec [J2000]	Obs_date	AOR_key	AOT_type	Obs_mode	Modules	Version
Sz76	15h49m30.7s	-35d49m51.4s	2005-09-09	0015916288	irsstare	TargetFixedSingle	SL1,SL2,LL1,LL2	S13.2.0
IM_Lup	15h56m09.2s	-37d56m06.4s	2004-08-30	0005644800	irsstare	TargetMulti	SL1,SL2,LL1,SH,LH	S13.2.0
RU_Lup	15h56m42.3s	-37d49m15.5s	2004-08-30	0005644800	irsstare	TargetMulti	SL1,SL2,LL1,SH,LH	S13.2.0
Sz84	15h58m02.5s	-37d36m02.8s	2004-03-25	0005644288	irsstare	TargetFixedSingle	SL1,SL2,LL1,LL2	S13.2.0
RY_Lup	15h59m28.4s	-40d21m51.2s	2004-08-30	0005644544	irsstare	TargetFixedSingle	SL1,SL2,LL1,SH,LH	S13.2.0
SSTc2d_J160115.9-415334	16h01m15.9s	-41d53m33.8s	2005-09-09	0015914240	irsstare	TargetMulti	SL1,SL2,LL2	S13.2.0
SSTc2d_J160145.9-415824	16h01m45.9s	-41d58m24.5s	2005-09-09	0015912960	irsstare	TargetFixedSingle	SL1,SL2,LL2	S13.2.0
SSTc2d_J160159.6-415306	16h01m59.6s	-41d53m05.9s	2005-09-09	0015914240	irsstare	TargetMulti	SL1,SL2,LL2	S13.2.0
EX_Lup	16h03m05.5s	-40d18m24.9s	2004-08-30	0005645056	irsstare	TargetFixedSingle	SL1,SL2,LL1,SH,LH	S13.2.0
RXJ1603.2-3239	16h03m11.8s	-32d39m20.2s	2005-09-09	0015917312	irsstare	TargetFixedSingle	SL1,SL2,LL1,LL2	S13.2.0
Sz96	16h08m12.6s	-39d08m33.4s	2006-03-15	0016755200	irsstare	TargetFixedSingle	SL1,SL2,LL1,LL2	S13.2.0
Sz102	16h08m29.7s	-39d03m11.2s	2004-03-25	0009407488	irsstare	TargetFixedSingle	SL1,SL2,SH,LH	S13.2.0
AS_205	16h11m31.4s	-18d38m26.1s	2004-08-28	0005646080	irsstare	TargetFixedSingle	SL1,SL2,SH,LH	S13.2.0
SSTc2d_J161148.7-381758	16h11m48.7s	-38d17m57.8s	2005-08-13	0015738112	irsstare	TargetFixedSingle	SL1,SL2,LL1,LL2	S13.2.0
SSTc2d_J161159.8-382338	16h11m59.8s	-38d23m37.5s	2005-08-14	0015737856	irsstare	TargetFixedSingle	SL1,SL2,LL1,LL2	S13.2.0
RXJ1615.3-3255	16h15m20.2s	-32d55m05.1s	2005-09-09	0015916800	irsstare	TargetFixedSingle	SL1,SL2,LL1,LL2	S13.2.0
Haro_1-1	16h21m34.7s	-26d12m27.0s	2005-03-12	0009833472	irsstare	TargetFixedSingle	SL1,SL2,LL1,SH,LH	S13.2.0
SSTc2d_J162145.1-234232	16h21m45.2s	-23d42m31.8s	2005-09-09	0015919872	irsstare	TargetFixedSingle	SL1,SL2,LL1,LL2	S13.2.0
SSTc2d_J162148.5-234027	16h21m48.5s	-23d40m27.3s	2006-03-15	0015919617	irsstare	TargetFixedSingle	SL1,SL2,LL1,LL2	S13.2.0
SSTc2d_J162148.5-234027	16h21m48.5s	-23d40m27.4s	2006-03-15	0015920897	irsstare	TargetMulti	SL1,SL2,LL1,LL2	S13.2.0
SSTc2d_J162221.0-230403	16h22m21.0s	-23d04m02.6s	2006-03-15	0015920897	irsstare	TargetMulti	SL1,SL2,LL1,LL2	S13.2.0
SSTc2d_J162230.2-232224	16h22m30.2s	-23d22m24.0s	2006-03-15	0015920129	irsstare	TargetMulti	SL1,SL2	S13.2.0
SSTc2d_J162244.9-231713	16h22m44.9s	-23d17m13.4s	2006-03-15	0015920129	irsstare	TargetMulti	SL1,SL2	S13.2.0
SSTc2d_J162245.4-243124	16h22m45.4s	-24d31m23.9s	2006-03-15	0015920641	irsstare	TargetMulti	SL1,SL2,LL1,LL2	S13.2.0
SSTc2d_J162305.9-233818	16h23m05.8s	-23d38m17.8s	2006-03-15	0015920129	irsstare	TargetMulti	SL1,SL2	S13.2.0
SSTc2d_J162332.8-225847	16h23m32.9s	-22d58m46.9s	2006-03-15	0015920641	irsstare	TargetMulti	SL1,SL2,LL1,LL2	S13.2.0
Off_position_1	16h24m00.0s	-24d00m00.0s	2004-03-25	0005654272	irsstare	TargetFixedSingle	SH,LH	S13.2.0
Haro_1-4	16h25m10.5s	-23d19m14.5s	2005-03-12	0009833216	irsstare	TargetFixedSingle	LL1,SH,LH	S13.2.0
CRBR_2317.3-1925	16h26m18.8s	-24d26m0***s	2004-08-08	0005647360	irsstare	TargetFixedSingle	LL1,LL2	S13.2.0
VSSG1	16h26m18.9s	-24d28m19.7s	2004-08-28	0005647616	irsstare	TargetMulti	SH,LH	S13.2.0
GSS30-IRS1	16h26m21.4s	-24d23m04.1s	2004-08-28	0005647616	irsstare	TargetMulti	SH,LH	S13.2.0
DoAr_24E	16h26m23.4s	-24d21m00.1s	2004-08-28	0005647616	irsstare	TargetMulti	SH,LH	S13.2.0
GY23	16h26m24.1s	-24d24m48.1s	2004-08-28	0005647616	irsstare	TargetMulti	SH,LH	S13.2.0
VLA_1623-243	16h26m26.4s	-24d24m30.3s	2004-08-29	0009828096	irsstare	TargetFixedSingle	SH,LH	S13.2.0

Table 2—Continued

Target	RA [J2000]	Dec [J2000]	Obs_date	AOR_key	AOT_type	Obs_mode	Modules	Version
IRS14	16h26m31.0s	-24d31m05.2s	2005-08-12	0012664576	irsstare	TargetFixedSingle	SL1,SL2,LL1,SH	S13.2.0
WL12	16h26m44.2s	-24d34m48.4s	2004-08-28	0005647616	irsstare	TargetMulti	SH,LH	S13.2.0
Off_position_2	16h27m00.0s	-24d30m00.0s	2004-03-25	0005654528	irsstare	TargetFixedSingle	SH,LH	S13.2.0
OphE-MM3	16h27m05.9s	-24d37m08.2s	2005-03-12	0006370816	irsstare	TargetFixedSingle	SL1,SL2,LL1,LL2,SH,LH	S13.2.0
SR_21	16h27m10.3s	-24d19m12.5s	2004-08-28	0005647616	irsstare	TargetMulti	SH,LH	S13.2.0
GY224	16h27m11.2s	-24d40m46.7s	2004-08-29	0009829888	irsstare	TargetMulti	SH,LH	S13.2.0
WL19	16h27m11.7s	-24d38m32.2s	2004-08-29	0009829888	irsstare	TargetMulti	SH,LH	S13.2.0
SSTc2d_J162715.1-245139	16h27m15.1s	-24d51m38.9s	2006-03-15	0016754688	irsstare	TargetFixedSingle	SL1,SL2,LL1,LL2	S13.2.0
WL20S	16h27m15.7s	-24d38m45.6s	2004-08-29	0009829888	irsstare	TargetMulti	SH,LH	S13.2.0
IRS37	16h27m17.6s	-24d28m56.5s	2004-08-28	0005647616	irsstare	TargetMulti	SH,LH	S13.2.0
IRS42	16h27m21.5s	-24d41m43.1s	2004-08-28	0005647616	irsstare	TargetMulti	SH,LH	S13.2.0
WL6	16h27m21.8s	-24d29m53.3s	2004-08-28	0005647616	irsstare	TargetMulti	SH,LH	S13.2.0
CRBR_2422.8-3423	16h27m24.6s	-24d41m03.3s	2004-03-25	0009346048	irsstare	TargetFixedSingle	SL1,SL2,SH,LH	S13.2.0
Elias32	16h27m28.4s	-24d27m21.4s	2005-09-09	0012664320	irsstare	TargetFixedSingle	SH,LH	S13.2.0
IRS46	16h27m29.4s	-24d39m16.3s	2004-08-29	0009829888	irsstare	TargetMulti	SH,LH	S13.2.0
VSSG17	16h27m30.2s	-24d27m43.4s	2004-08-28	0005647616	irsstare	TargetMulti	SH,LH	S13.2.0
IRS51	16h27m39.8s	-24d43m15.1s	2004-08-29	0009829888	irsstare	TargetMulti	SH,LH	S13.2.0
SR_9	16h27m40.3s	-24d22m04.0s	2004-09-02	0012027392	irsstare	TargetFixedSingle	SH,LH	S13.2.0
2MASS_16282-2432	16h28m13.7s	-24d31m39.0s	2004-08-29	0009829632	irsstare	TargetFixedSingle	SL1,SL2,LL1,LL2	S13.2.0
SSTc2d_J162816.7-240514	16h28m16.7s	-24d05m14.3s	2006-03-15	0016754944	irsstare	TargetFixedSingle	SL1,SL2,LL1,LL2	S13.2.0
V853Oph	16h28m45.3s	-24d28m19.0s	2005-03-12	0012408576	irsstare	TargetFixedSingle	LL1,SH,LH	S13.2.0
SSTc2d_J163023.8-245951	16h30m23.8s	-24d59m50.9s	2005-09-09	0015915008	irsstare	TargetMulti	SL1,SL2,LL2	S13.2.0
SSTc2d_J163027.1-245405	16h30m27.1s	-24d54m05.1s	2005-09-10	0015915264	irsstare	TargetMulti	SL1,SL2,LL2	S13.2.0
ROX42C	16h31m15.8s	-24d34m02.1s	2005-03-12	0006369792	irsstare	TargetFixedSingle	SH,LH	S13.2.0
ROX43A	16h31m20.1s	-24d30m05.1s	2005-09-09	0015914496	irsstare	TargetFixedSingle	LL1,SH,LH	S13.2.0
IRS60	16h31m30.9s	-24d24m39.7s	2005-09-09	0006370048	irsstare	TargetMulti	LL1,SH,LH	S13.2.0
Haro_1-16	16h31m33.5s	-24d27m37.1s	2005-09-09	0012664064	irsstare	TargetMulti	SH,LH	S13.2.0
SSTc2d_J163135.3-250832	16h31m35.3s	-25d08m32.4s	2005-09-10	0015915264	irsstare	TargetMulti	SL1,SL2,LL2	S13.2.0
IRS63	16h31m35.7s	-24d01m29.5s	2004-08-08	0009827840	irsstare	TargetFixedSingle	SH,LH	S13.2.0
SSTc2d_J163142.3-252501	16h31m42.3s	-25d25m01.2s	2005-09-09	0015915008	irsstare	TargetMulti	SL1,SL2,LL2	S13.2.0
L1689-IRS5	16h31m52.1s	-24d56m15.2s	2005-09-09	0012664064	irsstare	TargetMulti	SH,LH	S13.2.0
L1689-IRS7	16h32m20.8s	-24d30m29.1s	2005-09-09	0006370048	irsstare	TargetMulti	LL1,SH,LH	S13.2.0
Haro_1-17	16h32m21.9s	-24d42m14.7s	2004-08-29	0011827712	irsstare	TargetFixedSingle	SL1,SL2,LL1,SH,LH	S13.2.0
IRAS_16293-2422B	16h32m22.6s	-24d28m32.2s	2005-08-14	0015735808	irsstare	TargetFixedSingle	SL1,SL2,SH,LH	S13.2.0

Table 2—Continued

Target	RA [J2000]	Dec [J2000]	Obs_date	AOR_key	AOT_type	Obs_mode	Modules	Version
IRAS_16293-2422	16h32m22.9s	-24d28m36.1s	2004-08-29	0011826944	irsstare	TargetFixedSingle	SL1,SL2,SH,LH	S13.2.0
SSTc2d_J163322.9-251341	16h33m22.9s	-25d13m40.7s	2005-09-10	0015915264	irsstare	TargetMulti	SL1,SL2,LL2	S13.2.0
SSTc2d_J163346.2-242753	16h33m46.2s	-24d27m53.0s	2005-09-10	0015915264	irsstare	TargetMulti	SL1,SL2,LL2	S13.2.0
RNO_90	16h34m09.2s	-15d48m16.8s	2004-08-28	0005650432	irsstare	TargetMulti	SL1,SL2,LL1,SH,LH	S13.2.0
RNO_91	16h34m29.3s	-15d47m01.4s	2004-08-28	0005650432	irsstare	TargetMulti	SL1,SL2,LL1,SH,LH	S13.2.0
SSTc2d_J164136.3-235640	16h41m36.3s	-23d56m39.5s	2005-09-09	0015914752	irsstare	TargetFixedSingle	SL1,SL2,LL2	S13.2.0
Wa_Oph_6	16h48m45.6s	-14d16m35.9s	2006-03-15	0005650688	irsstare	TargetMulti	SL1,SL2,LL1,SH,LH	S13.2.0
V1121_Oph	16h49m15.3s	-14d22m08.6s	2006-03-15	0005650688	irsstare	TargetMulti	SL1,SL2,LL1,SH,LH	S13.2.0
IRAS_16544-1604	16h57m19.6s	-16d09m23.8s	2005-09-09	0005826816	irsstare	TargetFixedSingle	LL1,LL2,LH	S13.2.0
HD_163296	17h56m21.3s	-21d57m21.9s	2004-08-28	0005650944	irsstare	TargetFixedSingle	SH,LH	S13.2.0
HD_163296	17h56m21.3s	-21d57m21.9s	2004-08-28	0009830144	irsmap	TargetFixedSingle	SH,LH	S13.2.0
SSTc2d_J181617.4-23241	18h16m17.4s	-2d32m40.9s	2006-04-21	0015921153	irsstare	TargetFixedSingle	SL1,SL2,LL1,LL2	S14.0.0
SSTc2d_J182813.2+00313	18h28m13.2s	0d03m12.8s	2005-04-14	0013210368	irsstare	TargetMulti	SL1,SL2,LL1,LL2,SH	S13.2.0
SSTc2d_J182830.0+02015	18h28m30.0s	0d20m14.7s	2005-04-14	0013210624	irsstare	TargetMulti	SL1,SL2,LL1,LL2,SH	S13.2.0
SSTc2d_J182835.8+283548	18h28m35.8s	0d26m16.0s	2006-04-16	0015913985	irsstare	TargetMulti	SL1,SL2,LL2	S14.0.0
VV_Ser	18h28m47.9s	0d08m39.8s	2004-09-01	0005651200	irsstare	TargetFixedSingle	SL1,SL2,SH,LH	S13.2.0
SSTc2d_J182849.4+00604	18h28m49.4s	0d0-6m04.6s	2005-04-14	0013210624	irsstare	TargetMulti	SL1,SL2,LL1,LL2,SH	S13.2.0
SSTc2d_J182850.2+00950	18h28m50.2s	0d09m49.6s	2006-04-21	0013461505	irsstare	TargetMulti	SL1,SL2,LL1,LL2	S14.0.0
SSTc2d_J182850.4+00754	18h28m50.6s	0d07m54.0s	2005-09-09	0013460736	irsstare	TargetFixedSingle	LL1,LL2	S13.2.0
SSTc2d_J182850.9+04605	18h28m50.9s	0d46m05.6s	2006-04-18	0013459969	irsstare	TargetMulti	SL1,SL2,LL2	S14.0.0
SSTc2d_J182852.7+02824	18h28m52.7s	0d28m24.2s	2005-04-24	0013460224	irsstare	TargetFixedSingle	SL1,SL2,LL2	S13.2.0
SSTc2d_J182854.1+02930	18h28m54.1s	0d29m29.4s	2006-04-19	0013461249	irsstare	TargetMulti	SL1,SL2,LL1,LL2	S14.0.0
SSTc2d_J182854.5+02947	18h28m54.5s	0d29m47.0s	2006-04-19	0013460993	irsstare	TargetMulti	SL1,SL2,LL1,LL2	S14.0.0
SSTc2d_J182854.9+02952	18h28m54.9s	0d29m52.0s	2006-04-19	0013460993	irsstare	TargetMulti	SL1,SL2,LL1,LL2	S14.0.0
SSTc2d_J182859.5+03003	18h28m59.5s	0d30m02.9s	2006-04-19	0013461249	irsstare	TargetMulti	SL1,SL2,LL1,LL2	S14.0.0
SSTc2d_J182900.9+02931	18h29m00.9s	0d29m31.5s	2005-04-17	0013210112	irsstare	TargetMulti	SL1,SL2,LL1,LL2,SH	S13.2.0
SSTc2d_J182901.1+03145	18h29m01.1s	0d31m45.1s	2006-04-19	0013461249	irsstare	TargetMulti	SL1,SL2,LL1,LL2	S14.0.0
SSTc2d_J182901.2+02933	18h29m01.2s	0d29m33.2s	2006-04-21	0013461505	irsstare	TargetMulti	SL1,SL2,LL1,LL2	S14.0.0
SSTc2d_J182901.8+02946	18h29m01.8s	0d29m46.7s	2006-04-19	0013461249	irsstare	TargetMulti	SL1,SL2,LL1,LL2	S14.0.0
SSTc2d_J182901.8+02954	18h29m01.8s	0d29m54.3s	2005-04-17	0013210112	irsstare	TargetMulti	SL1,SL2,LL1,LL2,SH	S13.2.0
SSTc2d_J182902.6+03300	18h29m02.6s	0d33m00.3s	2006-04-18	0013459969	irsstare	TargetMulti	SL1,SL2,LL2	S14.0.0
SSTc2d_J182902.8+03009	18h29m02.9s	0d30m09.0s	2006-04-19	0013460993	irsstare	TargetMulti	SL1,SL2,LL1,LL2	S14.0.0
SSTc2d_J182904.4+03324	18h29m04.4s	0d33m23.7s	2006-04-21	0013461505	irsstare	TargetMulti	SL1,SL2,LL1,LL2	S14.0.0
SSTc2d_J182906.2+03043	18h29m06.2s	0d30m43.0s	2006-04-19	0013461249	irsstare	TargetMulti	SL1,SL2,LL1,LL2	S14.0.0

Table 2—Continued

Target	RA [J2000]	Dec [J2000]	Obs_date	AOR_key	AOT_type	Obs_mode	Modules	Version
SSTc2d_J182906.8+03034	18h29m06.8s	0d30m34.0s	2006-04-19	0013460993	irsstare	TargetMulti	SL1,SL2,LL1,LL2	S14.0.0
SSTc2d_J182909.8+03446	18h29m09.8s	0d34m45.8s	2005-04-14	0013210624	irsstare	TargetMulti	SL1,SL2,LL1,LL2,SH	S13.2.0
SSTc2d_J182914.0+01812	18h29m14.0s	0d18m12.0s	2006-04-18	0013459969	irsstare	TargetMulti	SL1,SL2,LL2	S14.0.0
SSTc2d_J182914.8+00424	18h29m14.8s	0d0-4m23.7s	2005-04-17	0013210112	irsstare	TargetMulti	SL1,SL2,LL1,LL2,SH	S13.2.0
SSTc2d_J182916.2+01822	18h29m16.2s	0d18m22.5s	2005-04-17	0013210112	irsstare	TargetMulti	SL1,SL2,LL1,LL2,SH	S13.2.0
SSTc2d_J182928.2+02257	18h29m28.2s	0d0-22m57.4s	2005-04-14	0013210368	irsstare	TargetMulti	SL1,SL2,LL1,LL2,SH	S13.2.0
SVS9	18h29m45.1s	1d18m47.0s	2004-09-02	0009828864	irsstare	TargetMulti	SL1,SL2	S13.2.0
SVS9	18h29m45.0s	1d18m47.0s	2005-09-09	0015913728	irsstare	TargetFixedSingle	LL2	S13.2.0
Serp-S68N	18h29m48.1s	1d16m42.5s	2004-09-01	0009828608	irsstare	TargetMulti	SH,LH	S13.2.0
EC69	18h29m54.4s	1d15m01.8s	2004-03-27	0009407232	irsstare	TargetMulti	SL1,SL2,SH,LH	S13.2.0
EC69	18h29m53.4s	1d00m00.0s	2005-04-14	0005826048	irsmap	TargetFixedSingle	SL1	S13.2.0
EC69	18h29m53.4s	1d00m00.0s	2005-04-14	0005825792	irsmap	TargetFixedSingle	SL1	S13.2.0
EC74	18h29m55.7s	1d14m31.6s	2004-03-27	0009407232	irsstare	TargetMulti	SL1,SL2,SH,LH	S13.2.0
EC74	18h29m56.2s	1d00m00.0s	2005-04-14	0005826048	irsmap	TargetFixedSingle	LL2	S13.2.0
EC74	18h29m56.2s	1d00m00.0s	2005-04-14	0005825792	irsmap	TargetFixedSingle	LL1	S13.2.0
Serp-SMM4	18h29m56.6s	1d13m15.1s	2004-09-01	0009828608	irsstare	TargetMulti	SH,LH	S13.2.0
Serp-SMM4	18h29m56.7s	1d13m15.8s	2005-04-14	0005826048	irsmap	TargetFixedSingle	LL2	S13.2.0
Serp-SMM4	18h29m56.7s	1d13m15.8s	2005-04-14	0005825792	irsmap	TargetFixedSingle	LL1	S13.2.0
EC82	18h29m56.9s	1d14m46.5s	2004-03-27	0009407232	irsstare	TargetMulti	SL1,SL2,SH,LH	S13.2.0
EC88	18h29m57.6s	1d13m00.6s	2004-03-27	0009407232	irsstare	TargetMulti	SL1,SL2,SH,LH	S13.2.0
EC90	18h29m57.8s	1d14m05.9s	2004-09-01	0009828352	irsstare	TargetFixedSingle	SL1,SL2,SH,LH	S13.2.0
EC92	18h29m57.9s	1d12m51.6s	2004-03-27	0009407232	irsstare	TargetMulti	SL1,SL2,SH,LH	S13.2.0
CK4	18h29m58.2s	1d15m21.7s	2004-03-27	0009407232	irsstare	TargetMulti	SL1,SL2,SH,LH	S13.2.0
Serp-SMM3	18h29m59.2s	1d14m00.3s	2004-09-01	0009828608	irsstare	TargetMulti	SH,LH	S13.2.0
EC118	18h30m00.6s	1d15m20.1s	2004-09-01	0011828224	irsstare	TargetFixedSingle	SL1,SL2,SH	S13.2.0
SVS8	18h30m11.5s	1d15m42.5s	2004-09-02	0009828864	irsstare	TargetMulti	SL1,SL2	S13.2.0
LkHA_348	18h34m12.6s	0d0-26m21.8s	2006-04-16	0009831424	irsstare	TargetFixedSingle	SL1,SL2,SH,LH	S14.0.0
R_CrA_IRS5	19h01m48.0s	-36d57m21.6s	2005-04-14	0009835264	irsstare	TargetFixedSingle	SL1,SL2,LL1,SH	S13.2.0
CrA_IRS7_A	19h01m55.3s	-36d57m22.0s	2005-04-14	0009835008	irsstare	TargetMulti	SL1,SL2,SH,LH	S13.2.0
CrA_IRS7_B	19h01m56.4s	-36d57m28.0s	2005-04-14	0009835008	irsstare	TargetMulti	SL1,SL2,SH,LH	S13.2.0
CrA_IRAS32	19h02m58.7s	-37d07m34.5s	2005-04-14	0009832192	irsstare	TargetFixedSingle	SL1,SL2,LL1,SH	S13.2.0
Cyg_OB2_No12	20h32m41.0s	41d14m28.9s	2004-10-23	0009834496	irsstare	TargetFixedSingle	LL1,SH,LH	S13.2.0
L1014_IRS	21h24m07.5s	49d59m09.0s	2004-10-23	0012116736	irsstare	TargetFixedSingle	SL1,SL2,LL1,LL2	S13.2.0
IRAS_23238+7401	23h25m46.6s	74d17m37.2s	2004-10-23	0009833728	irsstare	TargetFixedSingle	SL1,SL2,SH,LH	S13.2.0

Table 2—Continued

Target	RA [J2000]	Dec [J2000]	Obs_date	AOR_key	AOT_type	Obs_mode	Modules	Version
BF_Ori	5h37m13.3s	-6d35m00.6s	2004-10-03	0005638144	irsstare	TargetFixedSingle	SL1,SL2,LL1,SH,LH	S13.2.0
B1outflow	3h33m17.4s	31d09m36.0s	2005-09-08	0015915520	irsmap	TargetFixedSingle	SH	S13.2.0
Ced_110_IRS4-off	11h06m50.5s	-77d22m40.5s	2005-03-17	0013376512	irsmap	TargetFixedSingle	SH	S13.2.0
Sz102-off	16h08m28.9s	-39d03m14.9s	2005-03-18	0013377024	irsmap	TargetFixedSingle	SH	S13.2.0
IRS46-off	16h27m30.4s	-24d39m04.8s	2005-03-18	0013376000	irsmap	TargetFixedSingle	SH	S13.2.0
Haro_1-17_VSSG1-off	16h32m22.6s	-24d42m10.1s	2005-03-18	0013376256	irsmap	TargetMulti	SH	S13.2.0
SerpensCoreNW_1	18h29m50.4s	1d14m53.0s	2005-04-14	0005825792	irsmap	TargetFixedSingle	SL,LL	S13.2.0
SerpensCoreNW_2	18h29m50.5s	1d14m53.1s	2005-04-14	0005826048	irsmap	TargetFixedSingle	SL,LL	S13.2.0
EC74-69-CK4-off	18h29m58.7s	1d15m28.4s	2005-04-14	0013376768	irsmap	TargetMulti	SH	S13.2.0

Table 3. Calibration sources

Source	AOR	SL	LL	SH	LH
HD 166780	9529344	✓	✓	–	–
	9547264	✓	✓	–	–
	12601600	✓	✓	–	–
	12602880	✓	✓	–	–
	13521408	✓	✓	–	–
	13524992	✓	✓	–	–
HD 173511	8555776	✓	✓	–	–
	8561152	✓	✓	–	–
	9262848	✓	✓	–	–
	9265920	✓	✓	–	–
	10019584	✓	✓	–	–
	10047232	✓	✓	–	–
HR 5467	9094912	✓	✓	–	–
	9097984	✓	✓	–	–
	10019328	✓	✓	–	–
	10046976	✓	✓	–	–
	13520896	✓	✓	–	–
	13524480	✓	✓	–	–
HR 6348	9099520	✓	✓	–	–
	9101056	✓	✓	–	–
	13042176	✓	✓	–	–
	13046784	✓	✓	–	–
	13732352	✓	✓	–	–
	13774336	✓	✓	–	–
HR 7018	8555520	✓	✓	–	–
	8560896	✓	✓	–	–
	11814144	✓	✓	–	–
	11820544	✓	✓	–	–
	12001536	✓	✓	–	–
	12008704	✓	✓	–	–
HR 6688	13195008	–	–	✓	✓
	13349632	–	–	✓	✓
	13352960	–	–	✓	✓
	13513984	–	–	✓	✓

Table 3—Continued

Source	AOR	SL	LL	SH	LH
	13518592	–	–	✓	✓
	13732864	–	–	✓	✓
	13774848	–	–	✓	✓
	15334144	–	–	✓	✓
	15340288	–	–	✓	✓
	15669504	–	–	✓	✓
	15708160	–	–	✓	✓
	15708928	–	–	✓	✓
	15881216	–	–	✓	✓
	15883008	–	–	✓	✓
	16088832	–	–	✓	✓
	16093440	–	–	✓	✓
	16095744	–	–	✓	✓
	16294400	–	–	✓	✓
	16338432	–	–	✓	✓
	16338944	–	–	✓	✓
	16339456	–	–	✓	✓
	16339968	–	–	✓	✓
	16914432	–	–	✓	✓
	16912128	–	–	✓	✓
	16919040	–	–	✓	✓

Table 4. 1-σ flux calibration uncertainty (%) for high precision pointing

Order	— 1-σ uncertainty —			
	SL	LL	SH	LH
1	5.2	2.8	...	...
2	4.2	4.6	...	...
3	4.2	4.6	...	...
11	...	...	1.0	0.9
12	...	...	1.1	0.9
13	...	...	1.1	0.8
14	...	...	1.1	0.7
15	...	...	1.1	0.7
16	...	...	1.5	0.7
17	...	...	1.5	1.0
18	...	...	1.1	1.0
19	...	...	1.0	1.0
20	...	...	0.9	0.9

Table 5. List of Observed MIPS SED AORs

Target	RA	Dec	Obs_date	AOR_key	Chop	N_cyc	Version
CoKuTau4	04h41m16.79s	28d40m00.5s	2005-02-26	5800704	+1	4	S13.2.0
SXCha	10h55m59.74s	-77d24m39.9s	2005-03-06	5800960	+1	10	S13.2.0
Sz102	16h08m29.70s	-39d03m11.2s	2005-03-09	5801472	+2	20	S13.2.0
Haro1-1	16h21m34.69s	-26d12m27.0s	2005-03-09	5801728	+1	10	S13.2.0

Table 6. Input list for automatic feature identification

ID	em/abs/cnt	λ[a] [μm]	FWHM[b] [μm]	cont 1a[c] [μm]	cont 1b[c] [μm]	cont 2a[c] [μm]	cont 2b[c] [μm]
H2_S0	em	28.219	...	...	...	...	...
H2_S1	em	17.035	...	...	...	...	...
H2_S2	em	12.279	...	...	...	...	...
H2_S3	em	9.665	...	...	...	...	...
H2_S4	em	8.025	...	...	...	...	...
H2_S5	em	6.91	...	...	...	...	...
H2_S6	em	6.109	...	...	...	...	...
H2_S7	em	5.511	...	...	...	...	...
Ne_II	em	12.814	...	...	...	...	...
Ne_III	em	15.56	...	...	...	...	...
Fe_I	em	24.042	...	...	...	...	...
Fe_II	em	17.936	...	...	...	...	...
Fe_II	em	25.988	...	...	...	...	...
S_I	em	25.249	...	...	...	...	...
S_III	em	18.71	...	...	...	...	...
Si_II	em	34.82	...	...	...	...	...
PAH_11.3	em	11.3	0.1	10.5	10.9	11.6	12.1
PAH_12	em	12.7	0.3	11.9	12.3	13.0	13.6
PAH_6	em	6.2	0.2	5.7	6.05	6.5	6.8
PAH_7_8	em	7.7 & 8.6	0.7 & 0.4	6.8	7.10	9.0	9.3
CO_2	abs	15.15& 15.5	0.35 & 0.5	14.40	14.75	15.87	16.39
ICE_6	abs	6.0 & 6.85	0.4 & 0.3	5.40	5.65	7.20	7.60
SiO_s	abs/em	9.7 & 11.0	1.5 & 1.5	7.1	7.9	13.0	14.0
SiO_b	abs/em	18.52 & 22.0	3.0 & 3.0	13.2	14.7	25.	30.
SiO_l	em	34.0	2.0	30.5	31.5	36.0	37.5
Em_11.3	em	11.3	0.6	10	10.7	11.7	12.5
IRAC 3	cnt	5.7	...	...	...	...	...
IRAC 4	cnt	7.8	...	...	...	...	...
MIPS 24	cnt	23.5	...	...	...	...	...

[a]The center wavelength of the Gaussian fitting profile. When two wavelengths are listed, the fitting profile is composed of two Gaussian components.

[b]The full width at half maximum of the Gaussian fitting profile. When two FWHM are listed, the fitting profile is composed of two Gaussian components.

[c]The continuum is defined as from cont 1a to cont 1b on the short wavelength side of the feature and from cont 2a to cont 2b on the long wavelength side of the feature. — If the FWHM and continuum wavelengths are not defined, then the feature is either unresolved or a continuum feature. For unresolved features, the FWHM is set to the instrument resolution and the continuum regions are defined as; cont 1a= $\lambda - 4\times$FWHM, cont 1b= $\lambda - 1.5\times$FWHM, cont 2a= $\lambda + 1.5\times$FWHM, and cont 2b= $\lambda + 4\times$FWHM.

Note. — For the continuum features, IRAC 3, IRAC 4, and MIPS 24, the instrumental filter profiles are used (see Figure 15).

Table 7. List of Identified Gas-Phase Features

Feature Wavelength [μm]	H2_S0 28.2	H2_S1 17.0	H2_S2 12.3	H2_S3 9.7	H2_S4 8.0	H2_S5 6.9	H2_S6 6.1	H2_S7 5.5	Ne_II 12.8	Ne_III 15.6	Fe_I 24.0	Fe_II 17.9	Fe_II 26.0	S_I 25.2	S_III 18.7	Si_II 34.8
LDN1448_IRS1	-	-	-	-	-	-	-	-	?	-	-	✓	✓	-	-	✓
LDN1448_NA	-	✓	✓	-	-	-	-	-	✓	-	-	✓	-	-	-	✓
IRAS_03235+3004	-	-	-	-	-	-	-	-	-	-	-	✓	-	-	-	-
IRAS_03245+3002	-	?	-	-	-	-	-	-	-	-	-	-	-	-	-	-
L1455_SMM1	-	✓	-	-	-	-	-	-	✓	-	-	-	-	-	-	-
RNO_15	-	-	-	-	-	-	-	-	-	-	-	-	-	-	-	-
L1455_IRS3	-	-	-	-	-	-	-	-	?	-	-	-	-	-	-	-
IRAS_03254+3050	-	-	-	-	-	-	-	-	-	-	-	-	-	-	-	-
LkHA_325	-	-	-	-	-	-	-	-	-	-	-	-	-	-	-	-
LkHA_270	-	-	?	-	-	-	-	-	✓	-	-	-	-	-	-	-
LkHA_271	-	-	-	-	-	-	-	-	-	-	-	-	-	-	-	-
IRAS_03271+3013	-	✓	-*	-*	?	-*	-*	✓	-	-	-	✓	-	-	-	-
SSTc2d_J033036.0+303024	-	-	-	-	-	-	-	-	-	-	-	-	-	-	-	-
SSTc2d_J033037.0+303128	-	-	-	-	-	-	-	-	-	-	-	-	-	-	-	-
LkHA_326	-	-	-	-	-	-	-	-	-	-	-	-	-	-	-	-
SSTc2d_J033052.5+305418	-	-	-	-	-	-	-	-	-	-	-	-	-	-	-	-
IRAS_03292+3039	-	-	-	-	-	-	-	-	-	-	-	-	✓	-	-	✓
SSTc2d_J033241.7+311046	-	-	-	-	-	-	-	-	-	-	-	-	-	-	-	-
IRAS_03301+3111	-	-	-	-	-	-	-	-	?*	-	-	-	-	-	-	-
SSTc2d_J033314.4+310711	-	-	-	-	-	-	-	-	-	-	-	-	-	-	-	-
B1-a	-	-	-	-	-	-	-	-	✓	-	-	-	-	-	-	-
B1-c	-	-	-	-	-	-	-	-	-	-	-	-	-	-	-	-
B1-b	-	-	-	-	-	-	-	-	-	-	-	-	-	-	-	-
SSTc2d_J033327.3+310710	-	✓	?	✓	✓	✓	-	✓	✓	✓	-	✓	-	-	-	-
LkHA_327	-	-	-	-	-	-	-	-	-	-	-	-	-	-	-	-
SSTc2d_J033341.3+311341	-	-	-	-	-	-	-	-	-	-	-	-	-	-	-	-
IRAS_03380+3135	-	-	-	-	-	-	-	-	-	-	-	-	-	-	-	-
BD+31_634	-	-	-	-	-	-	-	-	-	-	-	-	-	-	-	-
SSTc2d_J034202.2+314802	-	-	-	-	-	-	-	-	-	-	-	-	-	-	-	-
SSTc2d_J034219.3+314327	-	-	-	-	-	-	-	-	-	-	-	-	-	-	-	-
RNO_19	-	-	-	-	-	-	-	-	-	-	-	-	-	-	-	-
IRAS_03406+3133	-	-	-	-	-	-	-	-	-	-	-	-	-	-	-	-
HH_211-mm	-	✓	?	-	-	-	-	-	-	-	-	-	✓	-	-	-

Table 7—Continued

Feature Wavelength [μm]	H2_S0 28.2	H2_S1 17.0	H2_S2 12.3	H2_S3 9.7	H2_S4 8.0	H2_S5 6.9	H2_S6 6.1	H2_S7 5.5	Ne_II 12.8	Ne_III 15.6	Fe_I 24.0	Fe_II 17.9	Fe_II 26.0	S_I 25.2	S_III 18.7	Si_II 34.8
SSTc2d_J034438.5+320801	-	✓	-	-	-	-	-	-	-	-	-	-	-	-	-	-
LkHA_330	-	-	-	-	-	-	-	-	-	-	-	-	-	-	-	-
IRAS_03439+3233	-	-	-	-	-	-	-	-	-	-	-	-	-	-	-	-
IRAS_03445+3242	-	-	-	-	-	-	-	-	-	-	-	✓	✓	-	-	✓
IRAS_03446+3254	-	?	-	-	-	-	-	-	?	-	-	-	-	-	-	-
IRAM_04191+1522	-	✓	-	-	-	-	-	-	-	-	-	-	-	-	-	-
Elias3_AOR1	-	-	-	-	-	-	-	-	-	-	-	-	-	-	-	-
Elias3_AOR2	-	-	-	-	-	-	-	-	-	-	-	-	-	-	-	-
LkCa_8	-	-	-	-	-	-	-	-	-	-	-	-	-	-	-	-
SSTc2d_J042838.9+265135	-	-*	-	-	-	-	-	-	-	-	-	-	-	-	-	-
IQ_Tau	-	-	-	-	-	-	-	-	?	-	-	-	-	-	-	-
FX_Tau	-	-	-	-	-	-	-	-	-	-	-	-	-	-	-	-
V710_Tau	-	-	-	-	-	-	-	-	-	-	-	-	-	-	-	-
RXJ0432.8+1735	-	-	-	-	-	-	-	-	-	-	-	-	-	-	-	-
Elias13	-	-	-	-	-	-	-	-	-	-	-	-	-	-	-	-
DN_Tau	-	-	-	-	-	-	-	-	-	-	-	-	-	-	-	-
CoKu_Tau_3	-	-	-	-	-	-	-	-	-	-	-	-	-	-	-	-
Tamura2_AOR1	-	-	-	-	-	-	-	-	-	-	-	-	-	-	-	-
Tamura2_AOR2	-	-	-	-	-	-	-	-	-	-	-	-	-	-	-	-
Elias15_AOR1	-	-	-	-	-	-	-	-	-	-	-	-	-	-	-	-
Elias15_AOR2	-	-	-	-	-	-	-	-	-	-	-	-	-	-	-	-
Elias16	-	-	-	-	-	-	-	-	-	-	-	-	-	-	-	-
Tamura8_AOR1	-	-	-	-	-	-	-	-	-	-	-	-	-	-	-	-
Tamura8_AOR2	-	-	-	-	-	-	-	-	-	-	-	-	-	-	-	-
CoKu_Tau_4	-	-	-	-	-	-	-	-	-	-	-	-	-	-	-	-
BF_Ori	-	-	-	-	-	-	-	-	-	-	-	-	-	-	-	-
RR_Tau	-	-	-	-	-	-	-	-	-	-	-	-	-	-	-	-
IRAS_08242-5050	-	-	-	-	-	-	-	-	✓	-	-	✓	-*	-	-	-
IRAS_08261-5100	-	-	-	-	-	-	-	-	-	-	-	-	-	-	-	-
IRAS_08267-3336	-	-	-	-	-	-	-	-	?	-	-	-	-	-	-	-
SX_Cha	-	-	-	-	-	-	-	-	-	-	-	-	-	-	-	-
SY_Cha	-	-	-	-	-	-	-	-	-	-	-	-	-	-	-	-
TW_Cha	-	-	-	-	-	-	-	-	-	-	-	-	-	-	-	-

Table 7—Continued

Feature Wavelength [μm]	H2_S0 28.2	H2_S1 17.0	H2_S2 12.3	H2_S3 9.7	H2_S4 8.0	H2_S5 6.9	H2_S6 6.1	H2_S7 5.5	Ne_II 12.8	Ne_III 15.6	Fe_I 24.0	Fe_II 17.9	Fe_II 26.0	S_I 25.2	S_III 18.7	Si_II 34.8
Ced_110_IRS4	-	✓	✓	-	-	-	-	-	✓	-	-	✓	-	-	-	-
Ced_110_IRS6	-	-	?	-	-	-	-	-	✓	-	-	-	-	-	-	-
B35	-	-	-	-	-	-	-	-	-	-	-	-	-	-	-	-
VW_Cha	-	-	-	-	-	-	-	-	✓	-	-	-	-	-	-	-
Hn_9	-	-	-	-	-	-	-	-	-	-	-	-	-	-	-	-
VZ_Cha	?	-	-	-	-	-	-	-	-	-	-	-	-	-	-	-
WX_Cha	-	-	-	-	-	-	-	-	-	-	-	-	-	-	-	-
ISO-Cha237	-	-	?	-	-	-	-	-	-	-	-	-	-	-	-	-
C7-11	-	-	-	-	-	-	-	-	-	-	-	-	-	-	-	-
HM_27	-	-	-	-	-	-	-	-	-	-	-	-	-	-	-	-
XX_Cha	-	-	-	-	-	-	-	-	-	-	-	-	-	-	-	-
HD_98922	-	-	-	-	-	-	-	-	-	-	-	-	-	-	-	-
HD_101412	-	-	-	-	-	-	-	-	-	-	-	-	-	-	-	-
T_Cha	-	-	-	-	-	-	-	-	✓	?	-	-	-	-	-	-
IRAS_12535-7623	-	-	-	-	-	-	-	-	-	-	-	-	-	-	-	-
ISO-ChaII_13	-	-	-	-	-	-	-	-	-	-	-	-	-	-	-	-
IRAS_12553-7651	-	-	-	-	-	-	-	-	-	-	-	-	-	-	-	-
Off_position_3	-	-	-	-	-	-	-	-	-	-	-	-	-	-	-	-
RXJ1301.0-7654	-	-	-	-	-	-	-	-	-	-	-	-	-	-	-	-
Sz50	-	-	-	-	-	-	-	-	-	-	-	-	-	-	-	-
ISO-ChaII_54	-	-	-	-	-	-	-	-	-	-	-	-	-	-	-	-
SSTc2d_J130234.5-772252	-	-	?*	-	-	-	-	-	-	-	-	-	-	-	-	-
DL_Cha	-	-	-	-	-	-	-	-	-	-	-	-	-	-	-	-
SSTc2d_J130718.0-774053	-	-	-	-	-	-	-	-	-	-	-	-	-	-	-	-
SSTc2d_J130827.2-774323	-	-	-	-	-	-	-	-	-	-	-	-	-	-	-	-
Sz62	-	-	-	-	-	-	-	-	-	-	-	-	-	?	-	-
IRAS_13546-3941	-	-	-*	-	-	-	-	-	?	-	-	-	-	-	-	-
HD_132947**	✓	?	-	-	-	-	-	-	-	-	-	-	-	-	-	-
HD_135344	-	-	-	-	-	-	-	-	-	-	-	-	-	-	-	-
IRAS_15398-3359	-	-	-	-	-	-	-	-	-	-	-	?	-	-	-	✓
HT_Lup_AOR1	-	-	-	-	-	-	-	-	-	-	-	-	-	-	-	-
HT_Lup_AOR2	-	-	-	-	-	-	-	-	-	-	-	-	-	-	-	-
GW_Lup	-	-	-	-	-	-	-	-	-	-	-	-	-	-	-	-

Table 7—Continued

Feature Wavelength [μm]	H2_S0 28.2	H2_S1 17.0	H2_S2 12.3	H2_S3 9.7	H2_S4 8.0	H2_S5 6.9	H2_S6 6.1	H2_S7 5.5	Ne_II 12.8	Ne_III 15.6	Fe_I 24.0	Fe_II 17.9	Fe_II 26.0	S_I 25.2	S_III 18.7	Si_II 34.8
HM_Lup	-	-	-	-	-	-	-	-	-	-	-	-	-	-	-	-
Sz73	-	-	-	-	-	-	-	-	✓	-	-	-	-	-	-	-
GQ_Lup	-	-	-	-	-	-	-	-	-	-	-	-	-	-	-	-
Sz76	-	-	-	-	-	-	-	-	-	-	-	-	-	-	-	-
IM_Lup	-	-	-	-	-	-	-	-	-	-	-	-	-	-	-	-
RU_Lup	-	-	-	-	-	-	-	-	-	-	-	-	-	-	-	-
Sz84	-	-	-	-	-	-	-	-	-	-	-	-	-	-	-	-
RY_Lup	-	-	-	-	-	-	-	-	-	-	-	-	-	-	-	-
SSTc2d_J160115.9-415334	-	-	-	-	-	-	-	-	-	-	-	-	-	-	-	-
SSTc2d_J160145.9-415824	-	-	-	-	-	-	-	-	-	-	-	-	-	-	-	-
SSTc2d_J160159.6-415306	-	-	-	-	-	-	-	-	-	-	-	-	-	-	-	-
EX_Lup	-	-	-	-	-	-	-	-	-	-	-	-	-	-	-	-
RXJ1603.2-3239	-	-	-	-	-	-	-	-	-	-	-	-	-	-	-	-
Sz96	-	-	-	-	-	-	-	-	-	-	-	-	-	-	-	-
Sz102	-	✓	✓	✓	-	-	-	-	✓	✓	-	✓	-	-	-	-
AS_205	-	-	-	-	-	-	-	-	-	-	-	-	-	-	-	-
SSTc2d_J161148.7-381758	-	-	-	-	-	-	-	-	-	-	-	-	-	-	-	-
SSTc2d_J161159.8-382338	-	-	-	-	-	-	-	-	-	-	-	-	-	-	-	-
RXJ1615.3-3255	-	-	-	-	-	-	-	-	?	-	-	-	-	-	-	-
Haro_1-1	-	-	-	-	-	-	-	-	✓	-	-	-	-	-	-	-
SSTc2d_J162145.1-234232	-	-	-	✓	-	-	-	✓*	-	-	-	-	-	-	-	-
SSTc2d_J162148.5-234027_AOR1	-	-	-	-	-	-	-	-	-	-	-	-	-	-	-	-
SSTc2d_J162148.5-234027_AOR2	-	-	-	-	-	-	-	-	-	-	-	-	-	-	-	-
SSTc2d_J162221.0-230403	-	-	-	-	-	-	-	✓*	-	-	-	-	-	-	-	-
SSTc2d_J162230.2-232224	-	-	-	-	-	-	-	-	-	-	-	-	-	-	-	-
SSTc2d_J162244.9-231713	-	-	-	-	-	-	-	-	-	-	-	-	-	-	-	-
SSTc2d_J162245.4-243124	-	-	-	-	-	-	-	-	-	-	-	-	-	-	-	-
SSTc2d_J162305.9-233818	-	-	-	-	-	-	-	-	-	-	-	-	-	-	-	-
SSTc2d_J162332.8-225847	-	-	-	-	-	-	-	-	-	-	-	-	-	-	-	-
Off_position_1	✓	✓	✓	-	-	-	-	-	-	-	-	-	✓	-	-	✓
Haro_1-4	-	-	-	-	-	-	-	-	?	-	-	-	-	-	-	-
CRBR_2317.3-1925	-	✓	-	-	-	-	-	-	-	-	-	-	-	-	-	-
VSSG1	✓	✓	✓	-	-	-	-	-	-	-	-	-	-	-	-	✓

Table 7—Continued

Feature Wavelength [μm]	H2_S0 28.2	H2_S1 17.0	H2_S2 12.3	H2_S3 9.7	H2_S4 8.0	H2_S5 6.9	H2_S6 6.1	H2_S7 5.5	Ne_II 12.8	Ne_III 15.6	Fe_I 24.0	Fe_II 17.9	Fe_II 26.0	S_I 25.2	S_III 18.7	Si_II 34.8
GSS30-IRS1	-	-	-	-	-	-	-	-	-	-	-	-	?	-	-	-
DoAr_24E	?	-	?	-	-	-	-	-	?	-	-	-	-	-	-	-
GY23	-	-	-	-	-	-	-	-	-	-	-	-	-	-	-	-
VLA_1623-243	✓	✓	✓	-	-	-	-	-	-	-	-	-	-	-	-	-
IRS14	✓	✓	✓	-	-	-	-	-	-	-	-	-	-	-	-	-
WL12	-	-	-	-	-	-	-	-	?	-	-	-	-	-	-	-
Off_position_2		✓		-	-	-	-	-	-	-	-	-	-	-	-	✓*
OphE-MM3	-	-	-	-	-	-	-	-	-	-	-	-	-	-	-	-
SR_21	?	-	-	-	-	-	-	-	-	-	-	-	-	-	-	-
GY224	-	-	-	-	-	-	-	-	-	-	-	-	-	-	-	-
WL19	?	-	-	-	-	-	-	-	-	-	-	-	-	-	-	-
SSTc2d_J162715.1-245139	-	-	-	-	-	-	-	-	-	-	-	-	-	-	-	-
WL20S	-	-	-	-	-	-	-	-	✓	-	-	✓	-	-	-	-
IRS37	-	-	-	-	-	-	-	-	✓	-	-	-	-	-	-	-
IRS42	-	-	-	-	-	-	-	-	-	-	-	-	-	-	-	-
WL6	-	-	-	-	-	-	-	-	-	-	-	-	-	-	-	-
CRBR_2422.8-3423	-	-	?	-	-	-	-	-	-	-	-	-	-	-	-	-
Elias32	-	-	?	-	-	-	-	-	-	-	-	-	-	-	-	-
IRS46	✓	-	-	-	-	-	-	-	-	-	-	-	-	-	-	-
VSSG17	✓	✓	-	-	-	-	-	-	-	-	-	?	-	-	-	✓
IRS51	-	-	-	-	-	-	-	-	-	-	-	-	-	-	-	-
SR_9	-	-	✓	-	-	-	-	-	?	-	-	-	-	-	-	-
2MASS_16282-2432	-	-	-	?*	-	-	-	-	-	-	-	-	-	-	-	-
SSTc2d_J162816.7-240514	-	-	-	-	-	-	-	-	-	-	-	-	-	-	-	-
V853Oph	-	-	✓	-	-	-	-	-	?	-	-	-	-	-	-	-
SSTc2d_J163023.8-245951	-	-	-	-	-	-	-	-	-	-	-	-	-	-	-	-
SSTc2d_J163027.1-245405	-	-	-	-	-	-	-	-	-	-	-	-	-	-	-	-
ROX42C	-	-	-	-	-	-	-	-	-	-	-	-	-	-	-	-
ROX43A	-	-	-	-	-	-	-	-	-	-	-	-	-	-	-	-
IRS60	-	-	-	-	-	-	-	-	-	-	-	-	-	-	-	-
Haro_1-16	-	-	-	-	-	-	-	-	-	-	-	-	-	-	-	-
SSTc2d_J163135.3-250832	-	-	-	-	-	-	-	-	-	-	-	-	-	-	-	-
IRS63	-	-	-	-	-	-	-	-	-	-	-	-	-	-	-	-

Table 7—Continued

Feature Wavelength [μm]	H2_S0 28.2	H2_S1 17.0	H2_S2 12.3	H2_S3 9.7	H2_S4 8.0	H2_S5 6.9	H2_S6 6.1	H2_S7 5.5	Ne_II 12.8	Ne_III 15.6	Fe_I 24.0	Fe_II 17.9	Fe_II 26.0	S_I 25.2	S_III 18.7	Si_II 34.8
SSTc2d_J163142.3-252501	-	-	-	-	-	-	-	-	-	-	-	-	-	-	-	-
L1689-IRS5	-	-	?	-	-	-	-	-	?	-	-	-	-	-	-	-
L1689-IRS7	-	-	-	-	-	-	-	-	-	-	-	-	-	-	-	-
Haro_1-17	-	✓	✓	-	-	-	-	-	-	-	-	-	-	-	-	-
IRAS_16293-2422B	-	✓	-*	-	-	-	-	-	-	-	-	-	-	✓	-	-
IRAS_16293-2422	-	✓	✓	-*	?	-	-	-	-	-	-	-	-	?	-	-
SSTc2d_J163322.9-251341	-	-	-	-	-	-	-	-	-	-	-	-	-	-	-	-
SSTc2d_J163346.2-242753	-	-	-	-	-	-	-	-	-	-	-	-	-	-	-	-
RNO_90	-	-	-	-	-	-	-	-	-	-	-	-	-	-	-	-
RNO_91	-	-	?	-	-	-	-	-	✓	-	-	✓	✓	-	-	-
SSTc2d_J164136.3-235640	-	-	-	-	-	-	-	-	-	-	-	-	-	-	-	-
Wa_Oph_6	-	-	-	-	-	-	-	-	-	-	-	-	-	-	-	-
V1121_Oph	-	-	-	-	-	-	-	-	-	-	-	-	-	-	-	-
IRAS_16544-1604	-	-	-	-	-	-	-	-	-	-	-	-	-	-	-	-
HD_163296_AOR1	-	-	-	-	-	-	-	-	-	-	-	-	-	-	-	-
HD_163296_AOR2	-	-	-	-	-	-	-	-	-	-	-	-	-	-	-	-
SSTc2d_J181617.4-23241	-	?	-	-	-	-	-	-	-	-	-	-	-	-	-	-
SSTc2d_J182813.2+00313	-	-	-	-	-	-	-	-	?	-	-	-	-	-	-	-
SSTc2d_J182830.0+02015	-	-	-	-	-	-	-	-	-	-	-	-	-	-	-	-
SSTc2d_J182835.8+283548	-	-	-	-	-	-	-	-	-	-	-	-	-	-	-	-
VV_Ser	-	-	-	-	-	-	-	-	-	-	-	-	-	-	-	-
SSTc2d_J182849.4+00604	-	-	-	-	-	-	-	-	-	-	-	-	-	-	-	-
SSTc2d_J182850.2+00950	-	-	-	-	-	-	-	-	-	-	-	-	-	-	-	-
SSTc2d_J182850.4+00754	-	✓	-	-	-	-	-	-	-	-	-	-	-	-	-	-
SSTc2d_J182850.9+04605	-	-	-	-	-	-	-	-	-	-	-	-	-	-	-	-
SSTc2d_J182852.7+02824	-	-	-	-	-	-	-	-	-	-	-	-	-	-	-	-
SSTc2d_J182854.1+02930	-	-	-	-	-	-	-	-	-	-	-	✓*	-	-	-	-
SSTc2d_J182854.5+02947	-	-	-	-	-	-	-	-	-	-	-	-	-	-	-	-
SSTc2d_J182854.9+02952	-	-	-	-	-	-	-	-	-	-	-	-	-	-	-	-
SSTc2d_J182859.5+03003	-	-	-	-	-	-	-	-	-	-	-	-	-	-	-	-
SSTc2d_J182900.9+02931	-	-	-	-	-	-	-	-	-	-	-	-	-	-	-	-
SSTc2d_J182901.1+03145	-	-	-	-	-	-	-	-	-	-	-	-	-	-	-	-
SSTc2d_J182901.2+02933	-	-	-	-	-	-	-	-	-	-	-	-	-	-	-	-

Table 7—Continued

Feature Wavelength [μm]	H2_S0 28.2	H2_S1 17.0	H2_S2 12.3	H2_S3 9.7	H2_S4 8.0	H2_S5 6.9	H2_S6 6.1	H2_S7 5.5	Ne_II 12.8	Ne_III 15.6	Fe_I 24.0	Fe_II 17.9	Fe_II 26.0	S_I 25.2	S_III 18.7	Si_II 34.8
SSTc2d_J182901.8+02946	-	-	-	-	-	-	-	-	-	-	-	-	-	-	-	-
SSTc2d_J182901.8+02954	-	✓	?	-	-	-	-	-	-	?	-	-	-	-	-	-
SSTc2d_J182902.6+03300	-	-	-	-	-	-	-	-	-	-	-	-	-	-	-	-
SSTc2d_J182902.8+03009	-	✓	-	-	-	-	-	-	-	-	-	-	-	-	-	-
SSTc2d_J182904.4+03324	-	-	-	-	-	-	-	-	-	-	-	-	-	-	-	-
SSTc2d_J182906.2+03043	-	-	-	-	-	-	-	-	-	-	-	-	-	-	-	-
SSTc2d_J182906.8+03034	-	?	-	-	✓	✓	✓	✓	-	-	-	-	-	-	-	-
SSTc2d_J182909.8+03446	-	-	-	-	-	-	-	-	-	-	-	-	-	-	-	-
SSTc2d_J182914.0+01812	-	-	-	-	-	-	-	-	-	-	-	-	-	-	-	-
SSTc2d_J182914.8+00424	-	-	-	-	-	-	-	-	-	-	-	-	-	-	-	-
SSTc2d_J182916.2+01822	-	-	-	-	-	-	-	-	-	-	-	-	-	-	-	-
SSTc2d_J182928.2+02257	-	-	-	-	-	-	-	-	✓	-	-	-	-	-	✓	-
SVS9_AOR1	-	-	-	-	-	-	-	-	-	-	-	-	-	-	-	-
SVS9_AOR2	-	-	-	-	-	-	-	-	-	-	-	-	-	-	-	-
Serp-S68N	-	✓	✓	-	-	-	-	-	-	-	-	-	-	✓	-	?
EC69_AOR1	-	✓	✓	-	-	-	-	-	-	-	-	-	-	-	-	?
EC69_AOR2	-	-	-	-	-	-	-	-	-	-	-	-	-	-	-	-
EC69_AOR3	-	-	-	-	-	-	-	-	-	-	-	-	-	-	-	-
EC74_AOR1	-	✓	✓	-	-	-	-	-	✓	-	-	-	-	-	-	-
EC74_AOR2	-	✓	-	-	-	-	-	-	-	-	-	-	-	-	-	-
EC74_AOR3	✓	-	-	-	-	-	-	-	-	-	-	-	-	-	-	-
Serp-SMM4_AOR1	✓	✓	✓	-	-	-	-	-	-	-	-	-	?	✓	-	✓
Serp-SMM4_AOR2	-	-	-	-	-	-	-	-	-	-	-	?	-	-	-	-
Serp-SMM4_AOR3	-	-	-	-	-	-	-	-	-	-	-	-	-	-	-	-
EC82	-	-	✓	-	-	-	-	-	?	-	-	-	-	-	-	-
EC88	-	-	-	-	-	-	-	-	-	-	-	-	-	-	-	-
EC90	-	-	-	-	-	-	-	-	-	-	-	-*	-	-	-	-
EC92**	-	-	✓	-	-	-	-	-	✓	-	-	-	-	-	-	-
CK4	-	✓	✓	-	-	-	-	-	-	-	-	-	-	-	-	✓
Serp-SMM3	-	✓	✓	-	-	-	-	-	-	-	-	✓	✓	✓	-	✓
EC118	-	✓	-	-	-	-	-	-	-	-	-	-	-	-	-	-
SVS8	-	-	-	-	-	-	-	-	-	-	-	-	-	-	-	-
LkHA_348	-	-	-	-	-	-	-	-	-	-	-	-	-	-	-	-

Table 7—Continued

Feature Wavelength [μm]	H2_S0 28.2	H2_S1 17.0	H2_S2 12.3	H2_S3 9.7	H2_S4 8.0	H2_S5 6.9	H2_S6 6.1	H2_S7 5.5	Ne_II 12.8	Ne_III 15.6	Fe_I 24.0	Fe_II 17.9	Fe_II 26.0	S_I 25.2	S_III 18.7	Si_II 34.8
R_CrA_IRS5	-	-	-	-	-	-	-	-	✓	?	-	-	-	-	✓	-
CrA_IRS7_A	-	-	-	-	-	-	-	-	✓	?	-	✓	-	-	✓	-
CrA_IRS7_B	-	✓	-	-	-	-	-	-	✓	-*	-	-	-	-	?	-
CrA_IRAS32	-	-	-	✓	-	-	-	-	✓	-	-	✓	-	-	-	-
Cyg_OB2_No12	-	-	-	-	-	-	-	-	✓	✓	-	-	-	-	✓	✓
L1014_IRS	-	-	-	-	-	-	-	-	-	-	-	-	-	-	-	-
IRAS_23238+7401	-	-	-	-	-	-	-	-	✓	-	-	-	-	-	-	-
BF_Ori	-	-	-	-	-	-	-	-	-	-	-	-	-	-	-	-

*Automated feature identification is suspect. Please check log file for details.

**A nearby source was within the slit for some modules. Please see log files for details. Frature identification is thus difficult.

Table 8. List of Identified Solid-state Features

Feature	PAH_11.3	PAH_12	PAH_6	PAH_7_8	CO_2	ICE_6	SiO_s	SiO_b	SiO_l	Em_11.3	irac3	irac4	mips24
Wavelength [μm]	11.3	12.7	6.2	7.7/8.6	15.1	6.0	9.7	18.6	34.0	11.3	5.8	8.0	24.0
Units	-	-	-	-	-	-	-	-	-	-	(mJy)	(mJy)	(mJy)
LDN1448_IRS1	-	-	-	-	✓	?	✓(A)	✓(E)	-	✓	377	456	2312
LDN1448_NA	-	-	-	-	✓	✓	✓(A)	✓(A)	-	-	63	145	3919
IRAS_03235+3004	-	-	-	-	✓	✓	✓(A)	-	-	-	10	11	497
IRAS_03245+3002	-	-	-	-	-	✓	-*	-	-	-	5	6	2525
L1455_SMM1	-	-	-	-	✓	✓	✓(A)	-	-	-	7	13	815
RNO_15	-	-	-	-	✓	?	✓(E)	✓(E)	-	?	706	1113	1769
L1455_IRS3	-	-	-	-	✓	?	-	? (E)	-	-	37	58	269
IRAS_03254+3050	-	-	-	-	✓	✓	✓(A)	-	-	-	214	225	1429
LkHA_325	-	-	-	-	-	-	✓(E)	? (E)	-	✓	329	408	435
LkHA_270	-	-	-	-	-	-	? (E)	-	-	-	347	360	556
LkHA_271	-	-	-	-	-	-	✓(E)	-	-	-	77	65	133
IRAS_03271+3013	-	-	-	-	✓	✓	✓(A)	✓(A)	-	-	17	37	1814
SSTc2d_J033036.0+303024	-	✓	-	-	?	?	✓(E)	✓(E)	-	✓	406	418	631
SSTc2d_J033037.0+303128	-	-	-	-	✓	?	✓(E)	? (E)	-	-	250	268	331
LkHA_326	-	-	-	-	?	?	✓(E)	? (E)	-	?	270	284	817
SSTc2d_J033052.5+305418	-	-	-	-	✓	-	✓(E)	? (E)	-	✓	35	43	115
IRAS_03292+3039	-	-	-	-	-	-	-	✓(E)	?	-	-	-	18
SSTc2d_J033241.7+311046	-	-	-	-	-	-	✓(E)	✓(E)	-	-	21	26	130
IRAS_03301+3111	-	-	-	-	-	?	✓(A)	-	-	-	335	639	4277
SSTc2d_J033314.4+310711	-	-	-	-	✓	-	-	✓(A)	-	-	-	-	120
B1-a	-	-	-	-	✓	✓	✓(A)	? (A)	-	-	72	84	1849
B1-c	-	-	-	-	✓	✓	✓(A)	-	-	-	76	159	1320
B1-b	-	-	-	-	✓	✓	✓(A)	? (A)	-	-	21	26	210
SSTc2d_J033327.3+310710	-	-	-	-	✓	?	? (A)	-	-	-	2	4	554
LkHA_327	-	-	-	-	-	-	✓(E)	-	✓	-*	811	805	1076
SSTc2d_J033341.3+311341	-	-	-	-	-	-	-	-	-	✓	81	85	175
IRAS_03380+3135	-	-	✓	✓	-	-	✓(A)	-	-	✓*	383	321	784
BD+31_634	-	-	-	-	-	-	✓(E)	-	-	-	29	49	169
SSTc2d_J034202.2+314802	-	-	-	-	✓	-	-	? (E)	-	-	-	-	138
SSTc2d_J034219.3+314327	-	-	-	-	-	-	✓(E)	-	-	✓	47	50	126
RNO_19	✓	✓	✓	✓	?*	-	? (A)*	-	-	✓	333	467	233
IRAS_03406+3133	-	-	-	-	-	-	✓(E)	? (E)	-	✓	191	230	530

Table 8—Continued

Feature	PAH_11.3	PAH_12	PAH_6	PAH_7_8	CO_2	ICE_6	SiO_s	SiO_b	SiO_l	Em_11.3	irac3	irac4	mips24
Wavelength [μm]	11.3	12.7	6.2	7.7/8.6	15.1	6.0	9.7	18.6	34.0	11.3	5.8	8.0	24.0
Units	-	-	-	-	-	-	-	-	-	-	(mJy)	(mJy)	(mJy)
HH_211-mm	?	-	-	-	-	-	✓(A)*	-	-	-	-	-	170
SSTc2d_J034438.5+320801	-	-	-	-	-	-	✓(E)	? (E)*	-	-	28	34	147
LkHA_330	✓	-	✓	?	?*	-	✓(E)	-	-	-	787	667	3270
IRAS_03439+3233	-	-	-	-	✓	?	✓(A)	-	-	-	109	133	694
IRAS_03445+3242	-	-	-	-	✓	✓	✓(A)	✓(A)	-	-	1066	1312	3574
IRAS_03446+3254	-	-	-	-	-	-	-	-	-	✓	120	155	473
IRAM_04191+1522	-	-	-	-	-	-	-	-	-	-	-	-	16
Elias3_AOR1	-	-	-	-	-	✓	✓(A)	-	-	-	861	495	-
Elias3_AOR2	-	-	-	-	-	✓	✓(A)	-	-	-	896	509	-
LkCa_8	-	-	-	-	-	-	✓(E)	? (E)	-	✓	-	-	305
SSTc2d_J042838.9+265135	-	-	-	-	?	-	-	-	-	-	-	-	31
IQ_Tau	-	-	-	-	-	-	✓(E)	? (E)	-	✓	-	-	518
FX_Tau	-	-	-	-	-	-	✓(E)	✓(E)	-	✓	-	-	486
V710_Tau	-	-	-	-	-	-	✓(E)	-	-	✓	-	-	297
RXJ0432.8+1735	-	-	-	-	-	-	-	-	-	-	28	16	18
Elias13	-	-	-	-	-	✓	✓(A)	-	-	-	1369	780	-
DN_Tau	-	-	-	-	-	-	-	? (E)	-	-	-	-	494
CoKu_Tau_3	-	-	-	-	✓	-	✓(E)	? (E)	-	✓	-	-	372
Tamura2_AOR1	-	-	-	-	-	-	✓(A)	-	-	-	373	217	-
Tamura2_AOR2	-	-	-	-	-	-	-	-	-	-	-	-	-
Elias15_AOR1	-	-	-	-	-	✓	✓(A)	-	-	-	518	304	-
Elias15_AOR2	-	-	-	-	✓	-	-	✓(A)	-	-	-	-	-
Elias16	-	-	-	-	-	✓	✓(A)	-	-	-	4258	2435	-
Tamura8_AOR1	-	-	-	-	-	✓	✓(A)	-	-	-	470	281	-
Tamura8_AOR2	-	-	-	-	✓	-	-	-	-	-	-	-	-
CoKu_Tau_4	-	-	-	-	?*	-	-	✓(E)	-	-	-	-	936
BF_Ori	-	-	-	-	✓	-	✓(E)	✓(E)	-	✓	605	1000	970
RR_Tau	✓	✓	✓	✓	-	-	✓(E)	✓(E)	?	?	1052	1380	1846
IRAS_08242-5050	-	-	-	-	✓	✓	✓(A)	✓(A)	-	-	637	1074	6545
IRAS_08261-5100	-	-	-	-	-	-	✓(A)	✓(E)	-	-	523	662	2850
IRAS_08267-3336	-	-	-	-	?	-	✓(E)	✓(E)	-	?	152	224	947
SX_Cha	-	-	-	-	?	-	✓(E)	? (E)	-	✓	-	-	760

Table 8—Continued

Feature	PAH_11.3	PAH_12	PAH_6	PAH_7_8	CO_2	ICE_6	SiO_s	SiO_b	SiO_l	Em_11.3	irac3	irac4	mips24
Wavelength [μm]	11.3	12.7	6.2	7.7/8.6	15.1	6.0	9.7	18.6	34.0	11.3	5.8	8.0	24.0
Units	-	-	-	-	-	-	-	-	-	-	(mJy)	(mJy)	(mJy)
SY_Cha	-	-	-	-	?	-	✓(E)	✓(E)	-	✓	-	-	456
TW_Cha	-	-	-	-	-	-	✓(E)	✓(E)	-	-	-	-	296
Ced_110_IRS4	?	-	-	-	✓	-	-	-	-	-	-	-	1042
Ced_110_IRS6	-	-	-	-	✓	-	✓(E)	-	-	-	-	-	1580
B35	-	-	-	-	✓	-	✓(E)	-	?	?	-	-	312
VW_Cha	-	-	-	-	-	-	✓(E)	-	-	✓	-	-	1352
Hn_9	-	-	-	-	✓	-	✓(E)	✓(E)	-	✓*	167	169	298
VZ_Cha	-	-	-	-	-	-	✓(E)	-	-	✓*	-	-	425
WX_Cha	-	-	-	-	-	-	✓(E)	-	-	✓	-	-	422
ISO-Cha237	-	-	-	-	✓	-	✓(E)	? (E)	-	✓*	-	-	862
C7-11	-	-	-	-	-	-	✓(E)	-	-	✓	-	-	303
HM_27	-	-	-	-	-	-	✓(E)	-	-	-	-	-	502
XX_Cha	-	-*	-	-	-	-	✓(E)	-	-	✓*	-	-	276
HD_98922	-	✓*	-	-	?	-	✓(E)	✓(E)	-	✓	-	-	21768
HD_101412	-	-	✓	✓	-	-	✓(E)	✓(E)	✓	✓	1773	2139	2414
T_Cha	✓	-	-	-	-	-	✓(E)	? (A)*	-	-	-	-	1329
IRAS_12535-7623	-	-	-	-	✓	-	✓(E)	? (E)	?	✓	-	-	437
ISO-ChaII_13	-	-	-	-	-	-	-*	-	-	-*	6	6	9
IRAS_12553-7651	-	-	-	-	✓	✓	✓(A)	✓(A)	-	-	565	586	3420
Off_position_3	-	?	-	-	-	-	-	-	-	-	-	-	-13
RXJ1301.0-7654	-	-	-	-	-	-*	✓(E)	✓(E)	-	?*	26	40	139
Sz50	-	-	-	-	-	-	✓(E)	-	-	✓	-	-	440
ISO-ChaII_54	-	?	-	-	✓*	✓	-	✓(E)	-	✓	319	219	630
SSTc2d_J130234.5-772252	-*	-*	-*	-*	-	-	-	-	-	-	1	3	-
DL_Cha	-	✓	-	-	-	-	-	✓(E)	-	✓	-	-	17159
SSTc2d_J130718.0-774053	-	-	-	-	-	-	✓(E)	-	-	?	7	7	-
SSTc2d_J130827.2-774323	-	-	-	-	-	-	-*	-	-	-	2	3	-
Sz62	-	-	-	-	-	-	-	? (E)	-	-	64	61	123
IRAS_13546-3941	-	-	-	-	✓	✓	-*	-	-	-	304	373	1229
HD_132947**	-	-	-	-	-	-	-	? (E)	-	-	123	36	93
HD_135344	✓	-	-	-	?*	-	✓(E)*	? (A)*	-	?	-	-	4579
IRAS_15398-3359	-	-	-	-	✓	✓	✓(A)	? (A)	-	-	48	85	1006

Table 8—Continued

Feature	PAH_11.3	PAH_12	PAH_6	PAH_7_8	CO_2	ICE_6	SiO_s	SiO_b	SiO_l	Em_11.3	irac3	irac4	mips24
Wavelength [μm]	11.3	12.7	6.2	7.7/8.6	15.1	6.0	9.7	18.6	34.0	11.3	5.8	8.0	24.0
Units	-	-	-	-	-	-	-	-	-	-	(mJy)	(mJy)	(mJy)
HT_Lup_AOR1	-	-	-	-	-	-	✓(E)	✓(E)	-	✓	1603	1937	3454
HT_Lup_AOR2	-	-	-	-	-	-	✓(E)	-*	-	?	1506	1985	3499
GW_Lup	-	-	-	-	-	-	✓(E)	-	-	?*	96	111	264
HM_Lup	-	-	-	-	-	-	✓(E)	✓(E)	-	✓	80	104	238
Sz73	-	-	-	-	?	?	✓(E)	✓(E)	-	✓*	302	391	1156
GQ_Lup	-	-	-	-	-	-	✓(E)	✓(E)	-	-	648	561	834
Sz76	-	-	-	-	-	-	✓(E)	-	-	-	24	28	69
IM_Lup	-	-	-	-	-	-	✓(E)	✓(E)	-	✓*	277	359	861
RU_Lup	-	-	-	-	-	?	✓(E)	? (E)	-	✓	1044	1166	3147
Sz84	-	-	-	-	-	-	-	? (A)*	-	-	17	11	33
RY_Lup	?	-	-	-	✓	?	✓(E)	✓(E)	-	-	813	891	2960
SSTc2d_J160115.9-415334	-	-	-	-	-	?	✓(A)	-	-	-	32	19	-
SSTc2d_J160145.9-415824	-	-	-	-	-	-	✓(A)	-	-	-	41	24	-
SSTc2d_J160159.6-415306	-	-	-	-	-	?	✓(A)	-	-	-	32	18	-
EX_Lup	-	-	-	-	-	-	✓(E)	✓(E)	-	✓	238	405	975
RXJ1603.2-3239	-	-	-	-	-	-	-	-	-	-	28	16	11
Sz96	?*	-	-	-	-	-	✓(E)	✓(E)	-	✓*	131	151	227
Sz102	-	-	-	-	✓	-	✓(E)	✓(E)	-	✓*	23	57	372
AS_205	-	-	-	-	-	-	✓(E)	✓(E)	-	✓	4909	5681	12367
SSTc2d_J161148.7-381758	-	-	-	-	-	-	-	-	-	?	10	10	26
SSTc2d_J161159.8-382338	-	-	-	-	-	-	✓(E)	-	-	✓	8	10	22
RXJ1615.3-3255	-	-	-	-	-	-	✓(E)	✓(E)	-	✓	40	60	412
Haro_1-1	-	-	-	-	-	-	✓(E)	✓(E)	-	?	79	96	479
SSTc2d_J162145.1-234232	✓	✓	-	-	✓*	-	-	-	-	-	14	16	343
SSTc2d_J162148.5-234027_AOR1	-	-	-	-	-	-	✓(E)	-	-	?*	8	14	92
SSTc2d_J162148.5-234027_AOR2	-	-	-	-	-	-	✓(E)	? (E)	-	✓	10	16	88
SSTc2d_J162221.0-230403	-	-	-	-	✓	-	✓(E)	✓(E)	-	✓	0	8	144
SSTc2d_J162230.2-232224	-	-	-	-	-	-	-	-	-	-	0	1	-
SSTc2d_J162244.9-231713	-	-	-	-	-	-	✓(E)	-	-	?	2	3	-
SSTc2d_J162245.4-243124	-	-	-	-	-	-	✓(E)	? (E)	-	✓	54	64	400
SSTc2d_J162305.9-233818	-	-	-	-	-	-	-	-	-	-	2	2	-
SSTc2d_J162332.8-225847	-	-	-	-	-	-	✓(E)	-	-	✓	27	26	39

Table 8—Continued

Feature	PAH_11.3	PAH_12	PAH_6	PAH_7_8	CO_2	ICE_6	SiO_s	SiO_b	SiO_l	Em_11.3	irac3	irac4	mips24
Wavelength [μm]	11.3	12.7	6.2	7.7/8.6	15.1	6.0	9.7	18.6	34.0	11.3	5.8	8.0	24.0
Units	-	-	-	-	-	-	-	-	-	-	(mJy)	(mJy)	(mJy)
Off_position_1	✓	✓	-	-	-	-	✓(A)	-	-	-	-	-	158
Haro_1-4	?	-	-	-	-	-	✓(E)	✓(E)	-	-	-	-	1058
CRBR_2317.3-1925	-	-	-	-	✓	-	-	-	-	-	-	-	78
VSSG1	✓	-	-	-	-	-	-	-	-	-	-	-	919
GSS30-IRS1	-	-	-	-	✓	-	✓(A)	-	-	-	-	-	69891
DoAr_24E	-	-	-	-	-	-	✓(E)	? (E)	-	✓	-	-	3799
GY23	-	-	-	-	?	-	✓(A)	-	-	✓	-	-	2409
VLA_1623-243	✓	-	-	-	-	-	✓(A)	-	-	-	-	-	201
IRS14	✓	?	-	✓	-	-	✓(A)	-	-	-	1906	1143	94
WL12	-	-	-	-	✓	-	✓(A)	✓(A)	-	-	-	-	7451
Off_position_2	?	-	-	-	-	-	✓(A)	-	-	-	-	-	191
OphE-MM3	-	-	-	-	-	-	✓(A)*	-	-	-	2	2	733
SR_21	?	-	-	-	✓*	-	-	-	-	?	-	-	18244
GY224	-	-	-	-	✓	-	-	-	-	?	-	-	1007
WL19	-	-	-	-	✓	-	✓(A)	-	-	-	-	-	249
SSTc2d_J162715.1-245139	-	-	-	-	-	-	✓(E)	✓(E)	-	✓	41	35	169
WL20S	-	-	-	-	✓	-	-	-	-	?	-	-	7140
IRS37	-	-	-	-	✓	-	✓(A)	? (A)	-	-	-	-	1217
IRS42	-	-	-	-	✓	-	-	? (E)	-	✓	-	-	3689
WL6	-	-	-	-	✓	-	✓(A)	✓(A)	-	-	-	-	4893
CRBR_2422.8-3423	-	-	-	-	✓	✓	✓(A)	✓(A)	-	-	184	180	1430
Elias32	-	-	-	-	✓	-	✓(A)	-	-	✓	-	-	813
IRS46	-	-	-	-	✓	-	✓(A)	-	-	?	-	-	1613
VSSG17	-	-	-	-	✓	-	✓(A)	-	?	✓	-	-	2091
IRS51	-	-	-	-	✓	-	-	-	-	✓	-	-	3143
SR_9	-	-	-	-	?	-	✓(E)	✓(E)	-	✓	-	-	1230
2MASS_16282-2432	-	-	-	-	-	-	-	-	-	-	0	0	3
SSTc2d_J162816.7-240514	-	-	-	-	-	-	✓(E)	✓(E)	-	✓	122	102	131
V853Oph	-	-	-	-	-	-	✓(E)	✓(E)	-	✓	-	-	690
SSTc2d_J163023.8-245951	-	-	-	-	-	-	? (A)	-	-	-	86	49	-
SSTc2d_J163027.1-245405	-	-	-	-	-	-	? (A)	-	-	-	453	259	-
ROX42C	-	?	-	-	-	-	✓(E)	✓(E)	-	✓	-	-	819

Table 8—Continued

Feature	PAH_11.3	PAH_12	PAH_6	PAH_7_8	CO_2	ICE_6	SiO_s	SiO_b	SiO_l	Em_11.3	irac3	irac4	mips24
Wavelength [μm]	11.3	12.7	6.2	7.7/8.6	15.1	6.0	9.7	18.6	34.0	11.3	5.8	8.0	24.0
Units	-	-	-	-	-	-	-	-	-	-	(mJy)	(mJy)	(mJy)
ROX43A	-	-	-	-	✓	-	✓(E)	✓(E)	?	✓	-	-	3638
IRS60	-	-	-	-	-	-	✓(E)	✓(E)	-	✓	-	-	1447
Haro_1-16	-	-	-	-	?	-	✓(E)	✓(E)	-	✓	-	-	1986
SSTc2d_J163135.3-250832	-	-	-	-	-	-	✓(A)	-	-	-	204	116	-
IRS63	-	-	-	-	✓	-	✓(A)	-	-	-	-	-	4064
SSTc2d_J163142.3-252501	-	-	-	-	-	-	? (A)	-*	-	-	99	53	-
L1689-IRS5	-	-	-	-	✓	-	-	-	-	-	-	-	3400
L1689-IRS7	-	-	-	-	?	-	✓(E)	-	-	-	-	-	426
Haro_1-17	?	-	-	-	-	-	✓(E)	✓(E)	-	-	78	100	257
IRAS_16293-2422B	-	-	-	-	-	-	✓(A)	-	-	-	0	0	1255
IRAS_16293-2422	-*	-	-	-	-	-	? (A)*	-	-	-	1	0	763
SSTc2d_J163322.9-251341	-	-	-	-	-	-	? (A)	-	-	-	111	64	-
SSTc2d_J163346.2-242753	-	-	-	-	-	-	✓(A)	-	-	-	145	93	-
RNO_90	-	-	-	-	-	-	✓(E)	✓(E)	-	?	1963	1975	3753
RNO_91	-	-	-	-	✓	✓	✓(A)	✓(A)	-	-	1435	1468	5614
SSTc2d_J164136.3-235640	?*	-	-	-	-	-	✓(A)	-	-	-	236	154	-
Wa_Oph_6	-	-	-	-	-	-	✓(E)	✓(E)	-	✓	841	907	912
V1121_Oph	-	-	-	-	✓	-	✓(E)	? (E)	-	✓	1117	2188	4031
IRAS_16544-1604	-	-	-	-	✓	-	-	-	-	-	-	-	764
HD_163296_AOR1	-	-	-	-	✓*	-	✓(E)	✓(E)	-	✓	-	-	15889
HD_163296_AOR2	-	-	-	-	?*	-	✓(E)	✓(E)	-	✓	-	-	16888
SSTc2d_J181617.4-23241	-	-	-	-	✓	-	-	-	-	✓	18	24	44
SSTc2d_J182813.2+00313	-	-	-	-	-	-	? (A)	-	-	?	762	533	217
SSTc2d_J182830.0+02015	-	-	-	-	-	-	-	-	-	-	1647	1191	658
SSTc2d_J182835.8+283548	-	-	-	-	-	-	✓(A)	-*	-	-	118	66	-
VV_Ser	-	-	✓	-	-	-	✓(E)	✓(E)	-	✓	3413	3743	3230
SSTc2d_J182849.4+00604	-	✓	-	-	-	-	✓(A)	-	-	?	3859	2265	890
SSTc2d_J182850.2+00950	-	-	-	-	-	-	✓(E)	✓(E)	-	✓	145	163	378
SSTc2d_J182850.4+00754	-	-	-	-	-	-	-	-	-	-	-	-	41
SSTc2d_J182850.9+04605	-	-	-	-	-	-	✓(A)	✓(E)[13]*	-	-	28	18	-
SSTc2d_J182852.7+02824	-	-	-	-	✓	✓	✓(A)	✓(A)	-	-	168	92	-
SSTc2d_J182854.1+02930	-	-	-	-	✓	✓	✓(A)	? (A)	-	-	48	72	1428

Table 8—Continued

Feature	PAH_11.3	PAH_12	PAH_6	PAH_7_8	CO_2	ICE_6	SiO_s	SiO_b	SiO_l	Em_11.3	irac3	irac4	mips24
Wavelength [μm]	11.3	12.7	6.2	7.7/8.6	15.1	6.0	9.7	18.6	34.0	11.3	5.8	8.0	24.0
Units	-	-	-	-	-	-	-	-	-	-	(mJy)	(mJy)	(mJy)
SSTc2d_J182854.5+02947	-	-	-	-	✓	✓	✓(A)	-	-	-	24	13	280
SSTc2d_J182854.9+02952	-	-	-	-	✓	✓	✓(A)	✓(A)	-	-	19	27	633
SSTc2d_J182859.5+03003	-	-	-	-	-	✓	✓(E)	-	-	?	42	45	82
SSTc2d_J182900.9+02931	-	-	-	-	✓*	?	✓(E)	✓(E)	-	-	307	375	884
SSTc2d_J182901.1+03145	-	-	-	-	✓	?	? (A)	-	-	?	75	73	86
SSTc2d_J182901.2+02933	-	-	-	-	✓*	-	✓(E)	-	-	?	103	117	831
SSTc2d_J182901.8+02946	-	-	-	-	✓	-	✓(E)	? (E)	-	✓*	33	61	527
SSTc2d_J182901.8+02954	-	-	-	-	-	✓	✓(A)	-	-	-	480	403	479
SSTc2d_J182902.6+03300	-	-	-	-	-	-	✓(A)	-	-	-	59	32	-
SSTc2d_J182902.8+03009	-	-	-	-	-	✓	? (A)	-	-	-	40	38	91
SSTc2d_J182904.4+03324	-	-	-	-	✓	?	✓(A)	-	-	?	113	156	620
SSTc2d_J182906.2+03043	-	-	-	-	✓	✓	✓(A)	? (A)	-	-	139	199	2719
SSTc2d_J182906.8+03034	-	-	-	-	✓	✓	✓(A)	-	-	-	16	24	2049
SSTc2d_J182909.8+03446	-	-	-	-	✓	-	✓(E)	✓(E)	-	?	1183	1129	1211
SSTc2d_J182914.0+01812	-	-	-	-	-	-	✓(A)	-	-	-	25	15	-
SSTc2d_J182914.8+00424	-	-	-	-	-	-	✓(A)	-	-	-	601	383	103
SSTc2d_J182916.2+01822	-	-	-	-	✓	✓	✓(A)	✓(E)*	-	-	440	431	1150
SSTc2d_J182928.2+02257	-	-	-	-	✓	-	-	✓(E)	-	✓	2464	2943	5238
SVS9_AOR1	-	-	-	-	-	-	✓(A)	-	-	-	137	74	-
SVS9_AOR2	-	-	-	-	-	-	-	-	-	-	-	-	-
Serp-S68N	-	-	-	-	✓	-	✓(E)	-	-	-	-	-	237
EC69_AOR1	-	-	-	-	-	-	✓(A)	-	-	-	23	11	140
EC69_AOR2	-	-	-	-	-	-	-	-	-	-	-	-	-
EC69_AOR3	-	-	-	-	-	-	-	-	-	-	-	-	-
EC74_AOR1	-	-	-	-	✓	-	✓(A)	✓(E)	-	-	114	132	220
EC74_AOR2	-	-	-	-	-	-	-	-	-	-	-	-	-
EC74_AOR3	-	-	-	-	-	-	-	✓(A)	-	-	-	-	798
Serp-SMM4_AOR1	-	-	-	-	-	-	-	-	-	-	-	-	120
Serp-SMM4_AOR2	-	-	-	-	-	-	-	? (E)	-	-	-	-	-
Serp-SMM4_AOR3	-	-	-	-	-	-	-	-	-	-	-	-	1224
EC82	-	-	✓	-	✓	-	✓(E)	✓(E)	-	✓	755	1307	4217
EC88	-	-	-	-	✓	✓	✓(A)	✓(A)	-	-	187	425	2126

Table 8—Continued

Feature	PAH_11.3	PAH_12	PAH_6	PAH_7_8	CO_2	ICE_6	SiO_s	SiO_b	SiO_l	Em_11.3	irac3	irac4	mips24
Wavelength [μm]	11.3	12.7	6.2	7.7/8.6	15.1	6.0	9.7	18.6	34.0	11.3	5.8	8.0	24.0
Units	-	-	-	-	-	-	-	-	-	-	(mJy)	(mJy)	(mJy)
EC90	-	-	-	-	✓	✓	✓(E)*	-*	-	✓	4941	5877	10165
EC92**	-	-	-	-	✓	✓	✓(E)*	? (E)	-	✓	263	356	2746
CK4	-	-	-	-	✓	?	✓(E)	✓(E)	-	✓	157	199	599
Serp-SMM3	-	-	-	-	✓	-	✓(A)	-	-	-	-	-	161
EC118	-	-	-	-	✓	✓	✓(A)	? (A)	-	-	578	310	-
SVS8	-	-	-	-	-	-	-	-	-	-	3	2	-
LkHA_348	-	-	-	-	-	-	✓(E)	✓(E)	?	?	7614	8392	2905
R_CrA_IRS5	-	-	-	-	✓	✓	✓(A)	-	-	-	1127	1452	8750
CrA_IRS7_A	-	-	-	-	✓	✓	✓(A)	✓(A)	-	-	708	1087	49127
CrA_IRS7_B	-	-	-	-	✓	✓	✓(A)	✓(A)	-	-	473	628	12689
CrA_IRAS32	-	-	-	-	✓	✓	✓(A)	-	-	-	15	11	3244
Cyg_OB2_No12	-	-	-	-	-	-	-	-	-	-	-	-	1898
L1014_IRS	-	?	-	-	✓	✓	✓(A)	✓(A)	-	-	22	23	103
IRAS_23238+7401	-	-	-	-	✓	✓	✓(A)	✓(A)	-	-	43	60	1533
BF_Ori	-	-	-	-	✓	-	✓(E)	✓(E)	-	✓	605	1000	970

*Automated feature identification is suspect. Please check log file for details.

**A nearby source was within the slit for some modules. Please see log files for details. Frature identification is thus difficult.

A. IRS Observation Logfile

Logfile for the Spitzer/IRS observation as shown in Figure 8.

```
Quality check file for Spitzer/IRS observation.

Source:        GW_Lup
Coordinates:   15h46m44.7s -34d30m35.4s [J2000]
Observer:      Neal Evans, OID 87
Program:       From Molecular Cores to Planets, continued
Obs. date:     2004-08-30
AOR:           0005643520
AOR label:     IRSS-0068
AOT type:      irsstare
Obs. mode:     TargetFixedSingle
Peak up mode:  --

IRS Pipeline: S13.2.0

Modules:       SL1, SL2, LL1, SH, LH

The longslit images of the SL2 and LL2 modules are severely undersampled
over most of their wavelength range. As a result the PSF extraction is
unstable for these modules. Therefore the PSF, PSF_sky, and the FullAp_sky
columns contain no data.

=============================================================

Data summary:
-------------
SL integration: 14*1*2 (tint*ndce*nexp)
SH integration: 121*2*2 (tint*ndce*nexp)
LL integration: 14*4*2 (tint*ndce*nexp)
LH integration: 60*4*2 (tint*ndce*nexp)

SL SNR:  20   STDEV:     5 [mJy]
SH SNR:  66   STDEV:     2 [mJy]
LL SNR:  34   STDEV:     7 [mJy]
LH SNR:  49   STDEV:     6 [mJy]

SL source size             :   1.1 [arcsec]
SL X-dispersion offset     :   0.2 [arcsec]
SL pointing offset estimate:   0.8 ...   0.8 [arcsec]
SH source size             :   0.4 [arcsec]
SH X-dispersion offset     :   0.9 [arcsec]
SH pointing offset estimate:  -0.9 ...  -0.6 [arcsec]
LL source size             :   1.9 [arcsec]
```

LL X-dispersion offset : 1.0 [arcsec]
LL pointing offset estimate: -0.9 ... -0.4 [arcsec]
LH source size : 0.0 [arcsec]
LH X-dispersion offset : -0.5 [arcsec]
LH pointing offset estimate: 1.3 ... 3.2 [arcsec]

==

Most prominant spectral absorption and emission features identified in the Spitzer/IRS spectrum of GW_Lup

IRAC3, IRAC4, and MIPS24 give the flux of the observed spectra, if possible with a correction for extended emission and pointing errors, convolved with the respective passbands.

SNR estimate is the peak intensity or peak optical depth of the feature over the residual rms after feature fitting.

N.B. The identification is done using an automated script.
Caution should therefore be taken at all times.

id	abs=2	lambda [um]	snr
	em=1	lambda [um]	snr
	cnt=-1	lambda [um]	flux [mJy]
SiO_s	1	9.700	17
Em_11.3	1	11.300	5
irac3	-1	5.702	96
irac4	-1	7.784	111
mips24	-1	23.512	264

#> ------------------
- The spectra are good
- Features identification is ok
- Em_11.3 could also be caused by a broad SiOs feature.

B. IRS Table Header

Header of IRS spectral table for the Spitzer/IRS observation as shown in Figure 8.

```
\c2d_irs_spectrum
\processing date Nov 2006
\char HISTORY ==============
\char HISTORY The spectrum presented in this table is a combination
\char HISTORY of all Spitzer/IRS c2d data for the object GW_Lup
\char HISTORY The data have been observed, reduced and verified by the
\char HISTORY Spitzer c2d legacy team:
\char HISTORY
\char HISTORY     'From Molecular Cores to Planet Forming Disks'
\char HISTORY          http://peggysue.as.utexas.edu/SIRTF/
\char HISTORY
\char HISTORY Before using this data please read the quality file accompanying
\char HISTORY this specific dataset and the complete documentation of the
\char HISTORY release of all the c2d legacy data.
\char HISTORY
\char HISTORY For questions please contact the Spitzer helpdesk
\char HISTORY          help@spitzer.caltech.edu
\char HISTORY who will answer your questions or forward them to one of
\char HISTORY the c2d IRS experts.
\char HISTORY ==============
\char NAXIS   =                    2 / STANDARD FITS FORMAT
\char ORIGIN  = '   c2d Legacy team' / Organization generating this FITS file
\char TELESCOP= '           Spitzer' /
\char INSTRUME= '              IRSX' /
\char EQUINOX = '            2000.0' / Equinox
\char CREATOR = '           S13.2.0' / SSC Pipeline Version
\char OBJECT  = '            GW_Lup' / Target Name
\char RA_HMS  = '      15h46m44.68s' / [hh:mm:ss.ss] Commanded RA as sexagesimal
\char DEC_DMS = '      -34d30m35.4s' / [dd:mm:ss.s] Commanded Dec as sexagesimal
\real RA_SLT  =          236.68617 / [deg] RA at slit center
\real DEC_SLT =          -34.50983 / [deg] DEC at slit center
\char DATE_OBS= '        2004-08-30' / Observation Date
\char AOT_TYPE= '          irsstare' / Observation Template Type
\char OBJTYPE = ' TargetFixedSingle' / Target Type
\char PEAKUP  = '                --' / Peakup
\char AORLABEL= '         IRSS-0068' / AOR Label
\char AORKEY  = '        0005643520' / AOR key. Astrnmy Obs Req Req
\char OBSRVR  = '        Neal Evans' / Observer Name
\char OBSRVRID= '                87' / Observer ID of Principal Investigator
\char PROGID  = '               172' / Program IDe
\char PROTITLE= 'From Molecular Cores to Planets, continued' / Program Title
\real SL_TINT =              14.68 / SL Ramp integration time
\int  SL_NDCE =                  1 / SL Commanded number of DCEs
```

```
\int  SL_NEXP =                    2 / SL Number of exposures per DCE
\real SH_TINT =               121.90 / SH Ramp integration time
\int  SH_NDCE =                    2 / SH Commanded number of DCEs
\int  SH_NEXP =                    2 / SH Number of exposures per DCE
\real LL_TINT =                14.68 / LL Ramp integration time
\int  LL_NDCE =                    4 / LL Commanded number of DCEs
\int  LL_NEXP =                    2 / LL Number of exposures per DCE
\real LH_TINT =                60.95 / LH Ramp integration time
\int  LH_NDCE =                    4 / LH Commanded number of DCEs
\int  LH_NEXP =                    2 / LH Number of exposures per DCE
\char SL_SIZE = '                1.1' / SL source size estimate
\char SL_XOFF = '                0.2' / SL cross dispersion offset
\char LL_SIZE = '                1.9' / LL source size estimate
\char LL_XOFF = '                1.0' / LL cross dispersion offset
\char SH_SIZE = '                0.4' / SH source size estimate
\char SH_XOFF = '                0.9' / SH cross dispersion offset
\char LH_SIZE = '                0.0' / LH source size estimate
\char LH_XOFF = '               -0.5' / LH cross dispersion offset
\real SLPE_PSF=                 0.77 / SL pointing offset for psf spectrum
\real SLPE_SRF=                 0.77 / SL pointing offset for fullap spectrum
\real LLPE_PSF=                -0.86 / LL pointing offset for psf spectrum
\real LLPE_SRF=                -0.42 / LL pointing offset for fullap spectrum
\real SHPE_PSF=                -0.91 / SH pointing offset for psf spectrum
\real SHPE_SRF=                -0.63 / SH pointing offset for fullap spectrum
\real LHPE_PSF=                 1.26 / LH pointing offset for psf spectrum
\real LHPE_SRF=                 3.20 / LH pointing offset for fullap spectrum
\real SL2Z_SRF=               0.0100 / SL order 2 zero level for fullap spectrum
\real SL3Z_SRF=               0.0100 / SL order 3 zero level for fullap spectrum
\char COMMENT ==============
\char COMMENT The longslit images of the SL2 and LL2 modules are
\char COMMENT severely undersampled over most of their wavelength range.
\char COMMENT As a result the PSF extraction is unstable for these modules.
\char COMMENT Therefore the PSF and the FullAp_sky columns contain no data.
\char COMMENT ==============
\char COMMENT The PSF_SRC and FULLAP_SRC columns contain the observed spectra
\char COMMENT corrected for extended emission within the IRS SH and LH aperture
\char COMMENT and flux loss due to pointing errors.
\char COMMENT Note that the extended emission correction uses a low resolution
\char COMMENT of the estimated sky and the resulting SRC spectrum may therefor
\char COMMENT still contain spectral features (e.g. H2 and PAH) from a
\char COMMENT spatially extended  component.
\char END
```

C. MIPS SED Namelist File

Namelist configuration file for the c2d MIPS SED data reduction for SX Cha.

```
write_lists = 1
have_uncertainties = 1
run_sed_fif = 1
run_mosaic_interp = 1
run_mosaic_coadder = 1
create_std_mosaic = 1
run_mosaic_subtract = 1
run_spectrum = 1
sigma_weighted_coadd  = 0
use_std_for_extract = 0
use_unc_for_extract = 1
create_unc_mosaic = 1

combine_clusters = 0

NICE = 0
verbose = 1
delete_intermediate_files = 1
save_namelist = 0

INTERP_DIR = Interp
COADDER_DIR = Coadd
OUTPUT_DIR = MIPS70/SED/mosaic

MOSAIC_PIXEL_RATIO_X = 1

IMAGE_STACK_FILE_NAME = data/MIPS70/SED/ImageList.txt
SIGMALIST_FILE_NAME = data/MIPS70/SED/SigmaList.txt
PMASK_FILE_NAME =  cal/fb674_MIPS70_PMASK.fits
DCE_STATUS_MASK_LIST = data/MIPS70/SED/MaskList.txt
CALIBRATION_TABLE_FILE_NAME = cal/MIPS70_SED_sample_calibration.tbl

DCE_Status_Mask_Fatal_BitPattern = 31744
PMask_Fatal_BitPattern =  16648

&SEDFIF
#in arcsec’s,
```

```
  EDGE = -100,
&END

&MOSAICINTIN
# INTERP_METHOD = 1(default), 2(Drizzle),3(Grid),4(Bicubic),
   INTERP_METHOD = 1,
&END

&SPECTRUM
   N_Columns =  5,
   Max_Bad_Pixels_In_Column = 20,
&END
```

D. MIPS SED Log File

Log file for the c2d MIPS SED data reduction for SX Cha.

```
Source:        SXCha
Coordinates:  10h55m59.74s  -77d24m39.9s [J2000]
Observer:      Neal Evans, OID 87
Program:       179
Obs. date:     2005-03-06
AOR:            5800960
AOR label:     MIPSE-0002

File list:
MOPEX extraction   = MIPSSED_MOPEXspec_SXCha.tbl
IRAF extraction    = MIPSSED_IRAFspec_SXCha.tbl
Plot of MOPEX+IRAF = MIPSSED_spec_SXCha.ps
```

E. MIPS SED Table Header

Header of MIPS SED spectral table for SX Cha.

```
\char HISTORY ==============
\char HISTORY The data presented in this table is the extracted MIPS-SED
\char HISTORY spectrum for the object SXCha
\char HISTORY The data have been observed, reduced and verified by the
\char HISTORY Spitzer c2d legacy team:
\char HISTORY
\char HISTORY     'From Molecular Cores to Planet Forming Disks'
\char HISTORY          http://peggysue.as.utexas.edu/SIRTF/
\char HISTORY
\char HISTORY Before using this data please read the quality file accompanying
\char HISTORY this specific dataset and the complete documentation of the
\char HISTORY release of all the c2d legacy data.
\char HISTORY
\char HISTORY For questions please contact the Spitzer helpdesk
\char HISTORY          help@spitzer.caltech.edu
\char HISTORY who will answer your questions or forward them to one of
\char HISTORY the c2d IRS experts.
\char HISTORY ==============
\mipssed data written by c2d routine irs2ipac
\processing time Mon Nov 20 15:32:49 2006
\int  SIMPLE  =                    1 / Standard FITS format
\int  BITPIX  =                    8 / 8-bits unsigned integers
\int  NAXIS   =                    0 / Empty Prime data matrix
\int  EXTEND  =                    1 / FITS extension may be present
\char ORIGIN  = 'c2d Legacy team'    / Organization generating this FITS file
\char DATE    = '2006-11-20'         / Date of writing: YYYY-MM-DD
\char TELESCOP= 'Spitzer '           /
\char INSTRUME= 'MIPSSED '           /
\char OBJECT  = 'SXCha   '           / Target Name
\char EQUINOX = '2000.0  '           /
\char OBSRVR  = 'Neal Evans'         / Observer Name
\int  OBSRVRID=                   87 / Observer ID of Principal Investigator
\int  PROGID  =                  179 / Program IDe
\char PROTITLE= 'From Molecular Cores to Planets, continued' / 0
\char COMMENT = ' dlimage library version  5.00' / comment
\char DATE_OBS= ' Thu Apr 20 17:53:08 2006' / Date-Time
\char INFILE  = ' MIPS70/SED/col3/mosaic_all_bicub/Mosaic/mosaic.fits' / Input_Image_Fi
\char UNCFILE = ' MIPS70/SED/col3/mosaic_all_bicub/Mosaic/mosaic_std.fits' / Input_Unc_
\int  NCOLUMNS=                    3 / N_Columns
\int  MAXBAD  =                   20 / Max_Bad_Pixels_In_Column
\int  HIGHP   =                    0 / HighPrecision
\real RESAMP  =            1.0000000 / Resample_Factor
\char CALFILE = ' cal/MIPS70_SED_sample_calibration.tbl' / Calibration_Table_Filename
```

```
\char OUTFILE = ' MIPS70/SED/col3/mosaic_all_bicub/Mosaic/sed.tbl' / Output_Table_Filen
\int  COLUMN1 =                    1 / Column_1
\int  COLUMN2 =                    2 / Column_2
\int  COLUMN3 =                    3 / Column_3
\real CONV    =         0.0022570000 / Conversion Factor
\char RA_HMS  = '5h10m26.9s'         / [hh:mm:ss.ss] Commanded RA as sexagesimal
\real RA_SLT  =            77.612300 / RA_Source
\char DEC_DMS = '-77d23m30.6s'       / [dd:mm:ss.s] Commanded Dec as sexagesimal
\real DEC_SLT =           -77.391800 / DEC_Source
\real CRVAL1  =          0.017694000 / CRVAL1_Source
\int  END     =                    0 / END
```

List of Figures

List of Tables